Politecnico di Torino

Corso di Laurea in Ingegneria Energetica e Nucleare

A. A. 2022/2023

Sessione di Laurea Marzo 2023

# Influence of load profiles and climatic zones on the installations of SOFC-based cogeneration systems in commercial buildings


**Relatori:**

Dr. Marta Gandiglio

Dr. Paolo Marocco

**Candidato:**

Davide Pepe

## Abstract

Even if significant efforts are being supported by a great part of Occidental Countries to switch from traditional thermochemical systems, based on fossil fuels to produce electrical and thermal power, to renewable energy sources-based technologies, according the latest international agreements between Countries aiming to mitigate the climate change, right now it is not possible to rely only on RES's to meet the energy needs of all the people in the word. In this context a combined heat and power (CHP) energy system based not on thermochemical but on more efficient electrochemical processes, could help the energy transition, using as well a fossil fuel as methane, but resulting in a strong reduction of pollutants and greenhouse gases (GHG) emission with respect to traditional fossil fueled energy systems.

This work wants to evaluate Solid Oxide Fuel Cell based systems potential in the context of distributed generation systems, applied on two different types of commercial buildings, evaluating priorly what kind of buildings are more suitable in terms of electrical and thermal load profiles and climatic conditions, to switch from the actual case, where most of them buy the electricity from the grid and produce thermal energy for space heating using fossil fuels fired boilers or electrical heat pumps, to combined heat and power systems fuel cell based. The entire analysis has been made using in input modeled end use load profiles of a typical meteorological year contained in a dataset supplied by The National Renewable Energy Laboratory (NREL). Firstly, comparisons in the electrical and thermal energy yearly demands of each type of commercial building are done, examining energy end uses and load profiles of different types of building in the same climate and for the same category of building, the influence of the climate zone on their energy behavior as magnitude and shape of load profiles, as well the ratio of electrical to thermal energy demand.

At the end of the aggregate analysis, four different climate zones from warm climates to colder ones and two categories of building are selected, among those that could be more suitable to a CHP SOFC based system installation, the average energy behavior per climate zone and building type is investigated and compared. A total of eight buildings modeled are analyzed, namely four hospitals and four hotels, selected as the most representative buildings per each category and climate, using a MATLAB code based on the minimization of the Euclidian distance for each building selected from the average electrical and thermal energy yearly consumptions of its category and climate of belonging.

Finally, a techno economic analysis is made for the eight buildings, evaluating the Levelized cost of electricity (LCOE) priorly on the SOFC system volume control, then on the control volume composed by the SOFC and the specific building. Buildings in cold climates, with a consistent electrical base load performs better with lower LCOE values. The study found that the lowest LCOE values were obtained for the largest hospital in the coldest climate zone and the largest hotel in the warmest climate zone. However, it was also noted that the buildings with the lowest LCOE values were not necessarily the ones with the highest electricity savings and thermal recovery from SOFC, due to the high investment costs and short stack lifespan of the technology. To explore a possible future scenario with lower investment costs, the LCOE values were recalculated, and it was found that the hospital in the mildest climate zone had the lowest LCOE value of 0.186 [€/kWh], and the hotel in the climate zone immediately before the coldest had an LCOE of 0.191 [€/kWh]. These results indicate the potential competitiveness of a similar energy system in the near future.

# Summary

## Nomenclature

| Indicator | Description | Unit of measure |
|---|---|---|
| EULP | End-Use Load Profiles | - |
| AMI | Advanced Metering Infrastructure | - |
| QOI | Quantity of Interest | - |
| SOFC | Solid Oxide Fuel Cell | - |
| CBECS | Commercial Building Energy Consumption Survey | - |
| AMY | Actual Meteorological Year | - |
| TMY | Typical Meteorological Year | - |
| LCOE | Levelized Cost Of Electricity | [$/kWh] |
| CHP | Combined Heat and Power | - |
| CCHP | Combined Cooling, Heat and Power | - |
| HVAC | Heating, Ventilation and Air Conditioning | - |
| E/T | Electric to Thermal ratio | - |
| TER | Thermal to Electric ratio | - |
| LHV | Lower Heating Value | [kWh/Sm$^3$] |

## List of figures

## List of tables

# Introduction

After a temporary decline in the global economy due to the COVID-19 pandemic, which led to a decrease in global energy consumption in 2020, the global economy recovered quickly in 2021, along with a significant increase in global energy demand by 5.4% [1] within a year. Projections for future energy demand indicate an increase in the global primary energy demand of approximately 1% per year until 2030, under the assumption that countries continue to implement their stated policies regarding the energy sector. The imperative to address climate change has led 87 countries and the European Union, in November 2022, to announce initiatives to achieve net-zero greenhouse gas (GHG) emissions within this century[2]. For example, the European Union has already adopted Fit for 55, a set of measures aimed at reducing GHG emissions by at least by a 55% [3]. In 2022, renewables contributed 30% of global power generation a record high compared to just a decade earlier when this value was barely 20% [2]. However, most of the world's energy production still relies on fossil fuels. In addition, in February 2022, the European Commission approved the Complementary Climate Delegated Act[4], which included natural gas in the European energy taxonomy to facilitate the energy transition from coal to renewables.

Regarding the global building sector, which includes both residential and commercial buildings, its final energy demand reached the 31% of global final energy demand in 2019, with the electricity component accounting for around the 18% of global electricity production[5]. Furthermore, their energy demand is expected to rise as it is strongly correlated with the building floor area, which is projected to increase by 20% from 2021 to 2030.

In this context, the use of more efficient cogeneration systems, such as fuel cells for building applications, could aid in the energy transition by reducing CO2 emissions and primary energy consumption, and emitting near-zero harmful pollutants compared to traditional internal combustion engines (ICEs)[6].

Numerous studies can be found in literature regarding the integration of fuel cell-based cogeneration systems in both residential and commercial buildings.

A study was conducted on the application of a SOFC CHP system to a model of a medium-sized office located in three different locations in the USA, with different climates and energy pricing structures[7]. The study achieved a significant reduction of more than 50% in $CO_2$ emissions, as compared to the baseline HVAC system, for two case studies, and a 14.5% reduction in the annual utility cost for the most efficient location. However, despite the not neglectable saving and due to the high capital and installation cost, a payback time is never reached during the system lifetime.

A study was conducted on the application of Phosphoric Acid Fuel Cell cogeneration systems to a supermarket in the UK [8]. In this work, a techno-economic study was performed comparing a PAFC- CHP against an ICE-CHP with a UK's cogeneration incentive mechanism implemented. The main results showed that fuel cell-based system had a payback time only 7 months higher than the reference case, and a 22% reduction in the fuel consumed.

Not only combined heat and power fuel cell systems, but also cooling systems that use part of the fuel cell heat to feed an absorption cooler, have been studied [9]. A SOFC based CCHP system model was developed and applied to a case study of a hospital in Shanghai. The optimal configuration resulted in an LCOE of 0.17 $/kWh, which was even lower than the baseline LCOE of 0.21 $/kWh, where electricity was procured from the grid, thermal energy was produced by a boiler, and cooling was provided by and electrical chiller. Furthermore, this system resulted in a 61% reduction of carbon emissions from an environmental point of view.

A similar case study in which cooling is provided using an absorption chiller is presented in [10], using a geometrically similar office model as the one studied by [7]. The study compared two offices in two cities in Qatar, and showed better results than the previous work, with a payback time of 7.8 years and a reduction in $CO_2$ emission of 30%, as well as reductions of ~90% in $NO_x$ and $SO_x$ emissions. These results were achieved thanks to an energy market structure in which natural gas costs are significantly lower than electricity costs, as well as the large summer cooling demand that can be met using the recovered heat and sending it to the absorption chiller.

One of the most comprehensive studies in the literature on CCHP systems applied to commercial buildings, compared five different types of buildings (hospitals, hotels, supermarket, offices, and schools) in five different climate zones, ranging from the coldest to the hottest. The study adopted a multi-criteria approach that simultaneously considered total efficiency, carbon emission reduction, air pollution cost saving, operation cost saving, simple payback time, and LCOE. The authors concluded that hospitals, hotels, and supermarkets generally perform better with a SOFC-CCHP based system, and warmer regions are characterized by slightly better performance. However, for the same building type, the overall performance is not predictable since it is at the same time a function of the climate, building type, electricity and natural gas prices, and carbon intensity.

Based on the literature review, the aim of this research is to improve energy efficiency in commercial buildings, resulting in reduced CO2, NOx, and Sox emissions, as well as decreased primary energy consumption compared to the reference case. The reference case involves the use of electricity from the grid and a gas-fired boiler for thermal load coverage through an HVAC system. This research proposes the installation of a cogeneration system based on SOFC and assesses its feasibility in two commercial building categories: hospitals and hotels. These buildings mostly rely on natural gas for heating purposes, as shown in Figure 1, and are characterized by the presence of a base load that enables the fuel cell to continuously generate electricity and meet part of the thermal load. The research will explore these buildings in four different climates. The primary input data for this research will be hourly electrical and thermal load profiles of modeled buildings, divided by end-use and obtained from an NREL dataset. To investigate the influence of building energy load profiles and climatic conditions on the cogeneration system's economy, the levelized cost of electricity (LCOE) will be calculated for each building selected. Additionally, the research will examine the potential impact of future technological advancements on the system's LCOE.

This study is organized into five sections. The first section provides the context of the study, including a literature review of similar work and the purpose of this study. In Section 1, a brief overview of the basic principles of SOFC operation is presented. Section 2 introduces and briefly describes the dataset used to obtain building energy load profiles as input data for subsequent analysis. Section 3 outlines the methodology used to select the most representative building for each climate and presents the technical and economic input data used in the LCOE calculations. In Section 4, comparisons of hourly load profiles on yearly and daily bases are presented and the LCOE results for buildings in the same category and different climates, as well as those in the same climate and different categories, are discussed. Additionally, a hypothetical future scenario is explored by varying the economic input data of SOFC technology, and new LCOE results are obtained and their relationship with building category and climate are discussed. Finally, in the last section, the main conclusions of the study are summarized.

Although similar studies have been conducted in the literature on the hotel, hospital,[11], and food retail sector [12], this work is novel in its detailed investigation across two very different types of commercial buildings, studying which type is more feasible to a FC-CHP energy system according to its climate zone and energy load profiles.

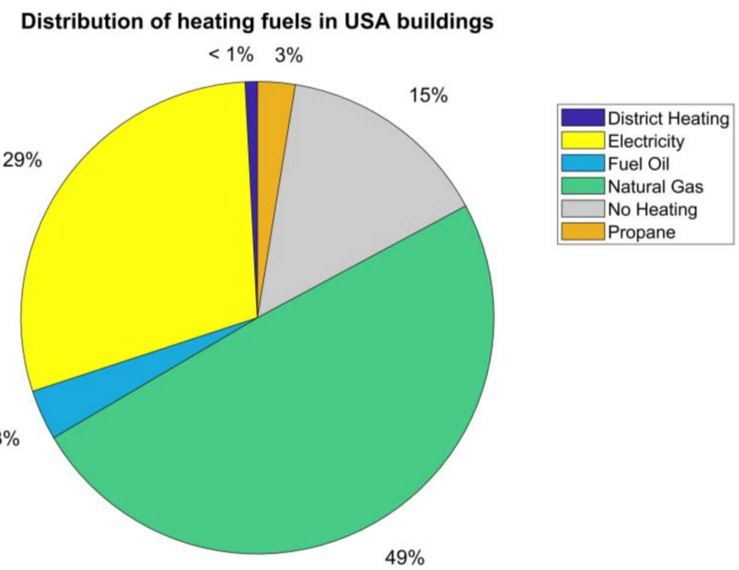


*Figure 1 - HVAC system heating fuels for all USA commercial building stock, author own elaboration from [13]*

# 1 SOFC-based cogeneration systems

A fuel cell is an electrochemical energy system capable of producing both electrical and thermal power with high efficiencies, low emissions, and no moving parts [14] The main components of a fuel cell in a conceptual diagram are an anode, a cathode, and an electrolyte layer that separates them, as shown in Figure 2. Conceptually, it can be thought of as a battery that does not need to be recharged but can continuously produce power as long as fuel and oxidant are provided, and the reaction products are removed. [15].

There are several types of fuel cells that can be classified based on the chemical characteristics of the electrolyte layer or their operating temperature. However, in this section, only a brief overview will be provided on the type of fuel cell that will be considered in this study as the CHP prime mover, i.e., solid oxide fuel cells.

The reactions that occur at the anode, when using a fuel containing carbon molecules as natural gas ($CH_4$) are the following:

$$H_2+O^{2-} \rightarrow H_2O+2e^- \qquad \textit{(Eq. 1)}$$

$$CO+O^{2-} \rightarrow CO_2+2e^- \qquad \textit{(Eq. 2)}$$

$$CH_4+4O^{2-} \rightarrow 2H_2O+CO_2+8e^- \qquad \textit{(Eq. 3)}$$

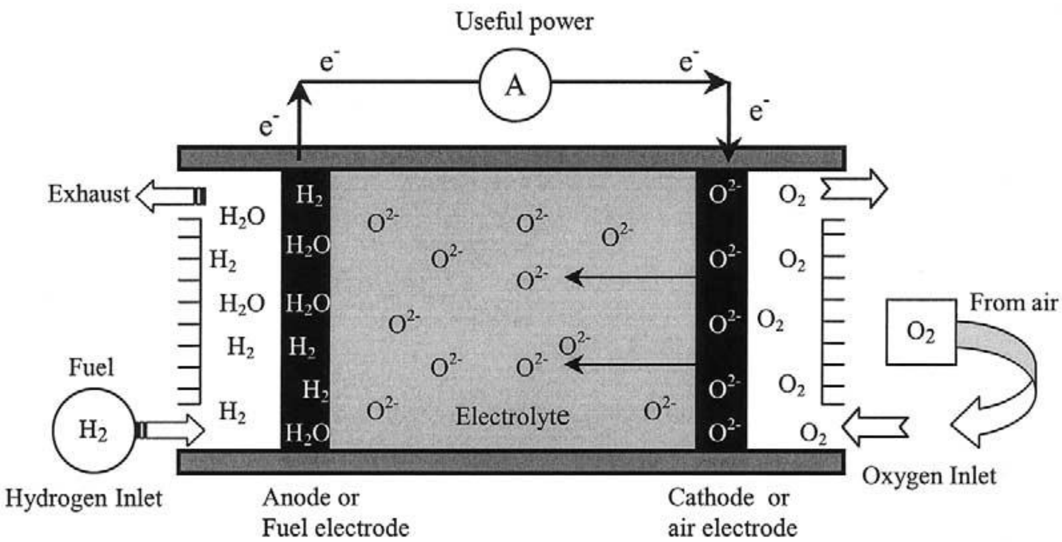


*Figure 2 - Conceptual scheme of a SOFC with anionic electrolyte[14]*

At the cathode side, where air flows throughout, only oxygen molecules participate to the reaction of reduction (Eq. 4 ), accepting electrons produced by oxidation reaction of the fuel molecules at the anode side and delivered by the external circuit.

$$O^2+4e^-\rightarrow 2O^{2-} \quad \textit{(Eq. 4 )}$$

The external flow of electrons from the anode to the cathode is a spontaneous process that generates electricity This electron flow is balanced by the migration of oxygen ions into the electrolyte in the opposite direction, specifically towards the anode in the case of an anionic electrolyte[16].

To provide a usable amount of energy, individual fuel cells must be connected in series to form a stack via bipolar plates, which consist of proper manifolds and flow fields that are electronically conductive. While the energy provided by a single cell is relatively low compared to conventional electrical technologies, the current density is high, and stacking multiple cells in series allows for a significant increase in power output.

## 1.1 Combined heat and power systems in commercial buildings

Solid oxide fuel cell (SOFC) stacks are an ideal technology for distributed generation (DG) or localized stationary power applications. This is because the high operating temperature range of 600-1000◦C enables the use of conventional hydrocarbon fuels, such as natural gas, with internal reforming. Additionally, SOFCs produce high-quality exhaust waste heat that can be used for cogeneration purposes. When operating on natural gas as fuel, SOFCs can eliminate almost all NOx, SOx, and particulate matter emissions, while reducing $CO_2$ emissions by up to 54% when compared to traditional fossil-fueled power plants [14].

These properties of SOFCs make them valuable for power generation scenarios where high-power reliability is needed, emission minimization or elimination is required, or biological waste gases are available for fuel.

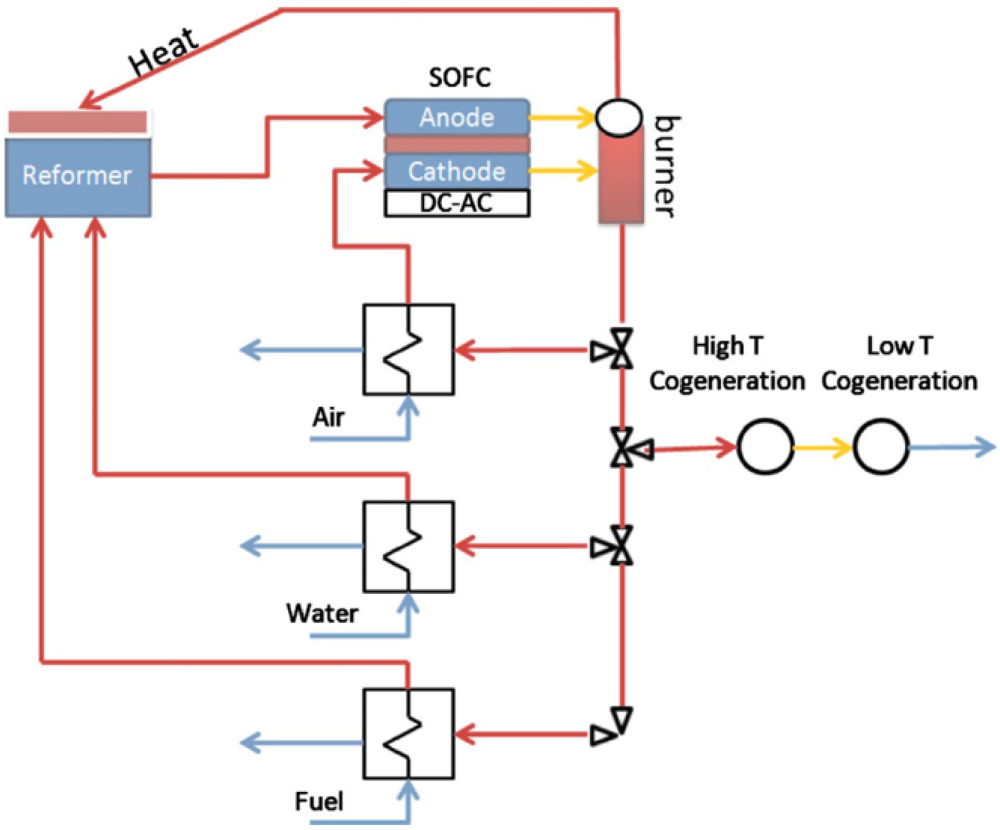


*Figure 3 - Basic layout of a generical SOFC-based CHP system [17]*

In Figure 3 depicts a possible simplified layout of a cogeneration system based on SOFC. The SOFC, which is the heart of the cogeneration system, is fueled with natural gas from the distribution network. In this figure, the reformer is shown as external to the stack, but its installation is not strictly necessary since the reforming reactions of natural gas can also occur inside the stack itself due to the high operating temperatures. Often, the installation of an external reformer is avoided to reduce investment costs[18] Depending on the composition of the incoming fuel, various reforming reactions may occur [18], such as steam reforming (Eq. 4), (Eq. 5), dry CO2 reforming (Eq. 6) or the water-gas shift reaction (Eq. 7):

$$CH_4+H_2O \rightarrow 3H_2+CO \quad \text{(Eq. 4)}$$

$$CH_4+2H_2O \rightarrow 4H_2+CO_2 \quad \text{(Eq. 5)}$$

$$CH_4+CO_2 \rightarrow 2H_2+2CO \quad \text{(Eq. 6)}$$

$$CO+H_2O+CO_2 \rightarrow 2H_2 \quad \text{(Eq. 7)}$$

The waste heat produced by the SOFC due to irreversible phenomena such as reaction activation, molecule diffusion, and ohmic losses is utilized to heat both the water loop of the HVAC system and the domestic hot water loop, enabling the recovery of thermal energy as a byproduct of electricity generation.

The amount of thermal energy introduced into the loop is determined by a percentage of the heat produced from the input design fuel consumption, taking into account the SOFC's efficiency. Additionally, the burner illustrated in the figure can be utilized to burn any excess fuel that is not recirculated to the SOFC anode, and it can potentially serve as the same boiler used by the existing HVAC system. Since electricity is generated in DC mode, it may be necessary to consider installing a DC-to-AC converter in this type of system. However, this thesis primarily focuses on the combined impact of building load profiles and climate zones on energy performance rather than on detailed system modeling, and therefore, the complete configuration of a cogeneration system is beyond its scope.

# 2 ComStock dataset

This chapter is divided into three subchapters and provides a brief description of the dataset from which the building load profiles used in the analysis are obtained.

The first subchapter describes the modeling process used to create the end-use load profiles, including the input data utilized to construct the dataset and gain insights into the nature of the building energy load profiles analyzed in this work.

The second subchapter presents the weather files used to simulate the buildings' energy behavior based on the outdoor weather conditions throughout the year.

The third and final subchapter lists the main characteristics of each building in the dataset, including geometrical properties and yearly energy behavior. These factors determine the shape and magnitude of the energy load profiles and are essential for understanding the building energy performance.

## 2.1 Introduction to the dataset

The commercial building stock dataset is part of a larger project called "End-Use Load Profiles for the U.S Building Stock," which also includes the Residential Building Stock database (ResStock). ComStock and ResStock are probabilistic representations of the building stock, each containing physics-based simulation models that represent the energy behavior of buildings. This overview focuses solely on the Commercial Building Stock (ComStock), as the present study analyzes commercial buildings exclusively and omits the residential portion of the dataset.

The complete dataset was created as part of a three-year project supported by the U.S Department of Energy (DOE), with contributions from researchers at the National Renewable Energy Laboratory (NREL), Lawrence Berkeley National Laboratory (LBNL), and Argonne National Laboratory (ANL).

COMSTOCK provides validated 15-minute resolution load profiles for the most common types of commercial buildings and end uses. It includes around 350,000 simulated commercial buildings, which represents 1.8 million actual commercial buildings in a 1:5 ratio. This is equivalent to 58 billion square feet (almost 5.4 billion square meters)[13]. The dataset is calibrated and validated to ensure accuracy and reliability in predicting the energy performance of commercial buildings in the United States.

The End-Use Load Profiles (EULP) are not measured but simulated energy profiles for end use, as stated in the project's final report. This is due to the high cost that would have been required for a direct submetering of a statistically representative sample of buildings, which would have been limited in spatial granularity and restricted in building types and energy end uses. Instead, a hybrid approach was adopted, which combined empirical data from various sources such as AMI's data and energy utilities surveys, along with physics-based simulation building stock models in OpenStudio® format as input for EnergyPlus™ modeling. Calibrated building models enable the analysis of various future scenarios, such as modifications to the thermophysical properties of buildings after implementing energy efficiency measures or changes in climate.

These end use load profiles are notable for several reasons, including their unprecedented scale of application with a large amount of empirical data and a high level of granularity in the building stock. Furthermore, the project incorporates a novel approach to sensitivity analysis and uncertainty quantification, which improves the accuracy and reliability of the load profiles. A concise logic flow diagram of the steps involved in generating the building stock models is shown in Figure 4.

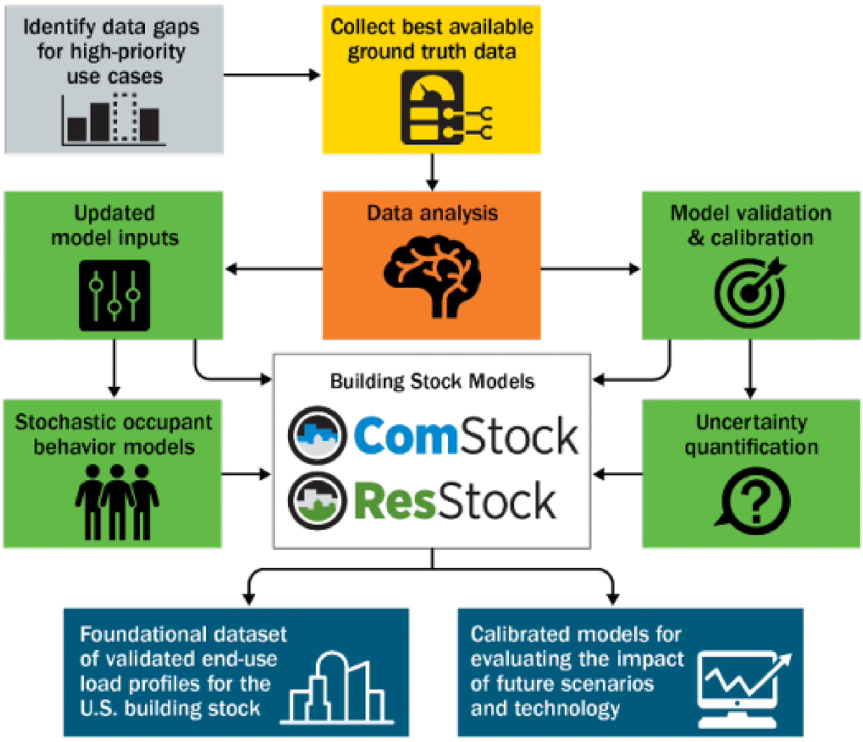


*Figure 4 - Block Summary of the End-Use Load Profiles for the U.S. Building Stock project [13]*

The authors of the project followed a four-step methodology to generate the ComStock (and ResStock) dataset.

First, the building stock was characterized using a conditional probability distribution obtained by combining data from various sources listed in Table 29 (APPENDIX A1), such as year of construction, location, and building type..

Secondly, quasi-random sampling using Sobol' sequences was employed to generate 350,000 samples to represent 1.8 million commercial buildings, with the number of samples determined through convergence testing to minimize uncertainty.

Thirdly, physics simulation was used to construct models from the samples, utilizing OpenStudio® to create the models, which were then simulated using EnergyPlus®

Finally, the model outputs were post-processed to obtain both annual and 15-minute resolution energy use load profiles for each sample, divided by end-use, such as electricity for heating in the case of a heat pump-based HVAC system or thermal energy from fuel consumption for a fossil fuel-based HVAC system.

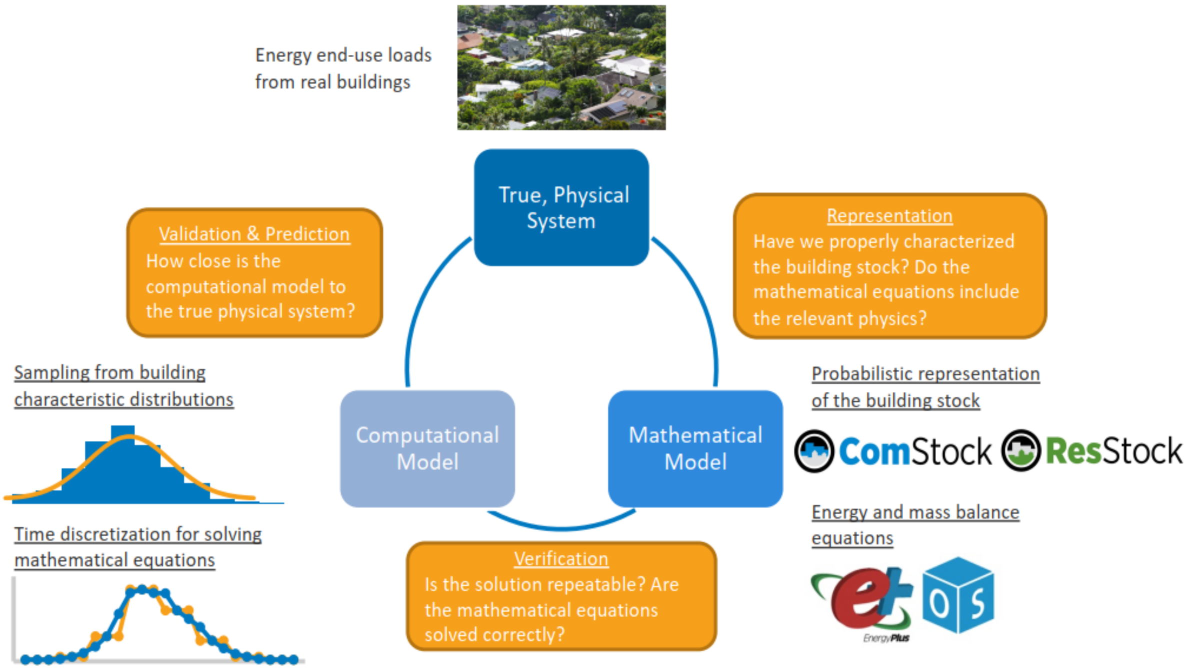


*Figure 5 - Verification, validation and prediction: relationship with real buildings, mathematical model and computational model[13]*

After obtaining a model, it is essential to ensure its reliability and provide users with information on the associated uncertainties. This process involves several steps, which are graphically summarized in Figure 5.

The first step is verification, which involves determining how the code (EnergyPlus®) correctly implements mass and energy equations and evaluating a narrow number of simulation outputs, called Quantity of Interest (QOI). Next, in the validation step, the accuracy of the model is evaluated by comparing the QOI output from ComStock against energy consumption data from various sources such as CBECS surveys, data of consumption reported by utilities, and commercial AMI data. Uncertainty quantification (UQ) is another critical step that involves calculating the uncertainties associated with the model's QOI output. Finally, calibration involves making improvements to the building models by comparing stock model outputs with empirical field data sources (as shown in Table 29 and Figure 6) which are corrected to reduce model error by evaluating the accuracy of QOI in output.

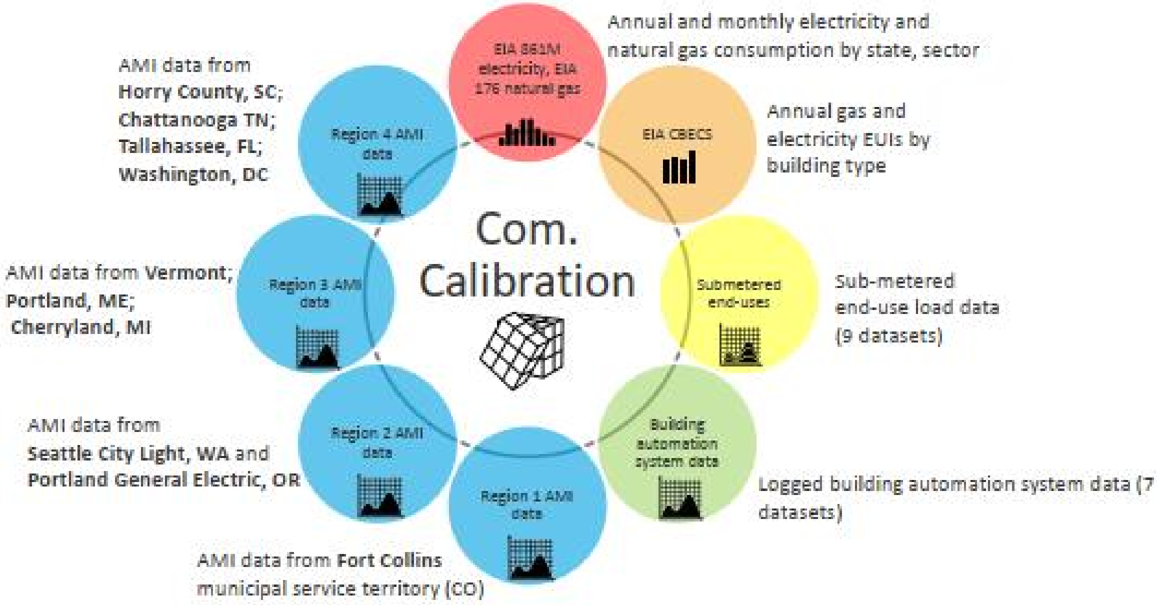


*Figure 6 - Data sources for ComStock models calibration and validation [13]*

Output correction is also an important step to correct the output of the model by comparing it with empirical data sources. However, it was not possible to apply this step to ComStock due to uncertainties related to the available commercial empirical data. Instead, a mathematical correction model was derived to correct the output of ResStock using available empirical data.

## 2.2 Weather input files

Weather conditions have a significant impact on a building's energy demand, as they can greatly affect its cooling and heating needs. Accurate weather input parameters are therefore crucial for realistic building energy behavior modeling. To obtain these parameters, the project collected weather-related data from nearly 1,000 weather stations located across the United States, providing information on temperature, relative humidity, pressure, wind speed, and direction. Solar radiation data, on the other hand, were obtained from satellite measurements. The ComStock dataset includes two versions of EULP characterized by different weather data files: one using the actual meteorological year in 2018 (AMY) and the other adopting a typical meteorological year (TMY3).

## 2.3 Buildings metadata

The buildings analyzed in this study possess unique characteristics, such as geometry-related properties, including total floor area and orientation, which can influence the magnitude of heating and cooling loads, occupancy schedules, and occupant density. These factors, in turn, can impact the shape of energy load profiles. In addition, information on the fuel type, HVAC system, and average efficiency of each building modeled is also listed, as they can affect the energy profiles. In the Results and Discussion chapter, some of the main building characteristics will be presented for each case study to investigate potential correlations between these factors and the shape of energy load profiles. Complete tables containing all metadata available for each building are provided in APPENDIX A1.

# 3 Methodology

The analysis conducted in this study can be conceptually divided into two main parts. The first part involves aggregating thousands of buildings by category and climate zones, comparing them across different climates, and characterizing their HVAC systems, fuel usage, and average electrical and thermal energy consumption in one typical year, divided by end use. The second part involves examining the specific load profiles of individual buildings, which requires a large amount of data since each building has its own yearly thermal and electrical load profiles at a 15-minute resolution. To handle this large amount of data, MATLAB is used, as it allows for the management of numerous variables.

## 3.1 Climate zones investigated

The climate zone in which a building is located is crucial in predicting the energy demand for space heating and cooling that will be covered by HVAC system operation, and thus, the expected performance of a cogeneration system, as analyzed in this study. Each building in the dataset is assigned to one of the 18 climate zones according to ASHRAE/IECC 2004, and a map of the USA with the division of climate zones is provided in **Error! Reference source not found.**[19]. These zones are defined based on heating degree days, average temperatures, and precipitation regimes[20].

Classifying buildings based on climate zones rather than their location in a specific state or city allows for an energy analysis that is independent of the geographical location of the building. This is particularly important in large countries where weather conditions can vary significantly within a single region, leading to biases in energy analysis. It also enables the extension of this study to other parts of the world with similar climatic conditions, as long as other relevant parameters are considered. Climate conditions alone, at the same building type, are not the only parameters that determine the load profiles and final energy consumption. Other factors such as occupant behavior and building thermophysical characteristics should also be considered.

A comprehensive list of ASHRAE climate zones in the USA is available in APPENDIX A1. It includes a description of the criteria used to define each climate zone, such as precipitation patterns, average temperatures, and heating degrees days.

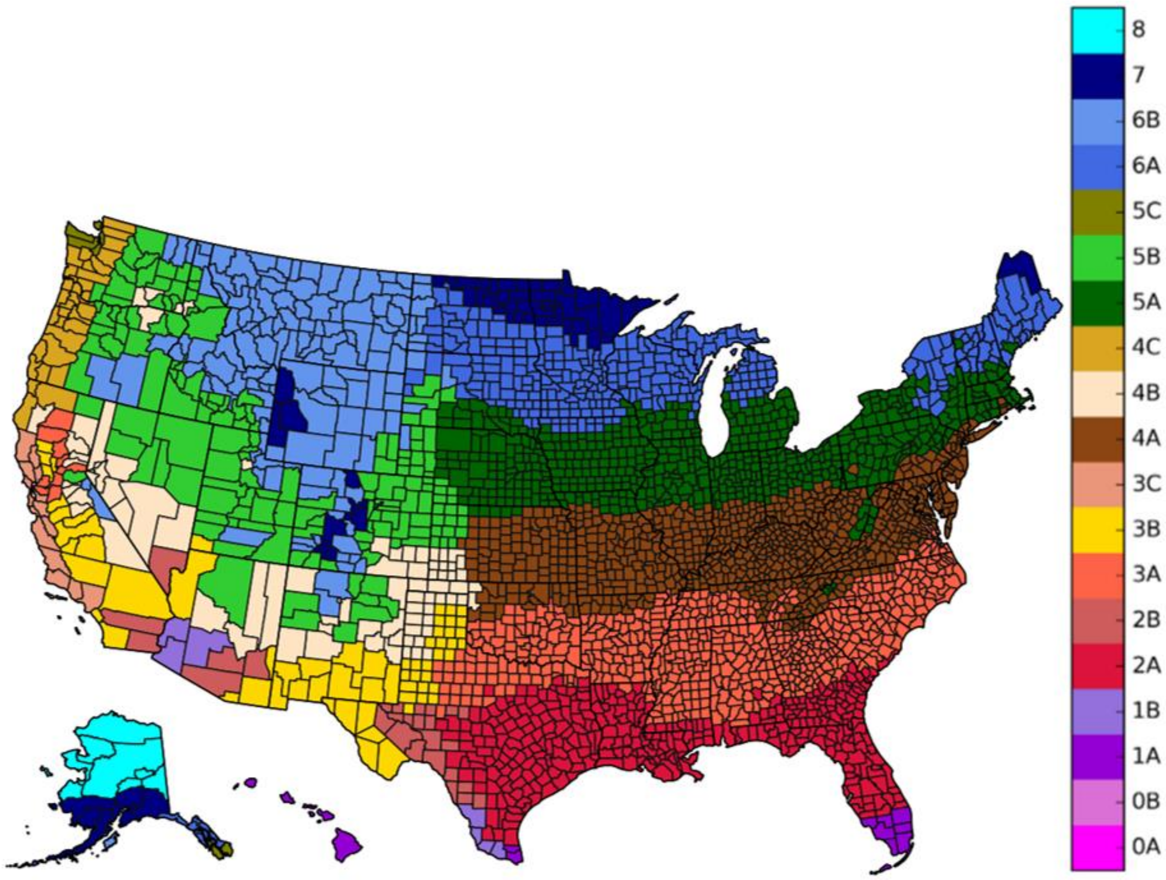


*Figure 7 - USA climate zones according to ASHRAE [21]*

The choice of which climate zones to investigate in this study is based on several considerations found in literature on similar studies and summarized in the following paragraph. These considerations highlight in which climate zones commercial buildings are generally more compatible with an SOFC-based cogeneration system or, conversely, show poor compatibility. Additionally, the total number of buildings in the dataset per each climate zone was also taken into account as some climates had a low number of buildings, which could impact the statistical significance of the results. TMY3 weather modeled buildings are chosen to reflect median weather conditions in a given place over a period of 30 years[22], as they would be more representative than a single year for a long-term analysis projected into future years.

E.J. Naimaster et al [7] conducted a techno-economic analysis of a SOFC-CHP system at different sizes, comparing the same modeled building type (a medium office) located in 3 very different climate zones 1A, 3A, 6A, Miami, Charlotte, and Minneapolis. The study concluded that installing this energy system in a medium office in California in not economically sustainable in terms of annual utility cost due to low thermal energy demand in winter, resulting in a drop in the cogeneration efficiency.

It is crucial to consider the matching of the electric and thermal demand of the building when designing an SOFC-CHP system. The study mentioned above suggests excluding buildings with low heating demand and looking at the ratio of the building's electrical load to thermal load (E/T), also known as its inverse thermal to electric ratio (TER). Matching the building's E/T ratio as closely as possible with that of the SOFC-CHP system is important to ensure that the energy supplied by the SOFC meets the electrical and thermal energy demand of the building as closely as possible.

The following considerations were taken into account when choosing which climate zones to analyze:

- Climate zone 1 was excluded as it is too hot to benefit from thermal energy co-produced by a cogeneration system. Additionally, it represents a very small portion of the USA's territory (Figure 7) and is not present in the European climate(Figure 8),
- Climate zone 2 has a large number of buildings (Table 1) but is still characterized by too high temperatures during the year.
- Buildings in climate zones from 6B going to colder climates, on the other hand, would have a high demand for thermal energy, but the number of buildings in these climates represented in the dataset is too small compared to other climates, as seen in Table 1.

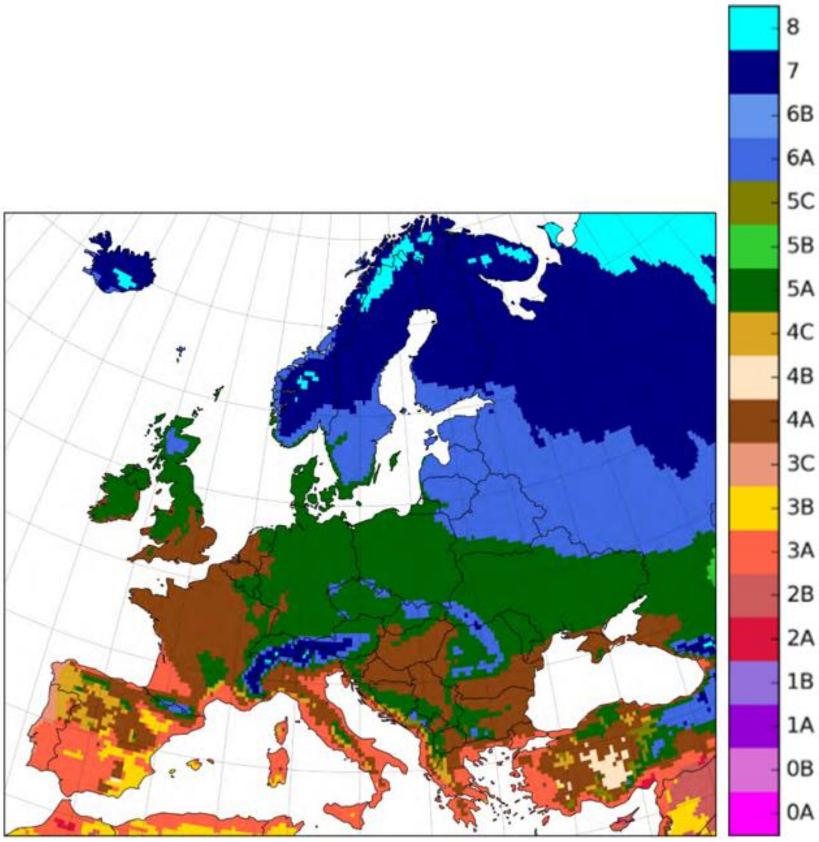


*Figure 8 - Europe climate zones according to ASHRAE[21]*

| Climate zone | 1A | 2A | 2B | 3A | 3B | 3C | 4A | 4B | 4C |
|---|---|---|---|---|---|---|---|---|---|
| **Buildings [%]** | 1.75 | 11.94 | 1.65 | 13.84 | 10.06 | 2.87 | 20.47 | 0.74 | 2.83 |
| **Climate zone** | **5A** | **5B** | **6A** | **6B** | **7** | **7A** | **7B** | **8** | |
| **Buildings [%]** | 22.97 | 4.15 | 5.29 | 0.70 | 0.13 | 0.52 | 0.06 | 0.02 | |

*Table 1 - Individual buildings count in ComStock dataset, author own elaboration from [13]*

Due to all the considerations mentioned earlier, this work only focuses on buildings located in four different climate zones, as listed in Table 2.

| IECC Climate Zone | IECC Moisture Regime | Type | Representative USA city | Representative European city |
|---|---|---|---|---|
| **3** | A | Warm, humid | Atlanta, GA | Rome, IT |
| **4** | A | Mixed, humid | Baltimore, MD | Turin, IT |
| **5** | A | Cold, humid | Chicago, IL | Berlin, DE |
| **6** | A | Cold, humid | Minneapolis, MN | Stockholm, SE |

*Table 2 - ASHRAE/IECC Climate zones analyzed, representative cities from[23],[21]*

## 3.2 Commercial buildings categories

Once the set of four climate zones to investigate has been selected, the next step is to determine which types of commercial buildings to analyze. The dataset includes 14 of the most common types of commercial buildings, as shown in Table 3.

| **1** | **Full-Service Restaurant** |
|---|---|
| **2** | Hospital |
| **3** | Large Hotel |
| **4** | Large Office |
| **5** | Medium Office |
| **6** | Outpatient |
| **7** | Primary School |
| **8** | Quick Service Restaurant |
| **9** | Retail Standalone |
| **10** | Retail Strip mall |
| **11** | Secondary School |
| **12** | Small Hotel |
| **13** | Small Office |
| **14** | Warehouse |

*Table 3 - Commercial building types in Comstock dataset, author own elaboration from* [13]

It is essential to consider the electrical baseload stability of buildings when evaluating the feasibility of implementing an SOFC-CHP system. Hotels and hospitals are two building types present in the dataset characterized by a relatively stable electrical baseload throughout the year, regardless of their climate or size, due to their continuous operation without any days of closure. This stability is crucial because SOFCs are unable to follow load variations and are susceptible to thermal cycles that can degrade the cell and shorten its lifespan.

Hospitals are known to consume a significant portion of the total energy used in the utility building sector, with studies showing they consume about 6% of the total energy [1], [2].

In one study comparing various distributed generation systems, a possible E/T value of 1.2 for a HTFC-CHP system was suggested for California, though this value depends on the specific technical data and operating conditions of the actual SOFC. The study authors also noted that hospitals are well-suited for CCHP technologies, even if only DHW demand is met by the technology, due to their E/T ratio between 0.9 and 1.69, coincident electrical and thermal demand, and peak loads not far from average loads.

Similarly, Yingjun Ruan et al. [24] found that hotels and hospitals are well-suited for combined heat and power technologies due to stable thermal load demands and a favorable heat-to-power ratio. Hotels in particular have coincident and flat electric and thermal loads, making them the most compatible with available DG technologies and an attractive target for CHP applications.

Therefore, in this work, the two categories of buildings investigated are hospitals and hotels located in the four previously selected climate zones.

### 3.2.1 Selection of buildings powered by natural gas

Initially, only buildings powered by HVAC systems fueled by natural gas are selected, while full electric buildings are excluded. This is because in full electric buildings, it would not be possible to recover thermal energy from SOFC for space heating. By selecting only buildings with natural gas or other fossil fuel HVAC systems, the E/T matching between SOFC and the building could be improved.

During the preliminary phase of aggregate building characterization, extensive investigations are conducted to determine the most installed HVAC systems and the fuels used to power them. This is done to determine their share in the USA market, as the dataset used has statistical significance for the characterization of building stock at an aggregate level. This exploration covers all climate zones in the dataset and all fuel types, in order to obtain a comprehensive understanding of the building stock's characteristics.

## 3.3 Energy characterization of building categories in different climate zones

During this phase of the analysis, the annual average electrical and thermal energy consumption of hospitals and hotels in each of the four selected climate zones is determined by end use. The comparison of buildings across different climate zones begins with identifying the most commonly used HVAC system type for each category of building within each climate zone. The aggregate specific electrical and thermal energy consumption is then compared with a focus on exploring the main components that constitute the majority of the energy consumption and their variability across different climates.

The characterization is carried out separately for hospitals and hotels, and the results for the two categories of buildings are ultimately compared. To eliminate the dependence on building surfaces and enable accurate comparison between buildings of different sizes, specific yearly energy values obtained by dividing energy consumption by floor area are used for comparison. Mean values and their standard deviations are calculated to characterize different clusters of numerous buildings that belong to different climatic zones. The standard deviation is calculated using the mathematical formulation provided in equation(Eq. 5 ).

$$\sigma_X = \sqrt{\frac{\sum_{i=1}^{N}(x_i - \overline{X})^2}{N}} \qquad (Eq.\ 5)$$

Where $x_i$ are the specific energy consumption values of the i-th individual building, $\bar{X}$ is the mean value of that value for the aggregated group of building considered, and $N$ is the number of buildings considered.

For each climate zone, the mean value of each end use is calculated, and the end uses with the highest impact on electricity consumption are selected. These selected end uses are then divided by the total electricity mean value to obtain an order of magnitude for each end use. Less impactful end uses are grouped in miscellaneous (Misc) including exterior lighting, heat recovery, heat rejection, electrical heating, pumping water systems, and refrigerators, also exploring their variability for the same climate and different building type and for the same building type in different climates. Electricity and thermal energy divided by end uses are compared, and their variability for the same building category across different climates is analyzed. Differences between hospitals and hotels are determined to identify the predominant end uses, with a focus on identifying the end uses of electrical and thermal energy that have the most impact on the total values and their relationship with the climate in which buildings are located. Finally, average E/T ratios are calculated, along with the minimum, maximum, and average electrical and thermal specific loads.

### 3.4 Selection of representative buildings for analysis

This chapter details the procedure for selecting individual buildings for load profile analysis and subsequent techno-economic analysis. Specific buildings with their characteristics and yearly load profiles are extracted for selected categories, and their specific hourly profiles are compared to evaluate the presence of a base load. Estimating their E/T ratio allows for the identification of which building category and climate zone could be more feasible for the installation of a SOFC-based CHP system. These buildings are then subject to a techno-economic analysis.

In order to ensure that the selected buildings are representative of their respective climate zones, the most common HVAC system fueled by natural gas for each building category in each climate zone is identified. Buildings equipped with this HVAC system and with annual electrical and thermal energy consumption per unit area closest to the mean specific energy values for their respective category in that particular climate zone are chosen. This guarantees that the selected buildings are representative of the larger population of buildings in that climate zone and can provide a more accurate picture of energy consumption patterns in that region.

In MATLAB, the Euclidian distance(Eq. 6 ) is calculated for each modeled building by comparing its actual yearly energy values to the mean values characterizing the specific category in a particular climate. This calculation is performed for every building of a fixed category and fixed climate zone. Then, for each category and climate, the building with the minimum distance is selected.

$$distance_i = \sqrt{(el_i - el_{avg})^2 + (th_i - th_{avg})^2} \quad \text{(Eq. 6 )}$$

The values of $el_i$ and $th_i$ represent the annual electricity and thermal energy consumption per unit area of the i-th building, respectively. The values $el_{avg}$ and $th_{avg}$ represents the mean values of electricity and thermal energy consumption per unit area for a category of building in a specific climate zone.

### 3.4.1 Energy characterizations of selected building models

The energy characteristics of the selected building models are analyzed in this phase. The end use load profiles of eight buildings, comprising one hospital and one hotel for each of the four climate zones, are compared. As the algorithm used to select the most representative building in terms of annual specific electricity and thermal energy consumption does not allow for a fixed surface area for all buildings, the comparisons between profiles are still based on the unit of area. This is because imposing this additional constraint would result in the extraction of building models with consumption values that are further away from the specific electricity and thermal consumption patterns characterizing each building category in each climate zone.

Initially, the hourly electrical and thermal profiles of buildings belonging to the same category are compared with an annual resolution to analyze the main patterns that occur across the four climate zones. Subsequently, the hourly electrical and thermal profiles of buildings belonging to the same category are compared on a daily basis for different climate zones. Four typical days corresponding to the two solstices and the two equinoxes of 2018 were compared, as the climatic data used to create the building models referred to the same year. It should be noted that Table 4 also includes the day of the week, as the buildings' schedules in terms of weekly opening hours are important when comparing the typical days. Even though hotels and especially hospitals do not have specific opening periods, their load profiles were obtained by taking into account different opening and closing times during weekdays and weekends.

| Typical day | Date | Day |
|---|---|---|
| Spring equinox | March 20th | Tuesday |
| Summer solstice | June 21th | Thursday |
| Autumn equinox | September 23 | Sunday |
| Winter solstice | December 21 | Friday |

*Table 4 -Typical days selected*

After comparing both annual and daily load profiles of the same building in different climatic zones, similar comparisons are carried out between hospitals and hotels belonging to the same climatic zones, identifying patterns that characterize the building category in the specific climatic zone.

### 3.5 Techno-economic analysis

A techno-economic analysis is conducted on the selected representative buildings from each climate zone. Technical data of the SOFC stack, such as electrical and thermal efficiency and nominal power, as well as economic data like investment cost and stack lifetime are considered as input data for the analysis. After defining all input data, the analysis proceeds to calculate the levelized cost of electricity (LCOE) for each building and climate zone. The analysis is first conducted by identifying the SOFC stack as the control volume, and subsequently including the specific building in which it is installed. Simultaneously with the LCOE calculations using the two control volume scenarios described above, the electrical energy coverage achieved by the SOFC during each year of the project's lifespan for each building, the thermal energy coverage, and the increase in natural gas purchased from the grid to feed the SOFC are also determined. The subsequent subchapters introduce the technical and economic input parameters for conducting these analyses, as well as the fundamental equations for defining the performance of the SOFC and for calculating the LCOE values with reference to the two different control volumes.

### 3.5.1 Input data

Technical and economic parameter of the SOFC and are listed in Table 5, including the SOFC investment cost $C_{INV,SOFC}$, fixed operating costs $C_{OPEX,fix}$, stack replacement cost $C_{repl}$, stack lifetime, as well as the electrical and thermal efficiency of the SOFC, assumed to be constant throughout the project lifetime, neglecting the performance degradation component that is encountered in reality.

Other fundamental parameters for economic analysis in general, and specifically for calculating the LCOE, include the discount rate "d", commissioning, and installation cost $C_{c\&i}$ and project lifetime "n”.

| Parameter | Value | Description |
|---|---|---|
| $C_{INV,SOFC}$ | 11,980 €/kW | Investment cost |
| $C_{OPEX,fix}$ | 1%/y of investment cost | |
| $C_{repl}$ | 45% of investment cost | Replacement cost |
| **Stack life** | 5 years | SOFC stack lifetime |
| **Electrical efficiency** | 49.1 | - |
| **Thermal efficiency** | 31 | - |
| **d** | 4% | Discount rate |
| $C_{c\&i}$ | 10% of investment cost | Commissioning & installation cost |
| **n** | 20yr | Project lifetime |

*Table 5 -Techno-economic input data [25], [26]*

### 3.5.2 Energy prices

Electricity and natural gas energy prices with all taxes included for commercial uses are obtained from the Eurostat database [27][28], with reference to Italy. The prices of natural gas and especially electricity fluctuate hourly, but for the analysis in this study, their average annual values were considered. The prices are divided into consumption bands in this phase of the analysis, six bands for electricity and five bands for natural gas, as listed in Table 6. Therefore, the results will certainly be influenced by the size of the individual building from which the annual purchase volumes are derived. Both gas and electricity prices were taken with reference to 2021, after the COVID-19 pandemic but before the war, to avoid any influences on the analysis due to geopolitical reasons.

| Natural gas price ranges [GJ] | Natural gas price [€/kWh] | Electricity price ranges [MWh] | Electricity price [€/kWh] |
|---|---|---|---|
| **<1,000** | 0.0868 | <20 | 0.3186 |
| **1,000<x<10,000** | 0.0615 | 20<x<500 | 0.246 |
| **10,000<x< 100,000** | 0.0432 | 500<x<2,000 | 0.2142 |
| **100,000<x< 1,000,000** | 0.0418 | 2,000<x<2,0000 | 0.1801 |
| **1,000,000<x<4,000,000** | 0.0522 | 20,000<x<70,000 | 0.1622 |
| **> 4,000,000** | 0.0468 | 70,000<x<150,000 | 0.1698 |
| | | >150,000 | 0.1675 |

*Table 6 - Prices of natural gas and electricity purchase for commercial buildings divided by consumption ranges, all taxes included*

### 3.5.3 SOFC sizing and modeling

The SOFCs installed in each analyzed building are designed to cover their respective electrical baseload. The baseload is calculated by determining the minimum value of hourly electrical power required by each building during a typical year. This ensures continuous operation of the SOFC throughout the year, preventing thermal cycles that would reduce its lifetime.

The equations implemented in MATLAB for the calculation of the hourly natural gas flow rate (Eq. 7 ) measured in $Sm^3/h$, the consequent annual natural gas consumption to fuel the SOFC(Eq. 8 ), measured in $Sm^3$ and the continuous thermal power output from the SOFC stack (Eq. 9 ), measured in kW, are listed below.

$$\dot{V}_{NG}=\frac{P_{el}}{\eta_{el}\cdot LHV_{NG}} \qquad \text{(Eq. 7 )}$$

$$NG_{SOFC}=\dot{V}_{NG}\cdot h \qquad \text{(Eq. 8 )}$$

$$P_{th,SOFC}=P_{el,SOFC}\cdot\frac{\eta_{th}}{\eta_{el}} \qquad \text{(Eq. 9 )}$$

LHV is the lower heating value associated with natural gas, a value of a 9.27 kWh/Sm$^3$ is adopted [25]..

| SOFC technical data | |
|---|---|
| **Electrical efficiency** | 49.1 |
| **Thermal efficiency** | 31 |
| **E/T** | 1.58 |

*Table 7 - SOFC techno-economic data[26]*

### 3.5.4 Levelized Cost of Energy (LCOE) and energy coverage analysis

The levelized cost of electricity (LCOE) is a key result of techno-economic analysis that allows for the comparison of the economic feasibility of different energy systems based on the unit price of electrical energy produced, measured in [€/kWh].

The LCOE is calculated by discounting the costs and revenues of the energy system over its entire lifetime, from the first year of installation to the end of its operational life. The LCOE is calculated in two different ways, by considering either only the SOFC as the control volume or the entire system composed of the building and the SOFC. This subsection presents the calculation of the LCOE produced by the SOFC using both methods.

In addition to the LCOE calculated using the two methods described above, the performance of the SOFC in terms of energy coupling with the building will also be calculated. This includes determining the amount of electricity and natural gas used for heating and domestic hot water production that each building is able to save annually thanks to the presence of the SOFC-based cogeneration system, as well as the increase in the percentage of gas purchased from the grid to fuel the SOFC stack compared to the base case. Finally, the LCOE with the SOFC and building as the control volume will be recalculated assuming electricity and gas prices that are no longer dependent on the annual consumption volumes of the building and considering a possible future scenario of technological evolution with lower investment costs and longer stack lifetimes. The results will be discussed in the final chapter.

#### *3.5.4.1 LCOE SOFC control volume*

The calculation of the LCOE [€/kWh] that considers only the control volume containing the SOFC is carried out by comparing the net present cost $C_{NPC}$ [€] with the total electrical energy produced by the SOFC, discounted through the discount rate over the project lifetime, as shown in (Eq. 10 )

$$LCOE=\frac{C_{NPC}}{\sum_{j=1}^{n} E_{el,SOFC,j}\cdot(1+d)^{-j}} \quad \text{(Eq. 10 )}$$

$$C_{NPC,CAPEX}=C_{INV,SOFC}+C_{c\&i} \quad \text{(Eq. 11 )}$$

$$C_{GRID,buy,NG,SOFC}=\sum_{t=1}^{8760}\left(P_{GRID,buy,NG}(t)\cdot c_{GRID,buy,NG}(t)\right) \quad \text{(Eq. 12 )}$$

The net present cost is defined in (Eq. 13 )where $C_{NPC,CAPEX}$ is the investment cost for the entire system discounted over the project lifetime and is the sum of the SOFC investment cost and commission and installing cost $C_{c\&i}$,(Eq. 11 ) while $C_{NPC,OPEX}$ (Eq. 14 ) is the sum from year 0 of system installation to the last year of the project's life of $C_{OPEX,j}$ which in this case is the annual cost of system maintenance, $C_{GRID,buy,NG,SOFC,j}$ which is the annual cost of gas purchased from the grid to fuel the SOFC(Eq. 12 ), and finally $C_{repl}$(if j=stack life) which is the stack replacement cost that appears when the calculation year coincides with the end of the stack's life..

$$C_{NPC}=C_{NPC,CAPEX}+C_{NPC,OPEX} \quad \text{(Eq. 13 )}$$

$$C_{NPC,OPEX}=\sum_{j=1}^{n}\frac{C_{OPEX,j}+C_{GRID,buy,NG,SOFC,j}+C_{repl}(\text{if } j=\text{stack life})}{(1+d)^{j}} \quad \text{(Eq. 14 )}$$

### 3.5.4.2 LCOE SOFC and building control volume

LCOE considering as control volume of the technoeconomic analyze the entire system composed by the SOFC and the building(Eq. 15 ), and differs in the definition of the OPEX term, that contains same element as before plus the $C_{GRID,buy,el}$ that is the electricity needed to the building bought from the grid because not covered by the cell operation and $C_{GRID,buy,NG,j}$ that now contain also the expenditure for natural gas bought form the grid to cover the remaining building thermal demand buying natural gas from the grid.

Last different element consists of the denominator $E_{el}$ that is no more only the total discounted electrical energy produced by the SOFC in the project lifetime but the total discounted electrical building consumption in the project lifetime.

$$LCOE=\frac{C_{NPC}}{\sum_{j=1}^{n}\left(E_{SOFC,prod,el,j}+E_{GRID,buy,el,j}\right)\cdot(1+d)^{-j}} \quad \text{(Eq. 15 )}$$

$$C_{NPC}=C_{NPC,CAPEX}+C_{NPC,OPEX}-C_{NPC,salv}+C_{repl} \quad \text{(Eq. 16 )}$$

$$C_{NPC,CAPEX}=C_{INV,SOFC}+C_{c\&i} \quad \text{(Eq. 17 )}$$

$$C_{NPC,OPEX}=\sum_{j=1}^{n}\frac{C_{OPEX,j}+C_{GRID,buy,el,j}+C_{GRID,buy,TOT,j}+C_{repl,}^{*}}{(1+d)^{j}} \quad \text{(Eq. 18 )}$$

$$C_{GRID,buy,EL}=\sum_{t=1}^{8760}\left(P_{GRID,buy,EL}(t)\cdot c_{GRID,buy,EL}(t)\right) \quad \text{(Eq. 19 )}$$

$P_{GRID,buy,EL}(t)$ is calculated as the sum of the hourly difference during the year between the building electrical load and SOFC nominal electrical power.

$$C_{GRID,buy,TOT,j}=C_{GRID,buy,NG,SOFC}+C_{GRID,buy,NG,residual} \quad \text{(Eq. 20 )}$$

$$C_{GRID,buy,NG,SOFC}=\sum_{t=1}^{8760}\left(P_{GRID,buy,NG,SOFC}(t)\cdot c_{GRID,buy,NG}(t)\right) \quad \text{(Eq. 21 )}$$

$$C_{GRID,buy,NG,residual}=\sum_{t=1}^{8760}\left(P_{GRID,buy,NG,residual}(t)\cdot c_{GRID,buy,NG}(t)\right) \quad \text{(Eq. 22 )}$$

$C_{GRID,buy,NG,residual}$ is calculated as the sum of the hourly difference during the year between the building thermal load and SOFC nominal electrical power.

### *3.5.4.3 LCOE future scenario*

The final analysis of this Master's thesis involves recalculating new LCOE values for the four hospitals and four hotels, assuming a future scenario in which the improvement of SOFC technology and an increase in sales volumes in the market lead to a reduction in the investment cost of the SOFC system by almost a quarter compared to the current value and a doubling of the stack's lifetime, as reported in Table 8, not considering, as a precautionary measure, any potential increase in efficiency.

| Parameter | Current | Target |
|---|---|---|
| Investment cost SOFC system | 11,980 €/kW | 3340 €/kW |
| SOFC stack lifetime | 5 yr | 10 yr |

*Table 8 - Future scenario tecnoeconomical parameter*

In addition, in this scenario, uniform electricity and natural gas purchase prices are adopted for all buildings (Table 9), calculated as the average of the values presented in Table 6, for both cost items. This is done to disassociate the greater economic convenience of the system from a favorable energy price structure for larger, more energy-intensive buildings, which would lead them to benefit from lower prices for both energy cost items compared to smaller buildings.

| Natural gas price [€/kWh] | Electricity price [€/kWh] |
|---|---|
| **0.0554** | **0.2083** |

*Table 9 - Average energy prices*

# 4 Results and discussions

## 4.1 Energy characterization of hospitals

The following subsections of this section present the results of the analyses conducted on hospitals. First, the hospital category is characterized in terms of the most used fuel for HVAC and the most widespread HVAC technology at an aggregate level. Then, energy end uses are investigated, and finally, the load profiles of modeled hospital buildings are shown and discussed.

### 4.1.1 Fuels and HVAC systems

Figure 9 displays the breakdown of the space heating fuel sources used in the hospital buildings across all climate zones. The proportion of hospitals with HVAC systems powered by electricity is comparable to those fueled by natural gas, although the percentage varies depending on the climate zone.

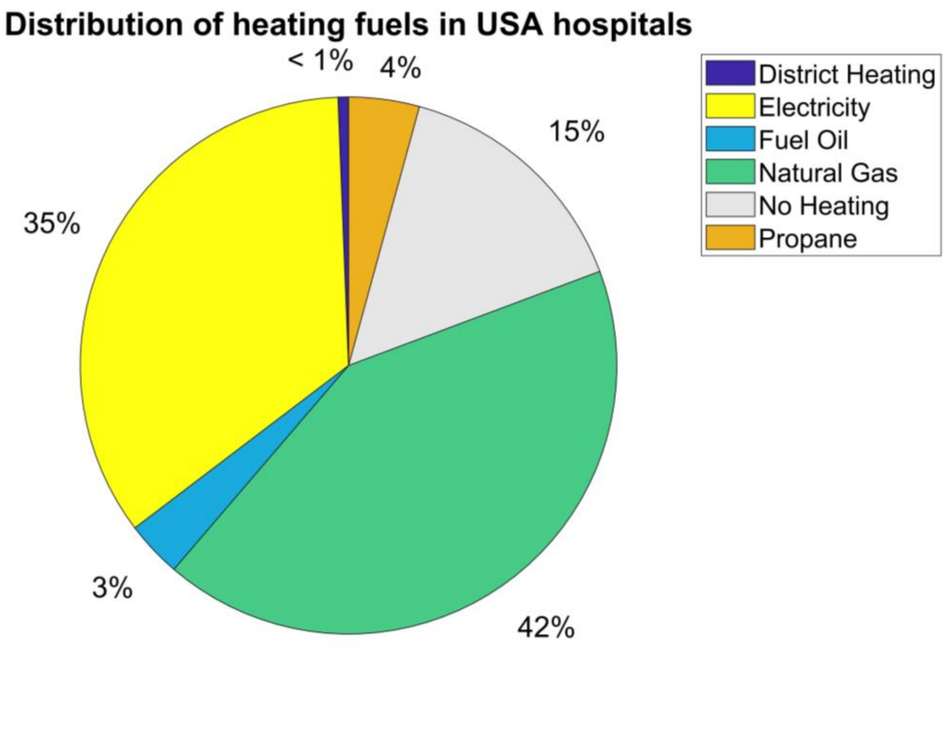


*Figure 9 - Distribution of heating fuels used in USA hospitals, author's own elaboration from [13]*

Table 10 lists the first five most common HVAC systems with their percentages on the total and a brief description.

The most common HVAC system in US hospitals is the packaged single zone heat pump (PSZ-HP), which is a fully electric HVAC system with a 34% share. However, its usage decreases in colder climates due to a reduced performance in heating mode at low temperatures.

| HVAC system | % |
|---|---|
| **PSZ-HP** | 33.96 |
| **VAV chiller with gas boiler reheat** | 16.42 |
| **PSZ-AC with no heat** | 14.53 |
| **VAV air-cooled chiller with gas boiler reheat** | 9.4 |
| **Fan coil air-cooled chiller with boiler** | 6.4 |

*Table 10 - Distribution of HVAC technologies in the USA hospital stock, author's own elaboration from* [13]

Across the four climates studied and considering only hospitals fueled by natural gas, the VAV chiller with gas boiler reheat is the most common HVAC system, with a share of 16.4% across the complete hospital stock in the dataset composed of all climates and all fuel types (Figure 10).

When considering hospitals in the four analyzed climates with natural gas-powered HVAC systems, this share increases to nearly 40%. This HVAC system remains the most prevalent even for each of the four climates, as shown in Figure 13, followed by the VAV air-cooled chiller with gas boiler reheat.

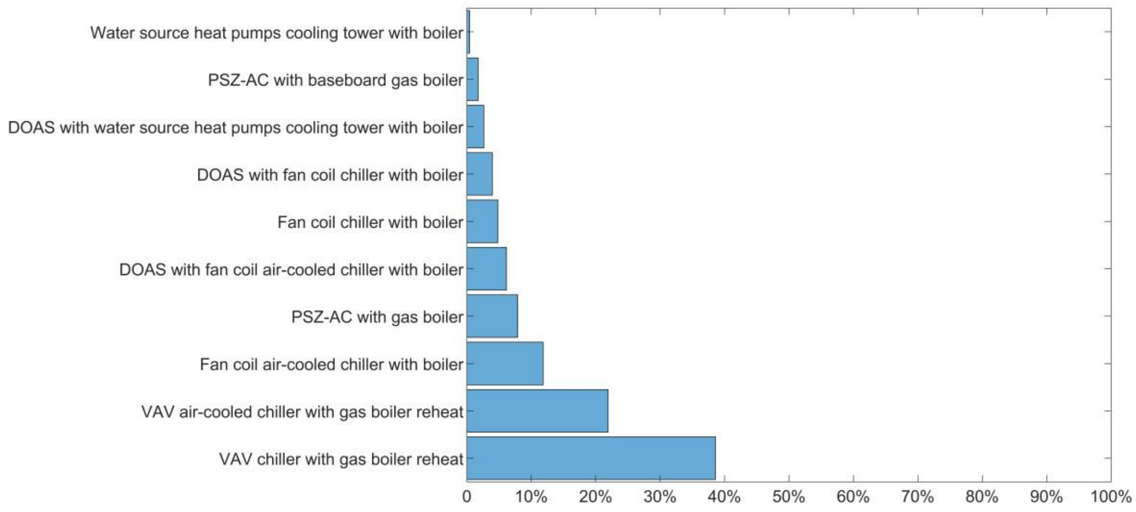


*Figure 10 - Natural gas HVAC systems in US hospitals, author's own elaboration from [11]*

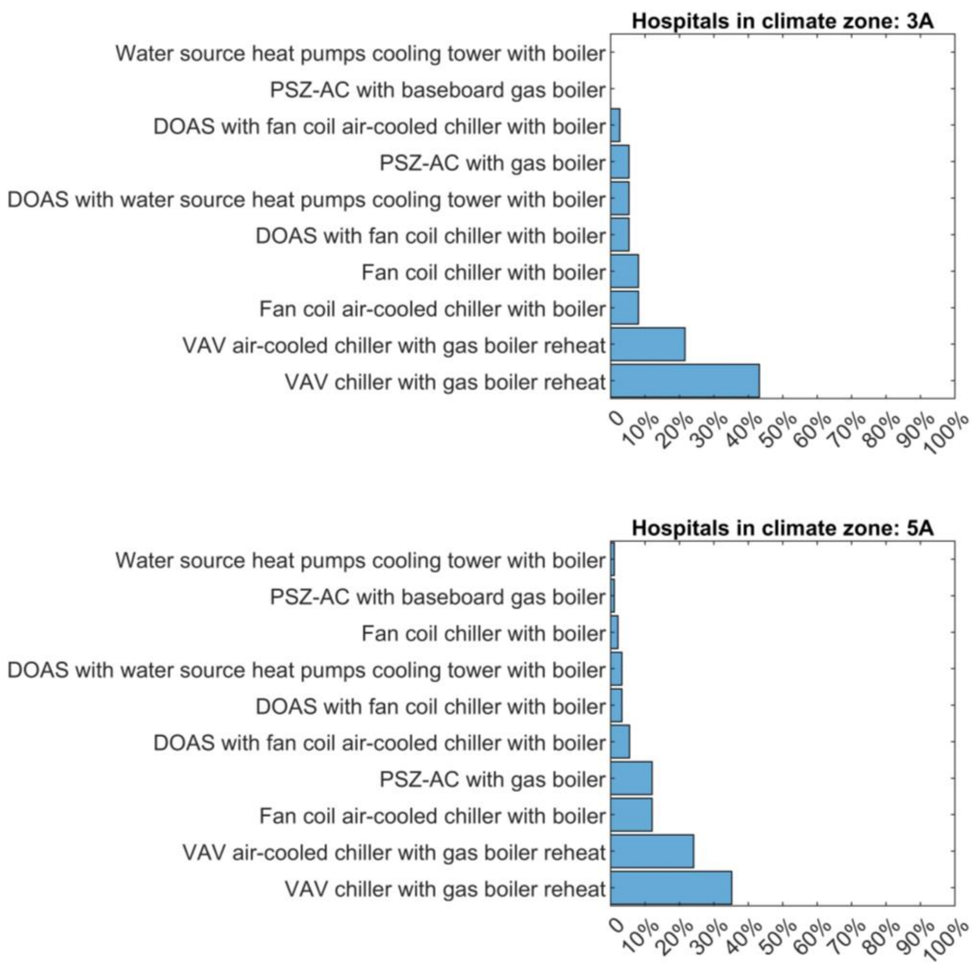


*Figure 11 - Natural gas HVAC systems in US hospitals by climate zones (3A – 5A), author's own elaboration from [11]*

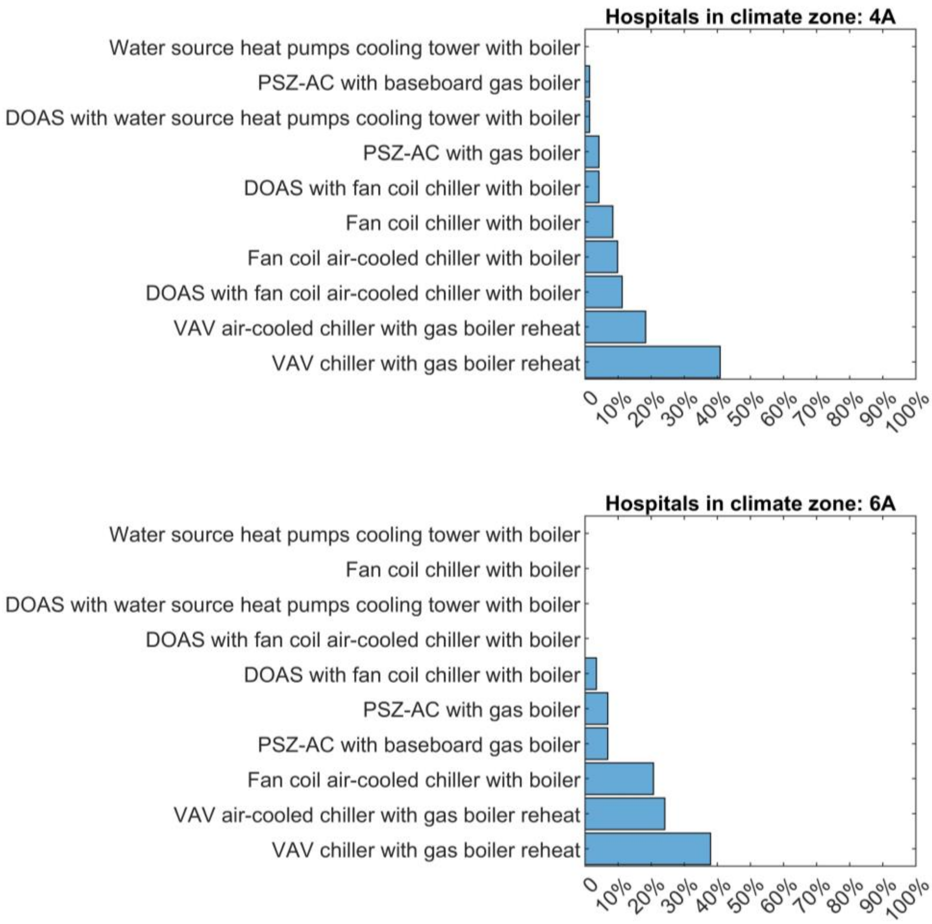


*Figure 12 - Natural gas HVAC systems in US hospitals by climate zones (4A – 6A), author's own elaboration from [11]*

### 4.1.2 Yearly electrical and thermal energy consumption: breakdown by end-use

It is observed that the total specific thermal energy consumed for space heating and hot water production increases from the hottest climate zone (3A) to the colder ones, as illustrated in Figure 13. On the other hand, the total specific electricity consumption follows an opposite trend, although this behavior is less noticeable.

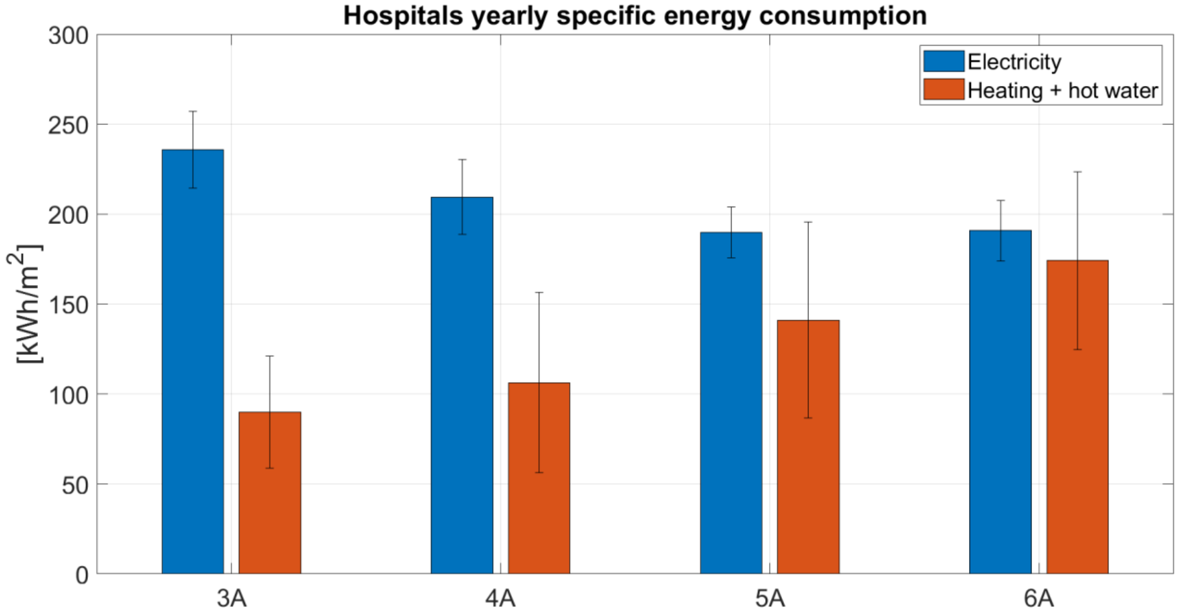


*Figure 13 - Comparing hospitals' specific energy consumption by climate zones*

The specific electricity consumption in hospitals has a relatively low standard deviation compared to thermal energy consumption. To identify the major contributors to the average electricity consumption per unit of area for each climate zone, a subset of the eleven different electricity end uses (APPENDIX A1),is considered in Figure 14. Figure 15 shows the same quantities with their average values, while in Figure 16 the minor contributors are shown.

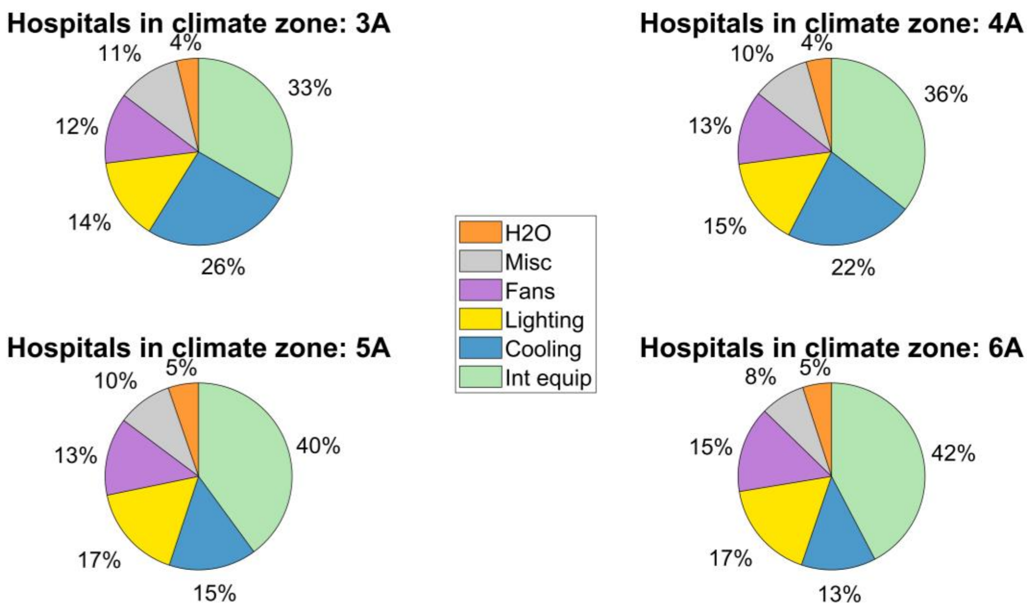


*Figure 14 - Composition of electricity end uses in hospitals*

Across all climate zones, the largest contributor to electricity consumption in hospitals is the "interior equipment," mainly consisting of medical machines, although its percentage varies. Although the standard deviation of interior equipment's electricity consumption varies slightly through different climates due to differences in installed technology, its average value remains almost constant, indicating no correlation with weather conditions, as expected.

The second most impactful end use on total electricity consumption is cooling energy, but only for the hot climate zone 3A and the warm climate zone 4A (Figure 14). In colder climate zones such as 5A and 6A, the fraction of cooling energy is overtaken by the fraction of energy for internal illumination. This trend is evident in Figure 15, which shows how the yearly cooling demand decreases progressively moving from hot to cold climates which shows that the yearly cooling demand decreases significantly from hot to cold climates. In fact, the average value of cooling energy consumption in the coldest climate zone, 6A, is less than half of the value in the hottest climate zone 3A.

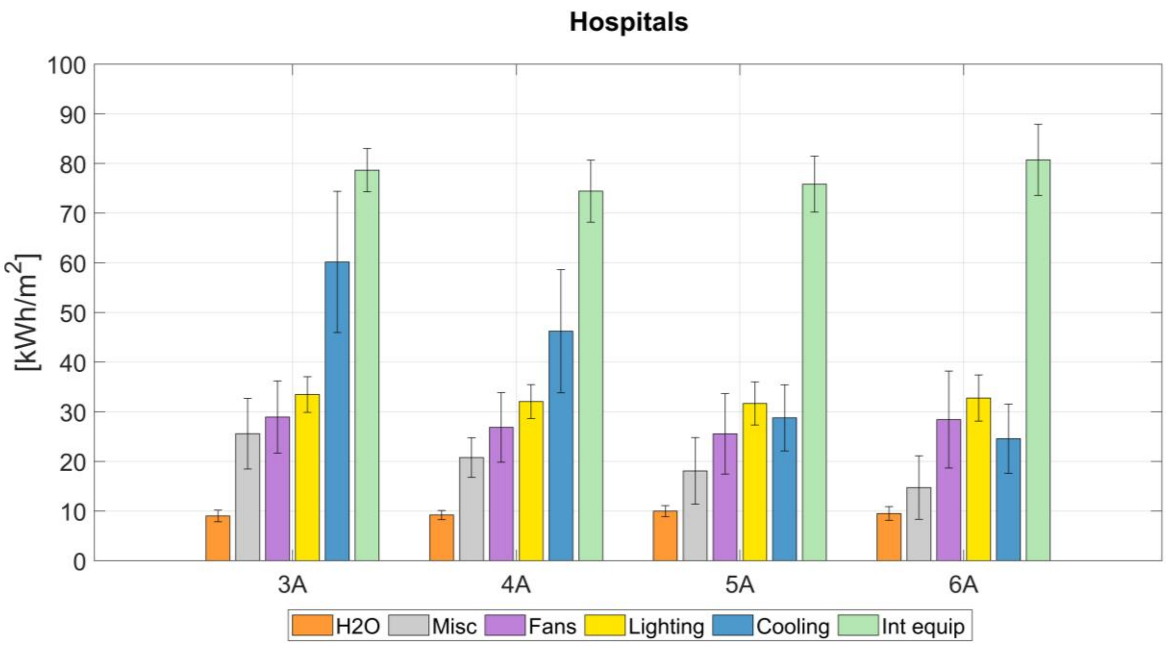


*Figure 15 - Electricity end use breakdown in hospitals by climate zones*

The average minor consumptions exhibit a slight decrease from hot to colder climates, both in terms of percentage and absolute values. Figure 18 illustrates the trend of the components that make up these minor consumptions, with the main end uses that cause this trend being the electricity consumed by water pumps, refrigerators, and heat rejection, all of which decrease from hot to cold climates.

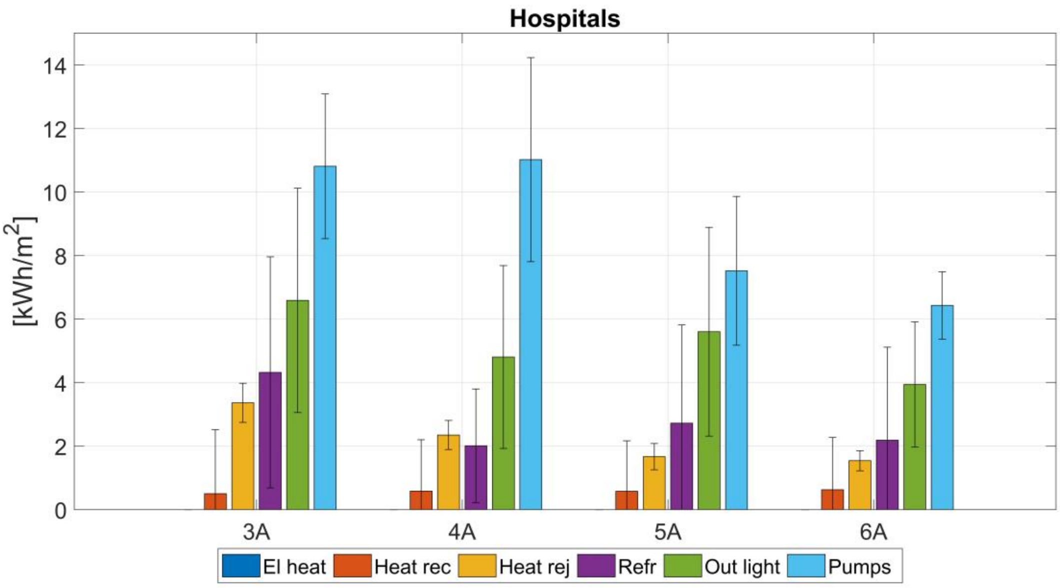


*Figure 16 - Minor electricity end uses consumption in hospitals*

Figure 17 shows the breakdown of thermal energy consumption by end uses for each climate zone. The contribution of thermal energy for hot water production to the total value decreases gradually going from hot to cold climates due to the increasing use of thermal energy for space heating purposes. However, it slightly increases in colder climates, not due to lower temperatures but more likely due to the longer duration of the winter season, which leads to an increased demand for hot water throughout the year. Thermal energy for space heating increases significantly, doubling its value from the hottest climate zone to the coldest one. However, its standard deviation is relatively high compared to the standard deviation associated with electricity consumption. This is because hospitals in each climate zone have different orientations, aspect ratios, and number of stories, which can impact their thermal energy needs.

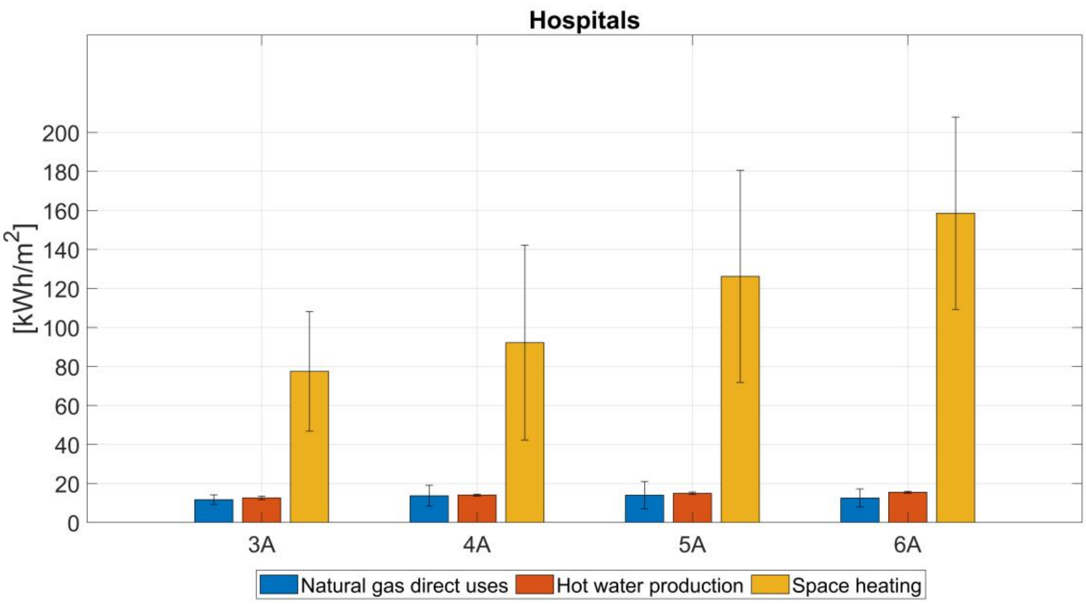


*Figure 17 - Thermal energy consumption in hospitals from natural gas-based end-use by climate zones*

### *4.1.3* Analysis of hourly load profiles and typical days

The main characteristics of the selected hospital buildings are summarized in Table 11.

The electric load profiles per unit of area of the four selected hospitals are presented in Figure 18. The electrical base loads per unit of area, which represent the minimum electricity consumption during non-cooling periods, are quite similar among all climates.

| Hospitals | | | | |
|---|---|---|---|---|
| **Climate zone** | Floor area $[m^2]$ | Rotation $[°]$ | Aspect ratio | Stories |
| **3A** | 6968 | 315 | 4 | 4 |
| **4A** | 13935 | 0 | 3 | 2 |
| **5A** | 6968 | 270 | 4 | 1 |
| **6A** | 69675 | 45 | 4 | 9 |

*Table 11 - Geometric properties of hospitals*

| Hospitals | | | | | | |
|---|---|---|---|---|---|---|
| Climat e zone | Electrical intensity $\left[\frac{kWh}{m^2\,y}\right]$ | Thermal intensity $\left[\frac{kWh}{m^2\,y}\right]$ | E/T | Average electrical Intensity climate $\left[\frac{kWh}{m^2\,y}\right]$ | Average thermal Intensity climate $\left[\frac{kWh}{m^2\,y}\right]$ | Avg E/T climate |
| **3A** | 253.04 | 93.08 | 2.72 | 235.82 | 90.03 | 2.62 |
| **4A** | 208.92 | 110.95 | 1.88 | 209.47 | 106.27 | 1.97 |
| **5A** | 188.15 | 143.59 | 1.31 | 189.89 | 141.13 | 1.34 |
| **6A** | 192.36 | 185.81 | 1.03 | 190.74 | 174.10 | 1.1 |

*Table 12 – Energy intensities of hospitals*

The base load during the summer season gradually decreases as the climate becomes colder, and so does the duration of the cooling season. Furthermore, the height of the maximum values of electricity consumed during summer also decreases when moving from hot to cold climates.

Regarding the shape of the profiles, the peaks in the electricity demand during the winter and fall season tend to flatten as the climate becomes colder (in zones 5A and 6A) due to the inactivity of HVAC in cooling mode. In contrast, in hot and warm zones (3A and 4A), cooling is sometimes needed even outside the cooling season.

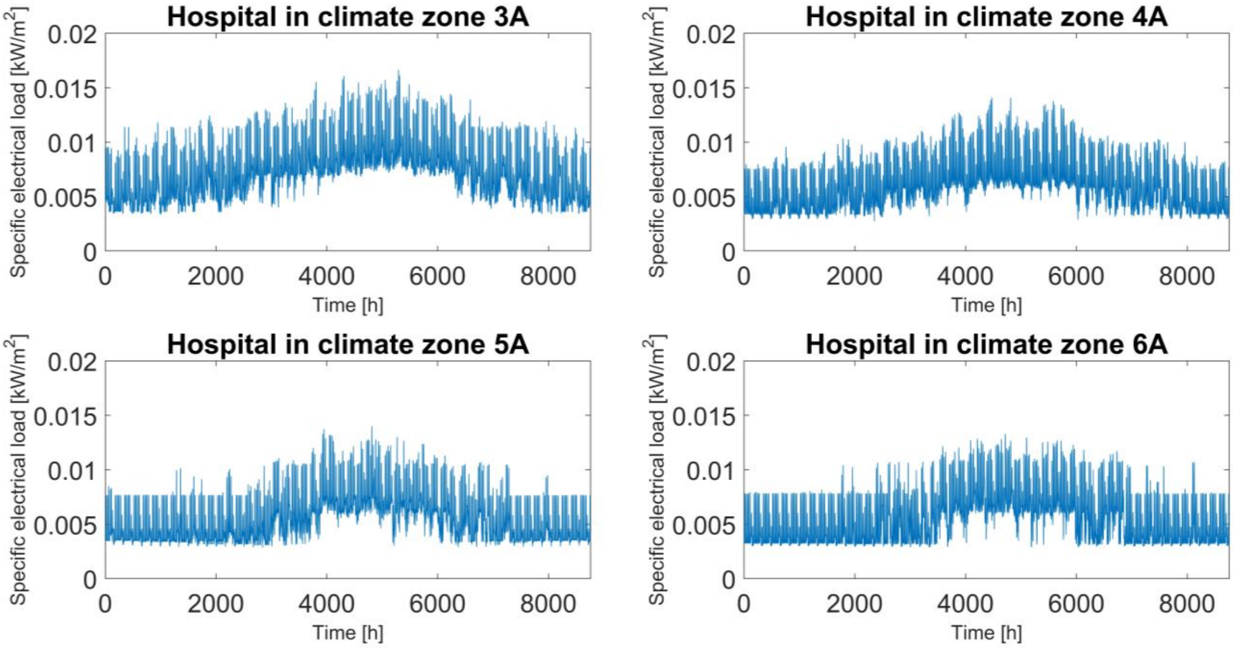


*Figure 18 - Hospitals: specific electrical load*

The thermal load profiles per unit of area of the selected hospitals are shown in Figure 19.

As expected, the thermal load increases as the climate becomes colder. The peak of the thermal load shifts towards the winter season, and the heating season's duration prolongs as the climate becomes colder. The shape of the thermal load profile exhibits sharp peaks during the winter season with a flatter profile during the rest of the year in all climates, but peaks become even more intense in colder climates.

In the hottest climate zone (3A) there is hardly any heating base load at the extremes of the graph, that correspond to winter season. The presence of a thermal base load commences from the 4A zone and becomes significant from 5A zone (first cold climate zone) moving towards colder climates. The heat energy peaks are the highest in the coldest climate zone (6A) and exceed ten times the base load.

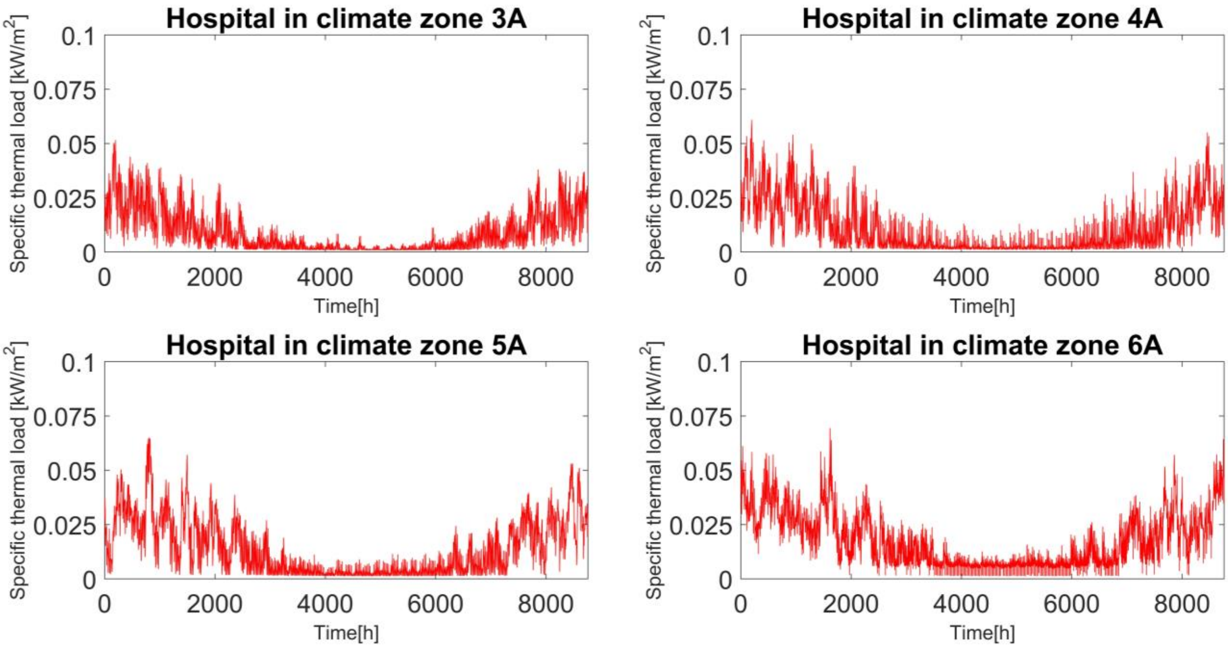


*Figure 19 - Hospitals specific thermal load profiles*

In Figure 20 hot water production thermal load profiles are compared because also hot water production is influenced by the climate. In terms of magnitude the profiles arise moving towards colder climates, while looking at their shape they all swing during the year with higher values in winter and a dip in summer. Moving towards colder climates they flatten and tend to be more uniform during the year.

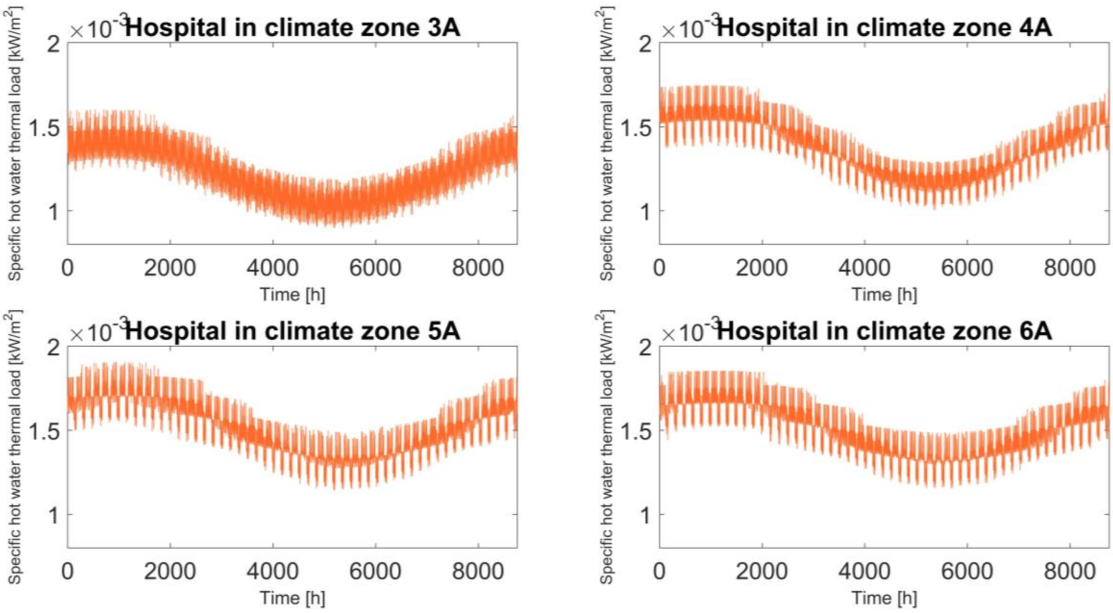


*Figure 20 - Hospitals specific thermal load profiles for hot water only*

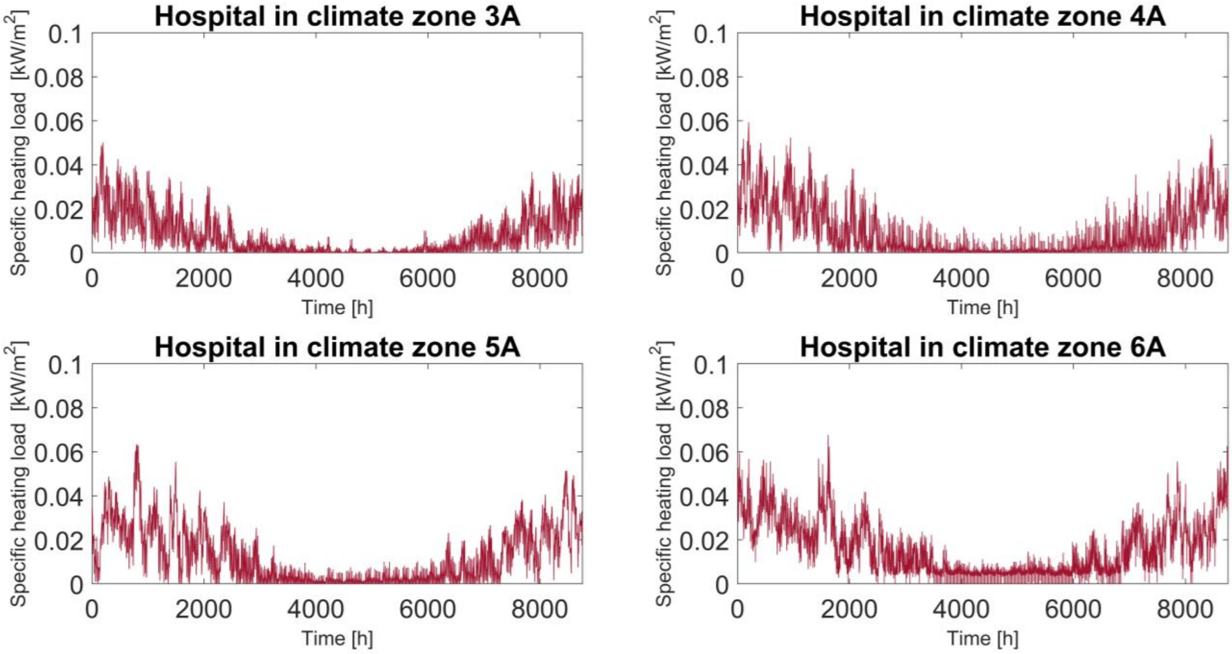


*Figure 21 - Hospitals specific thermal load profiles for heating only*

Figure 22 and Figure 23, show the yearly electrical and thermal load profiles, respectively, for the four hospitals located in the selected climate zones. The graphs depict the overlapping of the profiles to highlight the main differences in their base loads and peaks of demand. Analyzing the electrical demand in Figure 22, it can be observed that the hospital located in the coldest climate zone has the lowest base load per unit of area, even if the base loads of the four hospitals are very close to each other. On the other hand, the hospital located in the hottest climate zone shows the highest peaks of electrical demand throughout the year.

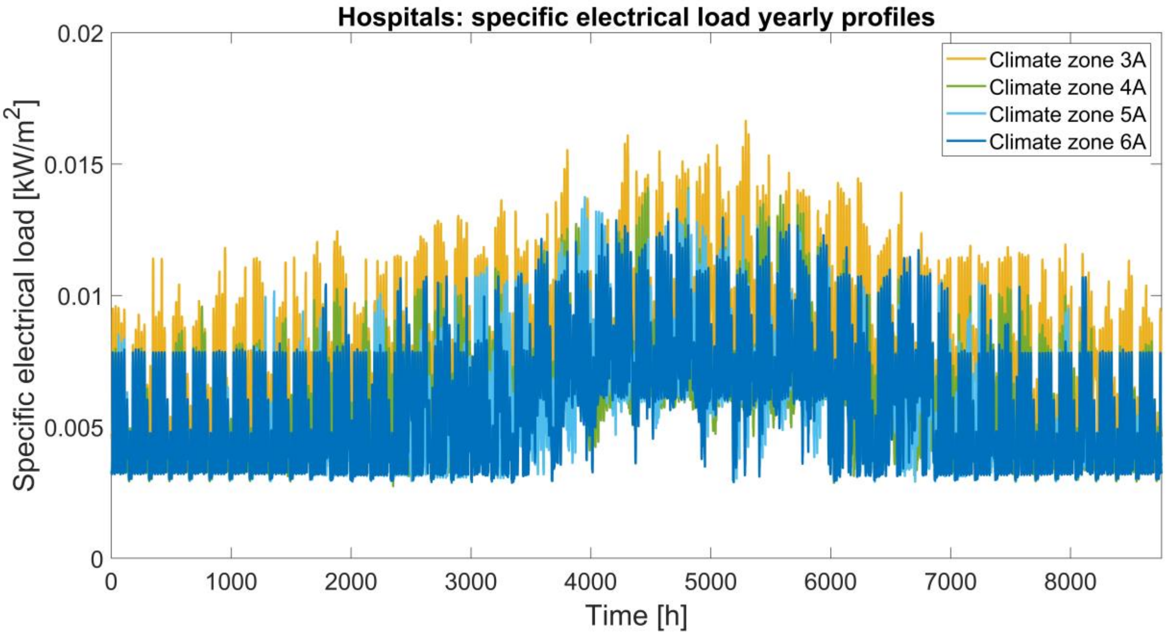


*Figure 22 - Hospitals: overlapped specific electrical load profiles*

Analyzing the thermal demand in Figure 23, it can be observed that the coldest climate zone has the highest thermal energy consumption even during the summer, while the hottest climate zone is mostly covered by the other three except for its lowest values of thermal demand during the winter. Interestingly, in some cases, climate zone 5A exceeds the colder climate 6A in terms of thermal demand

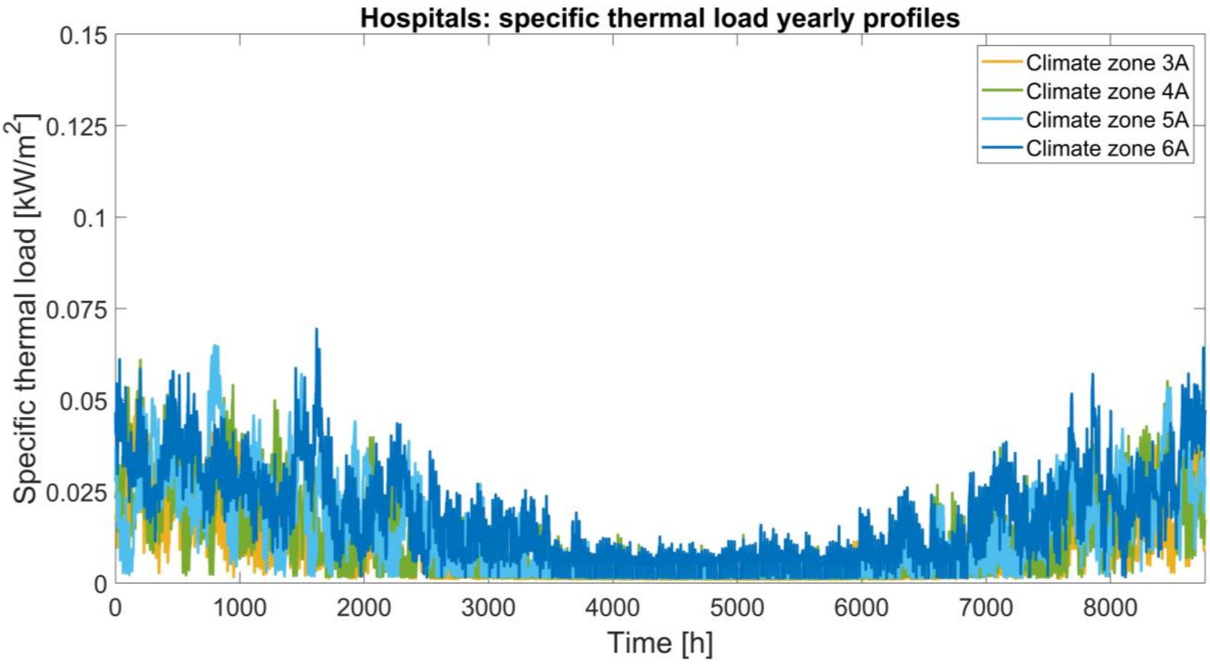

*Figure 23 - Hospitals: overlapped specific thermal load yearly profiles*

Typical days analysis was conducted to identify patterns in electricity and thermal energy demand throughout the year by analyzing four different typical days, i.e., 2 equinoxes and 2 solstices. Although hospitals are buildings that operate continuously 24/7, the generation of the models still considered opening and closing hours for the public, which can have an influence on the daily profiles and are therefore reported Table 13.

| | Weekday opening time | Weekday operating hours | Weekend operating hours | Weekend opening time |
|---|---|---|---|---|
| **3A** | 8:30 | 8 | 14.75 | 8:00 |
| **4A** | 7:15 | 11 | 11.25 | 6.15 |
| **5A** | 7:45 | 7.75 | 13.5 | 5:45 |
| **6A** | 7:00 | 9.5 | 8 | 10:00 |

*Table 13 - Hospitals schedules*

Figure 24 displays the typical days for electricity demand for the four selected hospitals in their respective climate zones. Overall, the selected hospitals exhibit similar patterns of electrical energy demand across different climate zones, with the same peak timing due to opening to the public hours, and main differences seen primarily in the magnitude rather than the shapes of the curves.

During the equinox days, the demand for electricity in all hospitals follows a similar trend, with a peak in the morning hours, a decrease during midday, and a further decrease moving towards the afternoon hours. However, during the spring equinox (March 20) and autumn equinox (September 23), hospitals in warmer climates consistently exhibit higher electricity loads than those in colder climates due to cooling purposes.

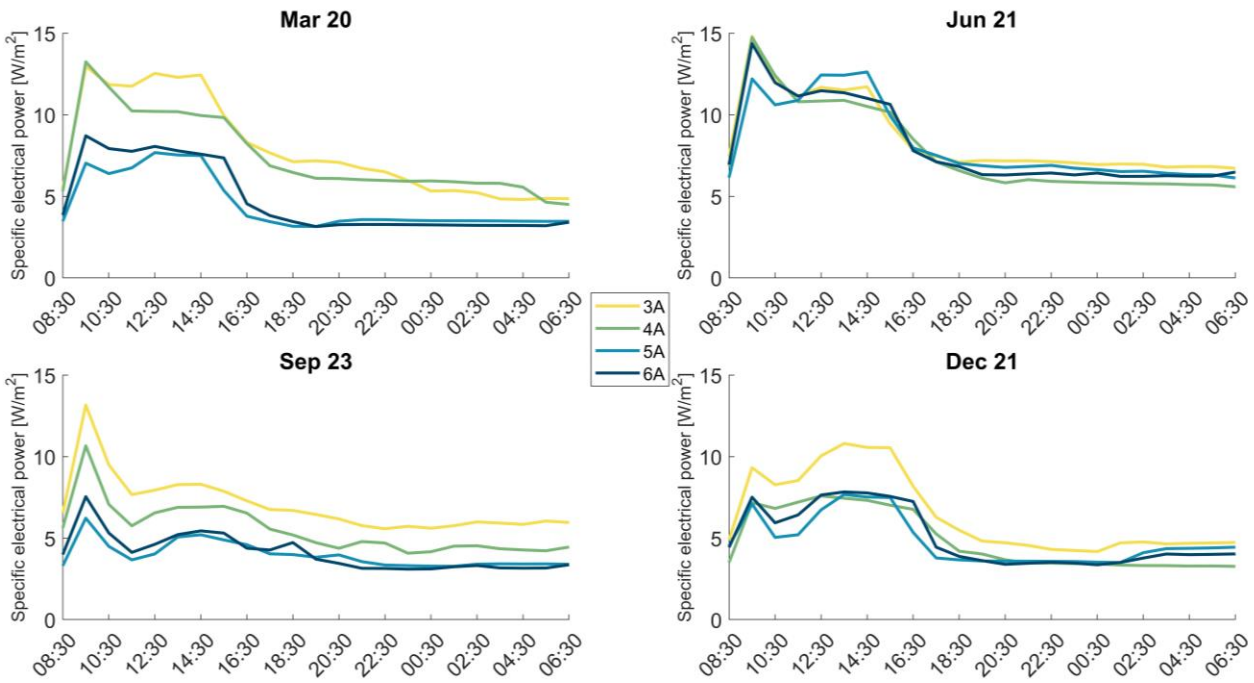


*Figure 24 - Comparison of specific electrical load profiles for typical days in hospitals*

Similarly, Figure 25 shows the typical days for thermal energy demand for the four selected hospitals in their respective climate zones. Hospitals located in colder climates (5A and 6A) exhibit significantly higher demand for heating during the spring equinox, highlighting the need for heating even towards the end of winter. For warmer climates (3A and 4A), apart from the peak in the morning hours and a slight rise towards the evening, there is practically no heating required during the rest of the day, with natural gas consumption only due to hot water demand.

During summer solstice the thermal energy demand is consistently flat for climates 3A and 4A, indicating no need for heating, while colder climates (5A and 6A) show a non-zero heating demand throughout the day, albeit small.

In the autumn equinox, the patterns of thermal energy demand are similar to those during the summer solstice in terms of shapes but with higher magnitude.

Finally, during the winter solstice, the shapes of the demand patterns are like those during the spring equinox, except for the duration of the morning peak load that is wider in winter. Additionally, in spring, the load magnitudes for the hot and mixed climates are similar, while in winter, the mixed zone is similar to the two cold climates, and the hottest climate 3A has significantly lower demand, with consumption nearing zero during the peak down timing at 14:30. Overall, the selected hospitals exhibit significant differences in the magnitude of their thermal energy demand across different climate zones, but for the same day considered, their shapes are quite similar.

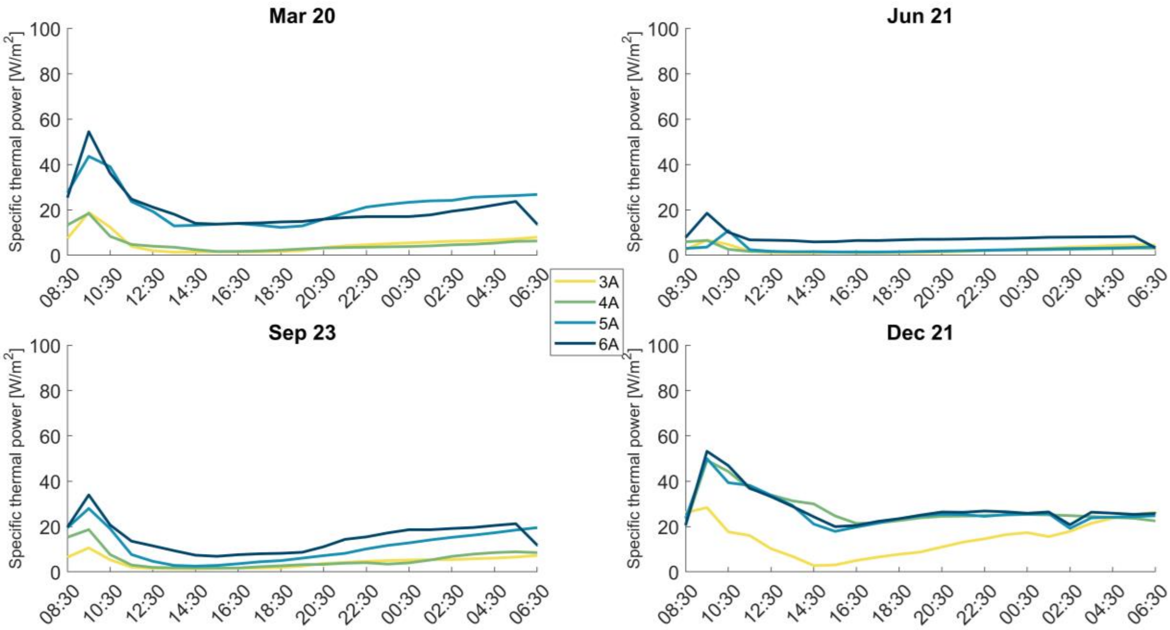


*Figure 25 - Comparison of specific thermal load profiles for typical days in hospitals*

## 4.2 Energy characterization of hotels

The following subsections of this section present the results of the analyses conducted on hotels. First, the hotel category is characterized in terms of the most used fuel for HVAC and the most widespread HVAC technology at an aggregate level. Then, energy end uses are investigated, and finally, the load profiles of modeled hotel buildings are shown and discussed.

### 4.2.1 Fuels and HVAC systems

Figure 26 shows the distribution of heating fuels used in hotels across all climates. Most hotels use natural gas, followed by electricity-driven heat pumps. However, hot climates exhibit a larger adoption of full electric HVAC systems and no heating, while both fuel types decrease in favor of natural gas fueled types going from hot to cold climates.

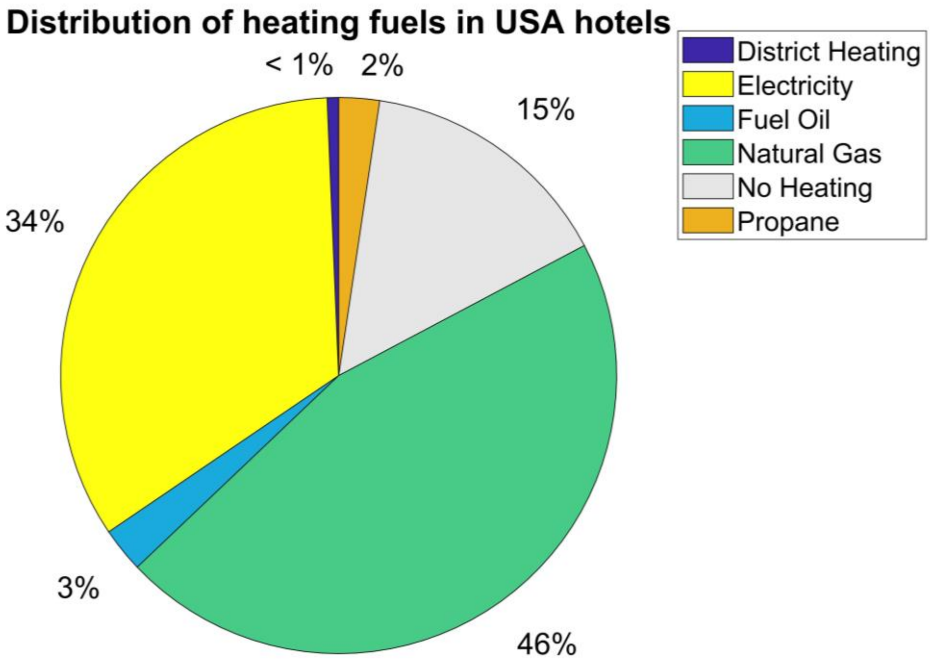


*Figure 26 - Distribution of heating fuels used in USA hotels, author's own elaboration from [11]*

According to Table 14, the Packaged Single Zone Air Conditioner with gas boiler (PSZ-AC with gas boiler) is the most common HVAC system in US hotels with a 16.45% share It uses natural gas in heating mode.

| HVAC system | % |
|---|---|
| **"PSZ-AC with gas boiler"** | 16.45 |
| **"Fan coil chiller with no heat"** | 14.89 |
| **"Fan coil air-cooled chiller with boiler"** | 8.60 |
| **"PTAC with baseboard electric"** | 7.89 |
| **"DOAS with water source heat pumps with ground source heat pump"** | 5.53 |

*Table 14 - Distribution of HVAC technologies in the USA hotel stock, author's own elaboration from [11]*

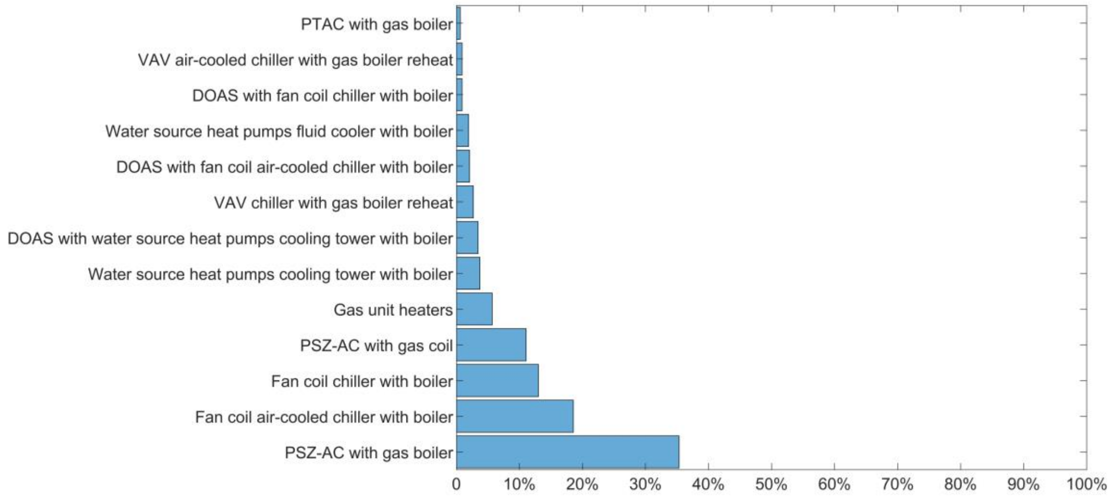


*Figure 27 - Natural gas HVAC systems in US hotels, author's own elaboration from [11]*

In the four climates studied and for hotels fueled by natural gas, it remains the most common HVAC system, with a share of over 35% (Figure 10).

This HVAC system remains the most prevalent even for each of the four climates, as shown in Figure 13, with higher adoption in colder climates.

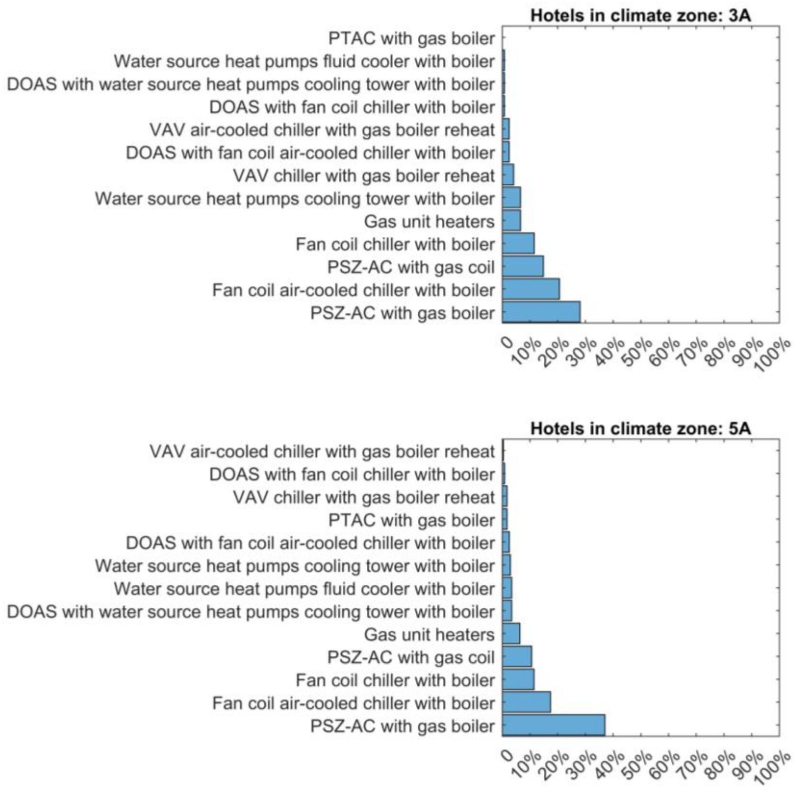


*Figure 28 - Natural gas HVAC systems in US hotels by climate zones (3A – 5A), author's own elaboration from [11]*

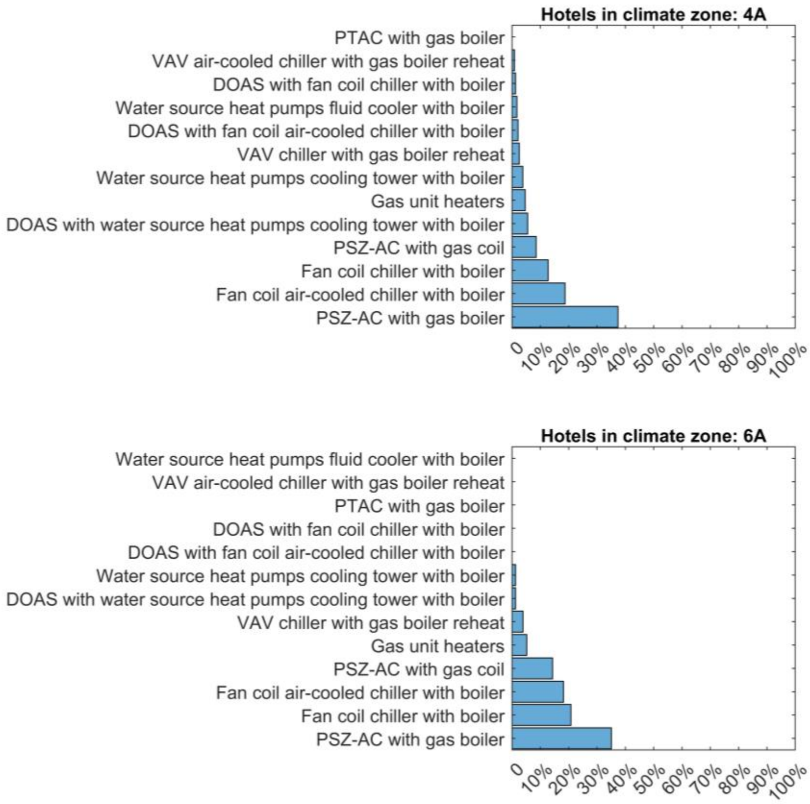


*Figure 29 - Natural gas HVAC systems in US hotels by climate zones (4A – 6A), author's own elaboration from [11]*

### 4.2.2 Yearly electrical and thermal energy consumption: breakdown by end-use

The graph presented in Figure 30 indicates that there is a gradual increase in the total specific thermal energy consumed for space heating and hot water production from the hottest climate zone (3A) to the coldest (6A), but the total specific electricity consumption does not decrease as expected with the reduction of summer cooling load going from hot to cold climates.

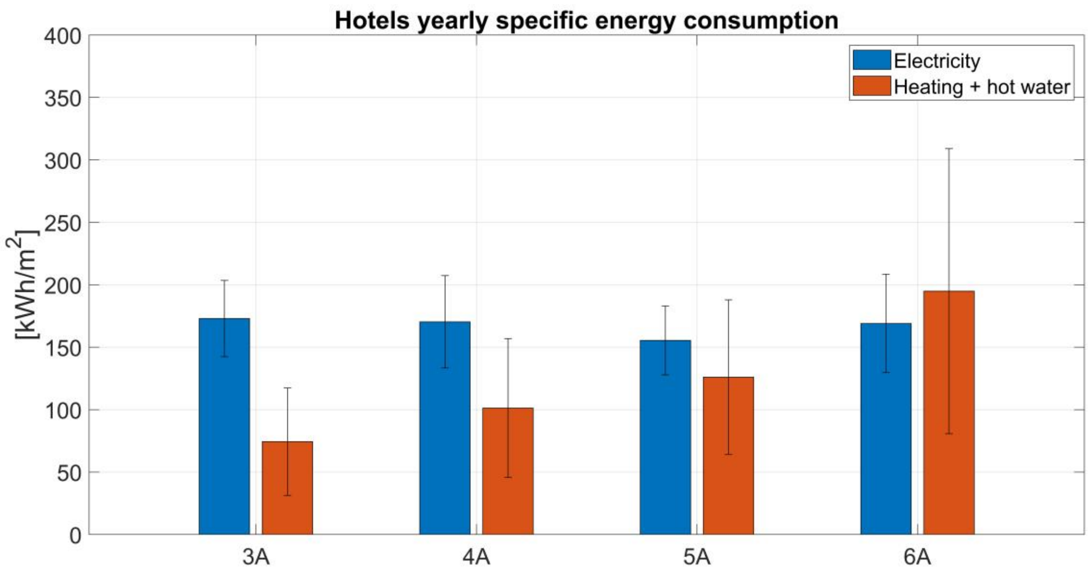


*Figure 30 - Comparing hotels' specific energy consumption by climate zones*

Despite the decrease in the share and absolute value of cooling energy on the total from the hottest to the coldest climate zones (20% to 7% and one third reduction, respectively), as shown in (Figure 31) and (Figure 32), the overall impact on the total energy consumption is not significant.

This is due to the simultaneous increase in electricity consumption for hot water production and minoritarian end uses, which occurs as the temperature decreases.

The increase in electricity consumption for exterior lighting and refrigerators in harsh climates could explain the increase in minoritarian consumption. However, these two factors have a high associated standard deviation, which is too large to fully explain the behaviors of their average values.

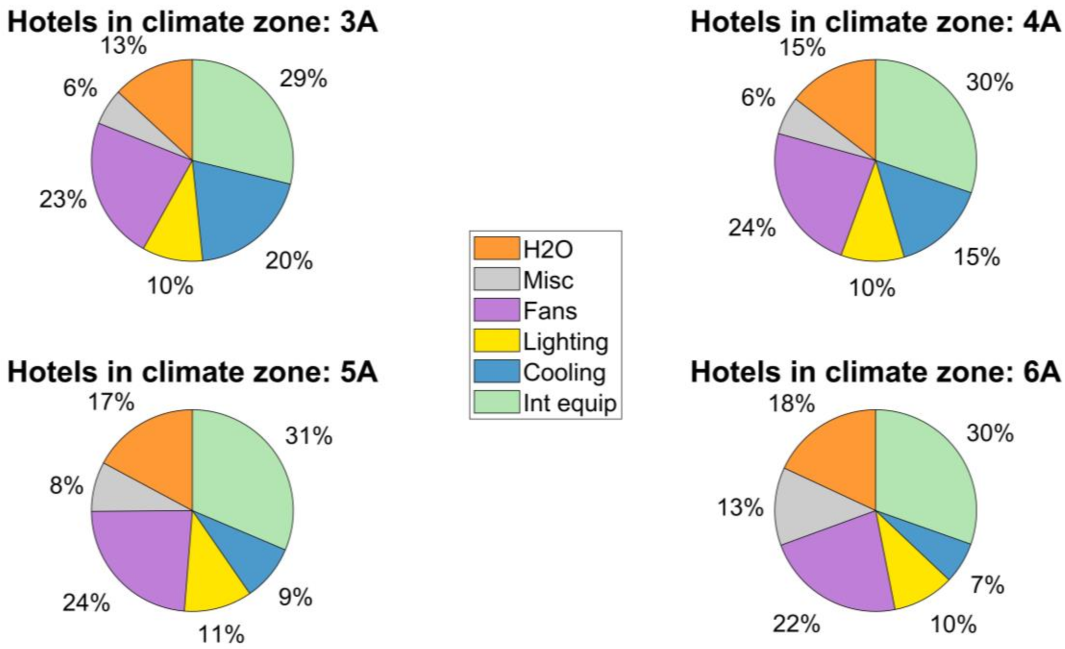


*Figure 31 - Composition of electricity end uses in hotels*

Across all climates zones, the largest contributor to electricity consumption in hotels is the "interior equipment," that for an hotel is composed by cleaning equipment as vacuums, washer, dryers, kitchens, or fitness rooms and pools, with a percentage (Figure 31) and an absolute value (Figure 32).

The second most impactful end use on total electricity consumption composition is the electricity to drive fans.

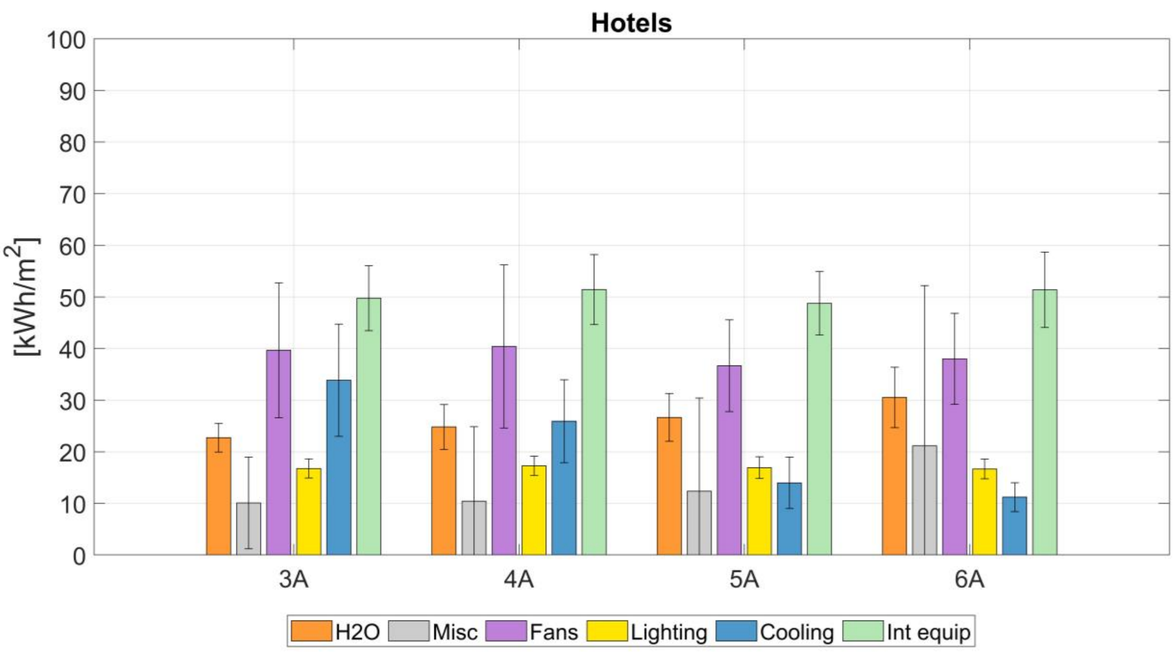


*Figure 32 - Electricity end use breakdown in hotels by climate zones*

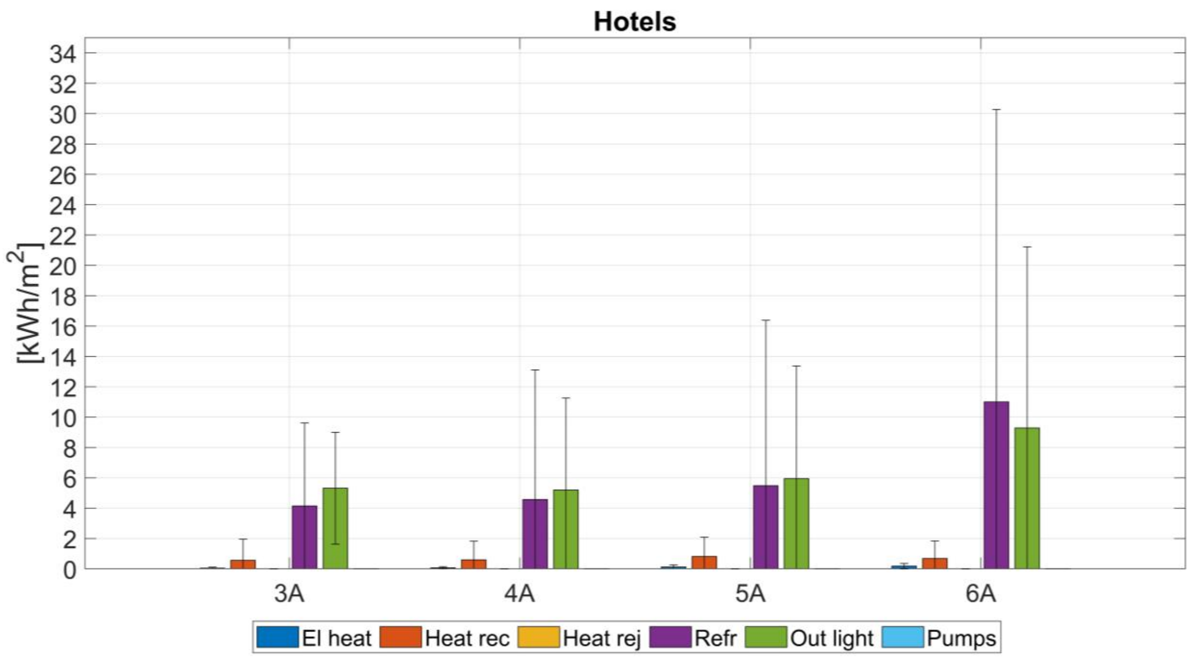


*Figure 33 - Minor electricity end uses consumption in hotels*

In Figure 34 the average yearly thermal energy consumption per climate is displayed. The thermal energy consumed for hot water production is relatively constant across different climates, unlike the hospital case shown in Figure 17.

However, the variability in energy consumed for hot water production can be observed in the electrical part shown in Figure 32.

On the other hand, the average thermal energy used for space heating is highly influenced by climate variations, with a significant increase towards colder climates. The high variability in space heating consumption is represented by the standard deviation error bar, which is primarily due to the variation in the number of stories ranging from 1 to 30, since buildings with an higher number of stories have an increased heating load and cooling load [30], [31], the aspect ratio (ratio of North/South facade vs. West/East facade) ranging from 1 to 6, orientation with respect to the North, and the age of the buildings that determine the transmittance values of walls and windows.

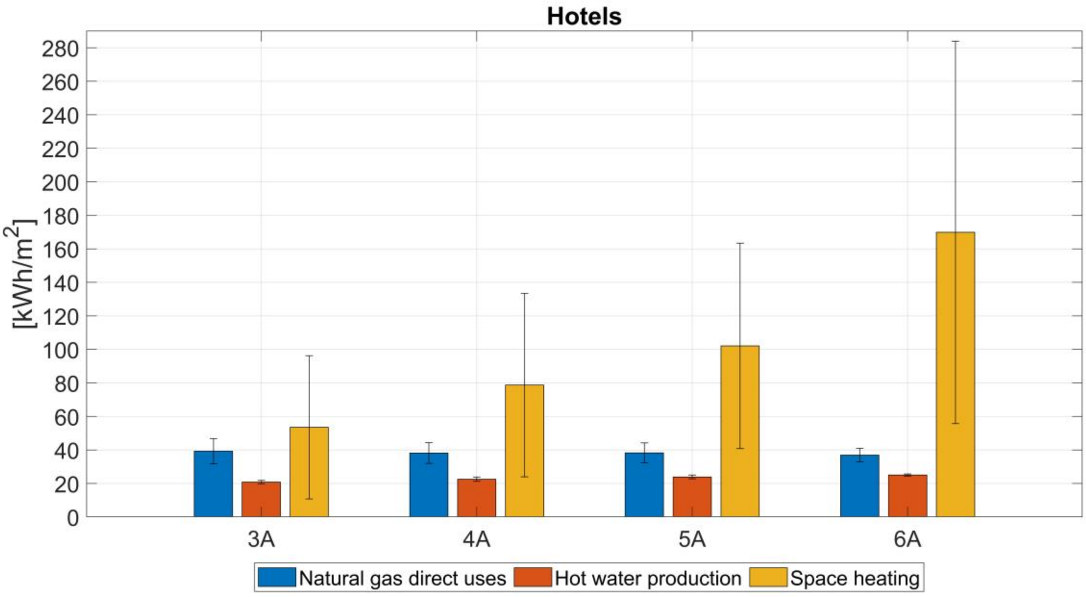


*Figure 34 - Thermal energy consumption in hotels from natural gas-based end-use by climate zones*

### 4.2.3 Analysis of hourly load profiles and typical days

The main characteristics of the selected hotel buildings are summarized Table 15

The electric load profiles per unit of area of the four selected hotels are then presented in Figure 35. The electrical base loads per unit of area, which represent the minimum electricity consumption during non-cooling periods, are different through different climates.

| Hotels | | | | |
|---|---|---|---|---|
| **Climate zone** | Floor area $[m^2]$ | Rotation [°] | Aspect ratio | Stories |
| **3A** | 32515 | 0 | 5 | 20 |
| **4A** | 13935 | 90 | 2 | 20 |
| **5A** | 6968 | 180 | 5 | 6 |
| **6A** | 13935 | 90 | 6 | 4 |

*Table 15 – Geometric properties of hotels*

| Hotels | | | | | | |
|---|---|---|---|---|---|---|
| **Climate zone** | **Electrical intensity $\left[kWh/m^2\,y\right]$** | **Thermal intensity $\left[kWh/m^2\,y\right]$** | **E/T** | **Average electrical Intensity climate $\left[kWh/m^2\,y\right]$** | **Average thermal Intensity climate $\left[kWh/m^2\,y\right]$** | **Avg E/T climate** |
| **3A** | 179.60 | 71.90 | 2.50 | 172.91 | 74.33 | 2.33 |
| **4A** | 168.49 | 104.23 | 1.62 | 170.33 | 101.26 | 1.68 |
| **5A** | 154.47 | 121.16 | 1.27 | 155.42 | 125.96 | 1.30 |
| **6A** | 166.88 | 181.87 | 0.92 | 168.99 | 194.86 | 0.87 |

*Table 16 – Energy intensities of hotels*

The base load during the summer season in the hottest climate, 3A, appears to be similar to the base load during the rest of the year, but the graph shows a faded region during summer. This indicates that although the minimum energy consumed during summer is still relatively high due to the high cooling load, the HVAC cooling power is lowered during the night, approaching shutdown levels.

Similarly, the other three climates follow this behavior during the summer, and their base load during the summer season gradually decreases as the climate becomes colder, along with the duration of the cooling season. In the coldest climate, 6A, there is almost no difference in comparison to the rest of the year, except for the peaks associated with the maximum power demand that are evident during the summer. Furthermore, the height of the maximum values of electricity consumed during summer also decreases when moving from hot to cold climates, except for the coldest climate, which has a behavior more similar to the mixed climate 4A than the cold climate 5A. This indicates that although this is the coldest climate, cooling load during the summer season is still high.

The peaks in the electricity demand outside of the cooling season are mostly present in the hottest climate zone 3A and are negligible in the colder zones.

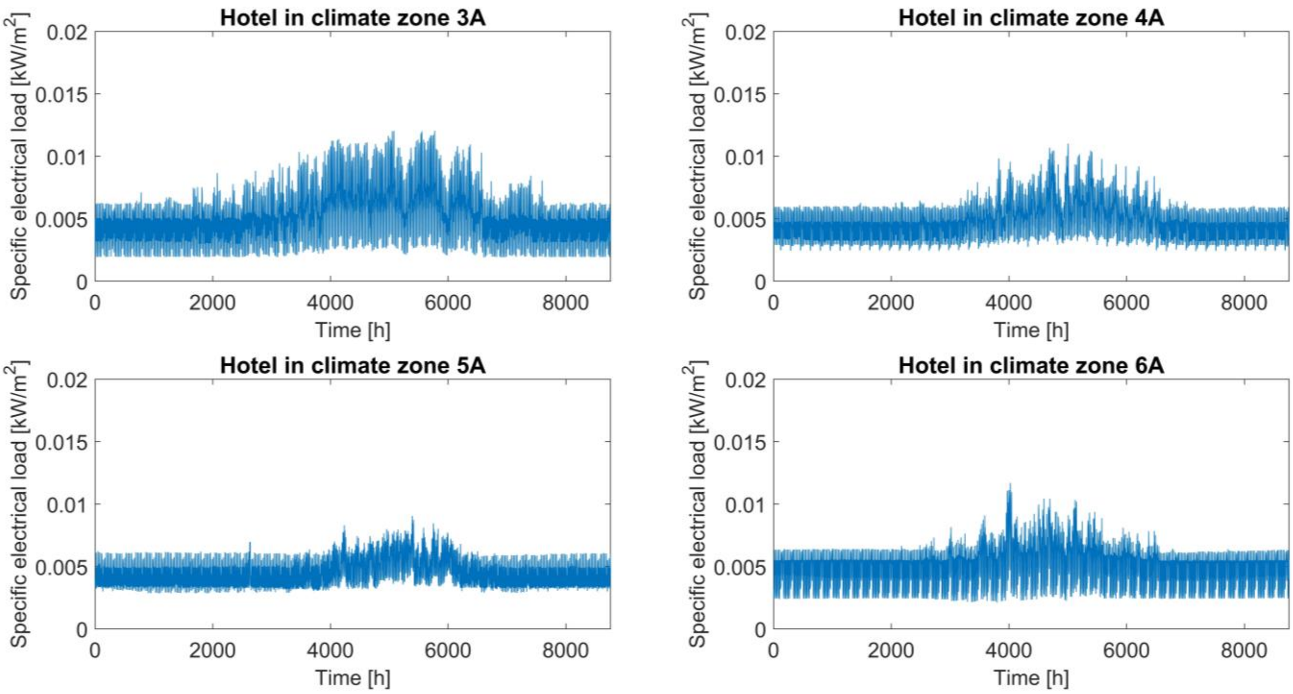


*Figure 35 - Hotels: specific electrical load profiles*

The thermal load profiles per unit of area of the selected hospitals are displayed in Figure 36Figure 19. The duration of the heating season is relatively short in the hottest climate (3A) and gradually increases in duration as the climate becomes colder. The shape of the thermal load profiles exhibits sharp peaks during the winter season with flatter profiles during the rest of the year in all climates, but the peaks become more intense and closer to each other in colder climates. Additionally, the minimum values of thermal loads increase moving towards colder climates.

Figure 38 emphasizes the importance of separating hot water demand from thermal demand analysis. By removing the contribution of hot water demand, it reveals that the heating load during summer is virtually zero in all climates, in accordance with the respective duration of the summer season. This further highlights the significance of distinguishing hot water demand from the overall thermal load profile analysis. Although hot water demand impacts the overall thermal load profile, its contribution is minimal when heating is performed, and varies from one to three orders of magnitude smaller depending on the season and the climate zone.

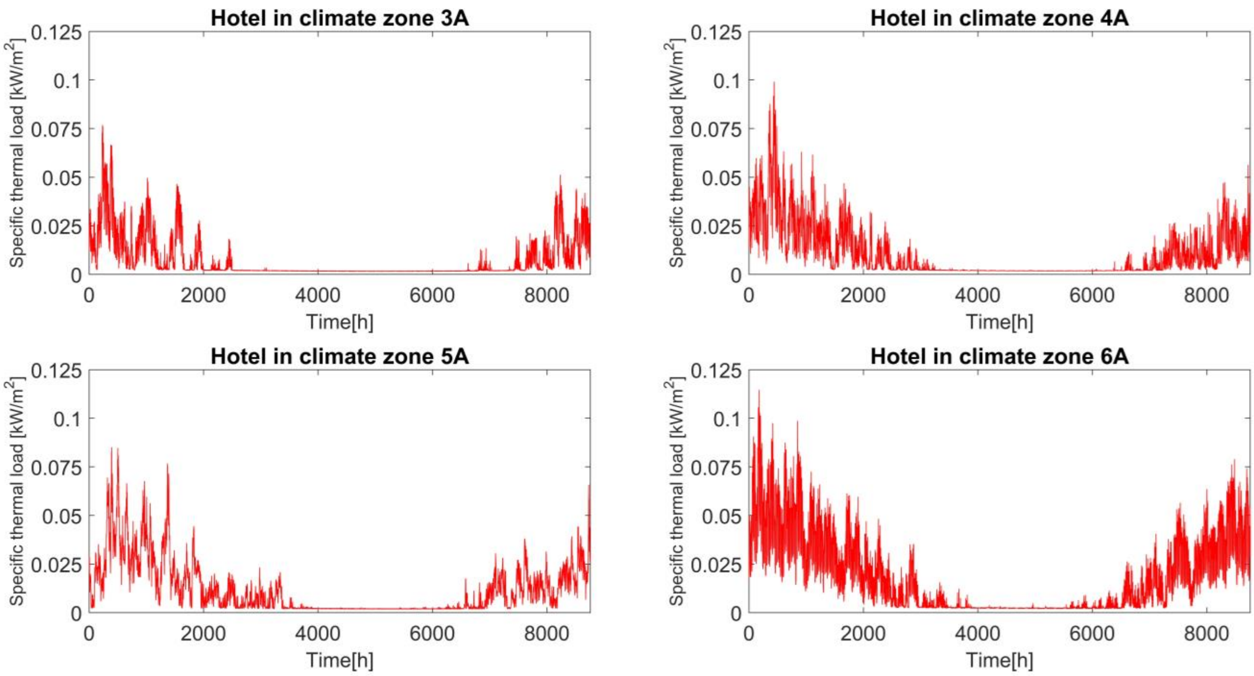


*Figure 36 - Hotels: specific thermal load profiles*

In Figure 37 the thermal load profiles for hot water production are compared. As the climates become colder, the magnitude of the profiles increases, and the shape of the profiles exhibits a swing throughout the year with higher values during the winter and a dip in summer. As the climates become colder, the profiles tend to flatten and become more uniform throughout the year. This suggests that hot water production demand is more consistent throughout the year in colder climates, whereas in warmer climates, there is a greater demand during the winter season.

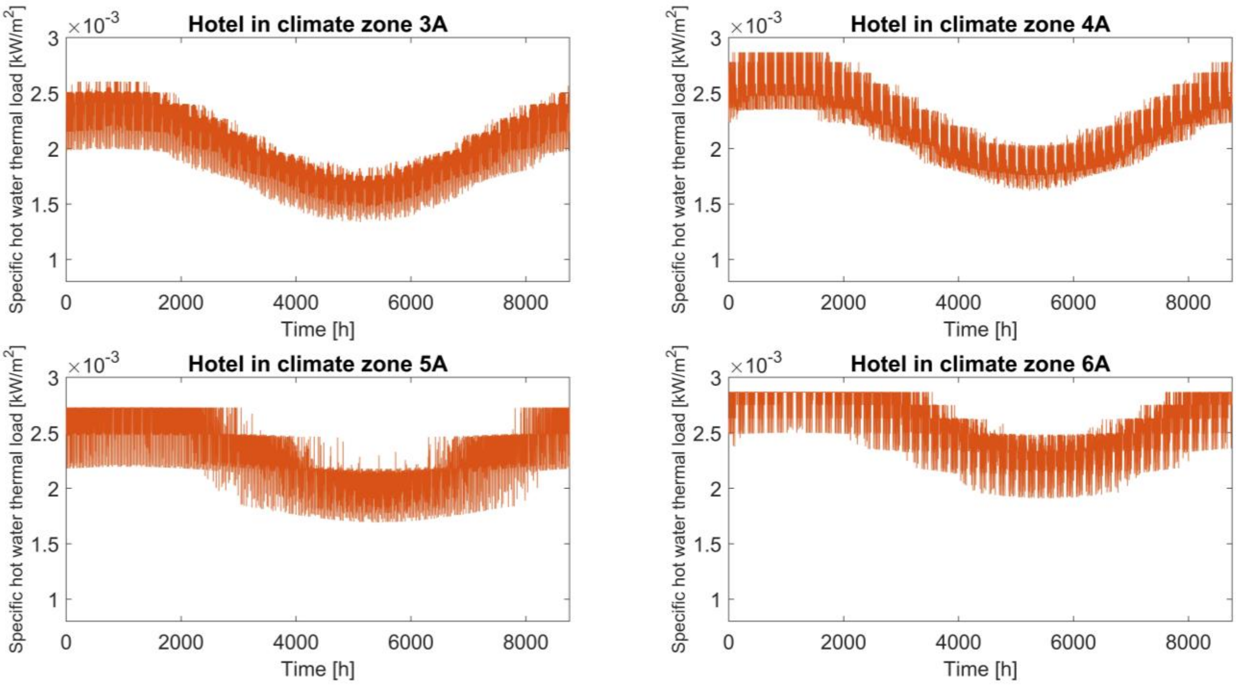


*Figure 37 - Hotels: specific thermal load profiles for hot water only*

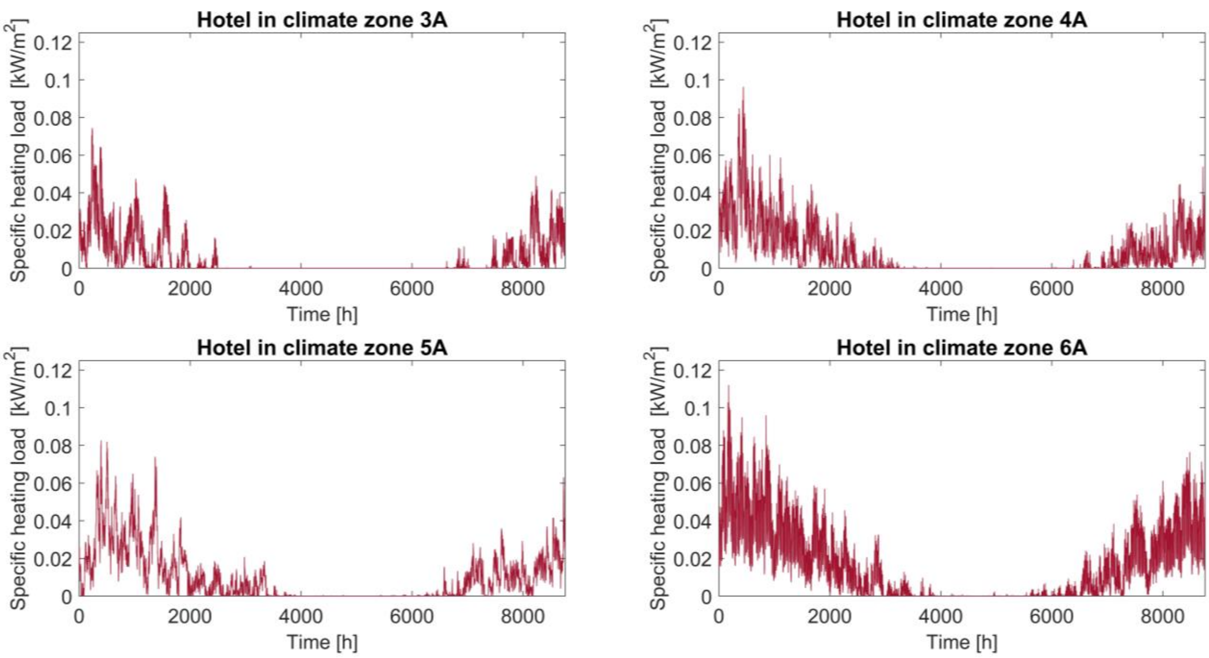


*Figure 38 - Hotels: specific thermal load profiles for heating only*

In Figure 39 and Figure 40, the yearly electrical and thermal load profiles, respectively, are displayed overlapped in the same graph to highlight the main differences in their base loads and peaks of demand.

Looking at the electrical profiles in Figure 39 it can be observed that the hotel in the hottest climate zone (ocra yellow) has the lowest base load per unit of area during the no-cooling season, while the hotel in the coldest climate (blue) has the lowest base load during the cooling period. However, the highest electricity demand during the no-cooling season comes from the hotel in the coldest climate. The hottest climate has the highest consumption for cooling during summer and the highest peaks, but in some cases, the purple curve reaches its peaks even for short periods of time, suggesting occasional spikes in electricity demand even in colder climates. This may be due to unexpected very high outdoor temperatures or changes in occupancy that result in increased electricity usage for cooling.

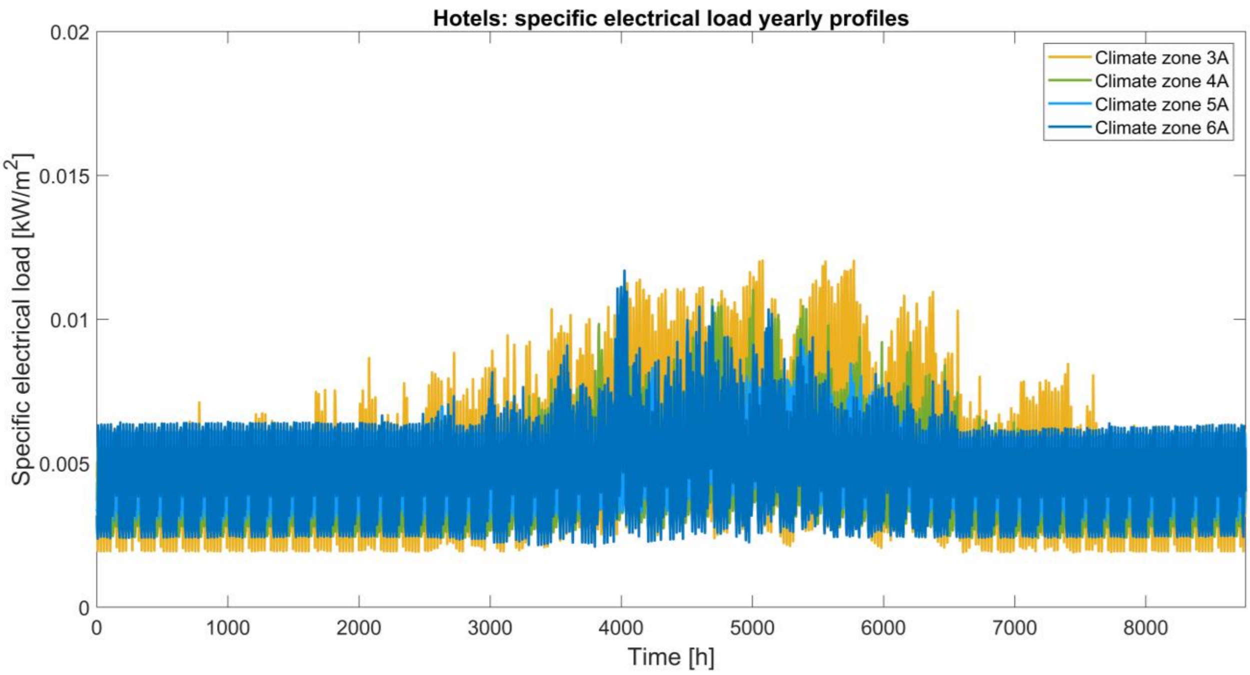


*Figure 39 – Hotels overlapped specific electrical load profiles*

Looking at Figure 40, the thermal demand of the hotel in the hottest climate zone is mostly visible in its minimum values during the heating season, as its maximum values are typically obscured by the other three climates. In contrast, the coldest climate shows prominent peaks in thermal demand, especially during its heating season from September to December. During this period, the other three curves are usually overshadowed. Although the thermal demand of the coldest climate is occasionally exceeded by climate zone 5A (light blue) and mixed climate 4A (green) for a few periods of a few days, it still has the highest thermal energy consumption overall, even during summer. Climate zone 5A sometimes surpasses the colder climate 6A in terms of thermal demand, but only for very brief periods.

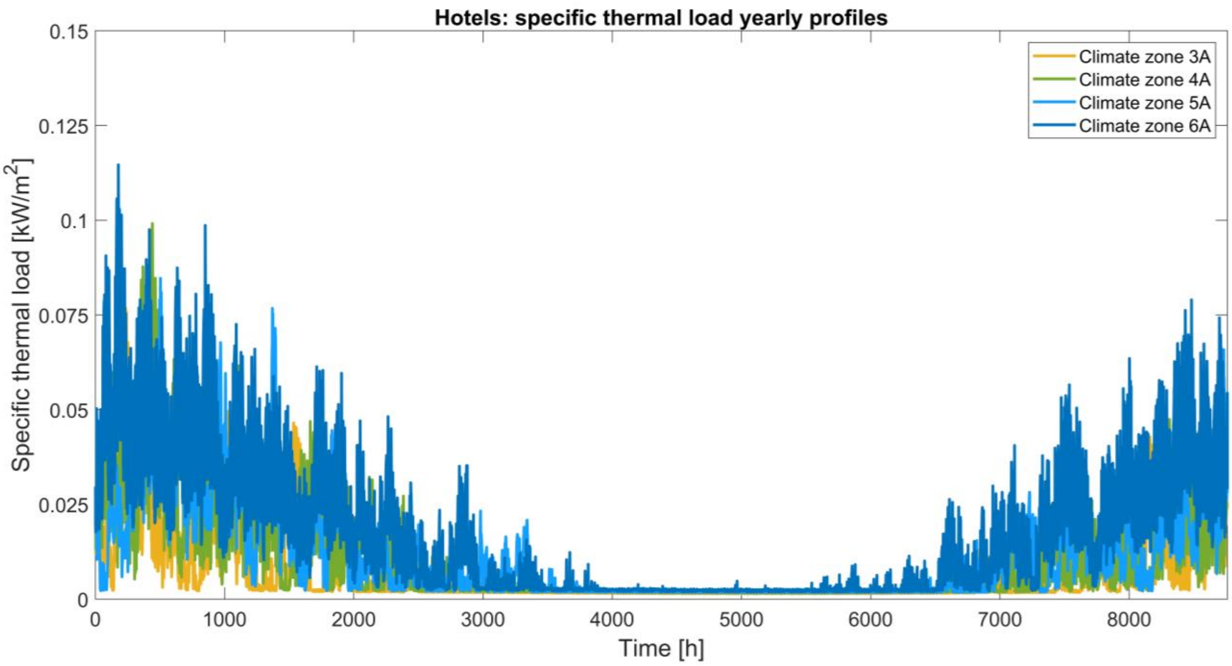


*Figure 40 – Hotels overlapped specific thermal load profiles*

When comparing the typical days, it is important not to overlook their weekly opening hours. Although hotels and especially hospitals do not have specific opening periods, their load profiles were still obtained by taking into account different opening and closing times during weekdays and weekends, that are reported in Table 17

| | Weekday opening time | Weekday operating hours | Weekend operating hours | Weekend opening time |
|---|---|---|---|---|
| **3A** | 10:45 | 12.5 | 10.5 | 11:15 |
| **4A** | 5:45 | 17 | 16.5 | 5:45 |
| **5A** | 8:15 | 14.75 | 8.5 | 9:00 |
| **6A** | 9:30 | 8.5 | 13.25 | 8.15 |

*Table 17 – Hotels' schedules*

Starting from the spring equinox, mixed zone hotel, cold zone hotel and coldest zone shows a similar then in their electrical loads, while the hotel in the hottest climate (yellow line) shows an highest profile during from about 12:30 until 16:30 Overall, the selected hospitals exhibit similar patterns of electrical energy demand across different climate zones, with the same peak timing due to opening to the public hours, and main differences seen primarily in the magnitude rather than the shapes of the curves.

During the equinox days, the demand for electricity in all hospitals follows a similar trend, with a peak in the morning hours, a decrease during midday, and a further decrease moving towards the afternoon hours. However, during the spring equinox (March 20) and autumn equinox (September 23), hospitals in warmer climates consistently exhibit higher electricity loads than those in colder climates due to cooling purposes.

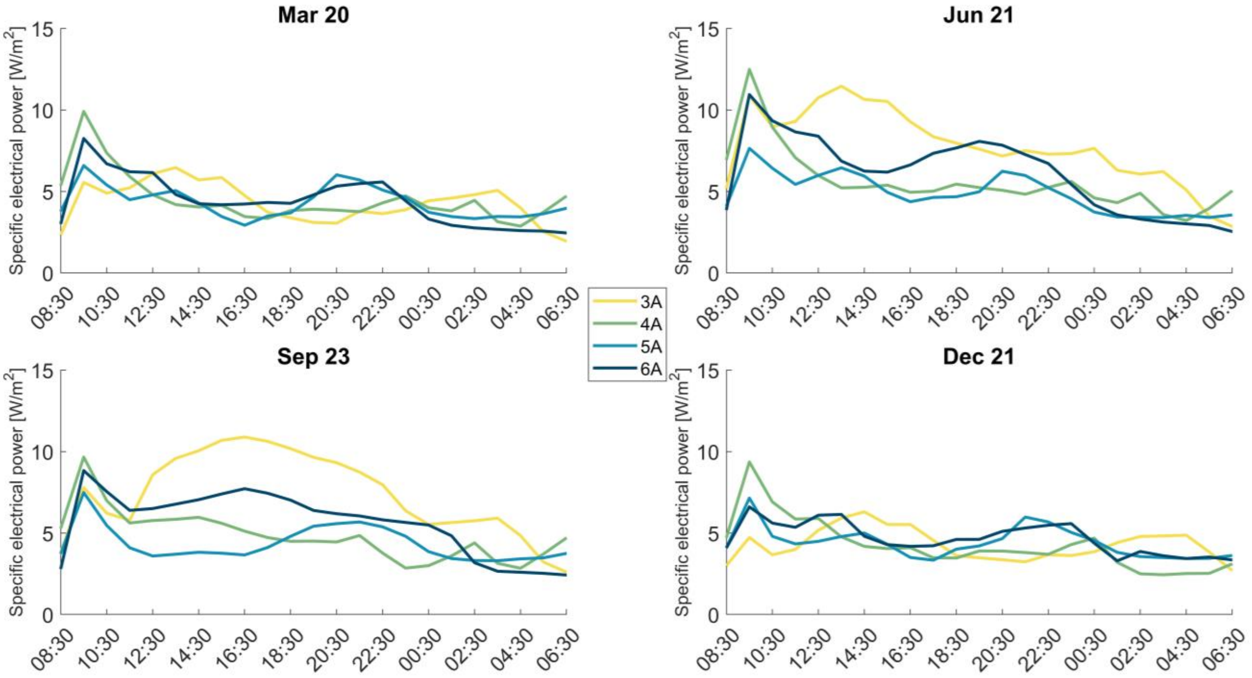


*Figure 41 - Comparison of specific electrical load profiles for typical days in hotels*

Similarly, Figure 25 shows the typical days for thermal energy demand for the four selected hospitals in their respective climate zones. Hospitals located in colder climates (5A and 6A) exhibit significantly higher demand for heating during the spring equinox, highlighting the need for heating even towards the end of winter. For warmer climates (3A and 4A), apart from the peak in the morning hours and a slight rise towards the evening, there is practically no heating required during the rest of the day, with natural gas consumption only due to hot water demand.

During summer solstice, the thermal energy demand is consistently flat for climates 3A and 4A, indicating no need for heating, while colder climates (5A and 6A) show a non-zero heating demand throughout the day, albeit small.

In the autumn equinox, the patterns of thermal energy demand are similar to those during the summer solstice in terms of shapes but with higher magnitude.

Finally, during the winter solstice, the shapes of the demand patterns are like those during the spring equinox, except for the duration of the morning peak load that is wider in winter. Additionally, in spring, the load magnitudes for the hot and mixed climates are similar, while in winter, the mixed zone is similar to the two cold climates, and the hottest climate 3A has significantly lower demand, with consumption nearing zero during the peak down timing at 14:30. Overall, the selected hospitals exhibit significant differences in the magnitude of their thermal energy demand across different climate zones, but for the same day considered, their shapes are quite similar.

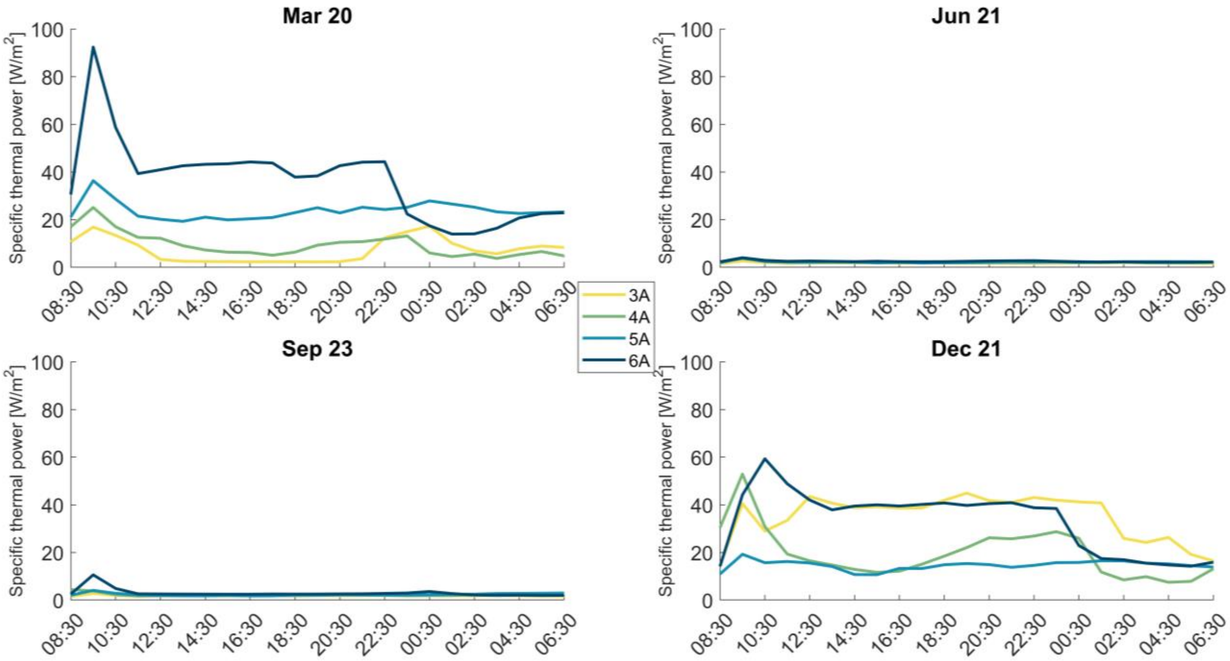


*Figure 42 - Comparison of specific thermal load profiles for typical days in hotels*

## 4.3 Hotels and hospitals compared

In this section, hotels and hospitals are compared in terms of their yearly average quantities. To determine the appropriate E/T ratio for a generic SOFC, Table 7 is referenced, and a possible value of 1.6 is calculated. The energy behavior of hotels and hospitals is then examined in Table 18 and Table 19 respectively, and it is found that it is more likely to find a building that matches the E/T ratio of the SOFC in climate zones 4A and 5A, which are a mixed zone and a cold zone, respectively. Climate zone 3A, which is too hot, exhibits a high E/T ratio due to high summer cooling loads and low winter heating loads. On the other hand, very cold climate zones such as 6A show the opposite situation.

| Hotels | Annual specific energy consumption [kWh/m²] | | | |
|---|---|---|---|---|
| ASHRAE Climate zone | | Electrical energy | Thermal energy | E/T |
| 3A | Min | 143.76 | 31.40 | 2.33 |
| | Avg | 172.91 | 74.33 | |
| | Max | 294.72 | 268.83 | |
| 4A | Min | 127.86 | 42.74 | 1.68 |
| | Avg | 170.33 | 101.26 | |
| | Max | 426.50 | 395.01 | |
| 5A | Min | 122.23 | 38.15 | 1.3 |
| | Avg | 155.42 | 125.96 | |
| | Max | 291.19 | 429.40 | |
| 6A | Min | 132.82 | 81.68 | 0.87 |
| | Avg | 168.99 | 194.86 | |
| | Max | 294.26 | 548.53 | |

*Table 18 - Hotels: specific energy consumption range by climate*

While the E/T ratios provide a useful estimate for identifying which building categories in which climates are most likely to be feasible for a SOFC-based cogeneration system, it is important to note that these ratios are calculated based on the averages of a large number of buildings. Therefore, they offer only a rough indication, and the actual E/T ratios may vary significantly within the same category of building in the same climate zone, as shown in Figure 17 and Figure 34. This large variability can be attributed to factors such as the building's age, orientation, aspect ratio, and number of stories, which can all impact its energy consumption patterns.

| Hospitals | Annual specific energy consumption [kWh/m²] | | | |
|---|---|---|---|---|
| ASHRAE Climate zone | | Electrical energy | Thermal energy | E/T |
| 3A | Min | 181.56 | 35.76 | 2.62 |
| | Avg | 235.82 | 90.03 | |
| | Max | 258.1 | 148.15 | |
| 4A | Min | 174.88 | 47.78 | 1.97 |
| | Avg | 209.47 | 106.27 | |
| | Max | 267.98 | 284.23 | |
| 5A | Min | 161.32 | 71.88 | 1.34 |
| | Avg | 189.89 | 141.13 | |
| | Max | 212.33 | 293.81 | |
| 6A | Min | 153.19 | 100.33 | 1.10 |
| | Avg | 190.74 | 174.10 | |
| | Max | 220.22 | 257.37 | |

*Table 19 - Hospitals: specific energy consumption range by climate*

### 4.3.1 Hourly load profiles: annual analysis

The following figures provide a comparison of the specific annual electrical and thermal profiles of hospitals and hotels located in the same climatic zone. In addition, the figures display the specific electrical base load used for sizing the SOFC, as well as the corresponding specific thermal power provided by the SOFC.

By examining Figure 43, it can be observed that the specific electricity consumption per square meter is generally lower in hotels than in hospitals, both in terms of base load and maximum electrical demand throughout the year. Moreover, hotels display a less oscillatory electrical profile compared to hospitals in the same climatic zone, both in terms of the difference between minimum and maximum demand and the peak demand during the period of the year outside of the cooling season. The greater difference between the minimum and maximum electrical demand in hospitals compared to hotels is mainly due to the fact that hospitals have a high electricity consumption associated with the use of sophisticated medical equipment characterized by high energy consumption that operates intermittently, leading to demand spikes when multiple devices are used simultaneously.

During the cooling season, represented by the increase in electrical demand in the center of the graph, hospitals show a longer cooling season than hotels. This can be observed from the central portion of the electrical profiles, which display another base load for hospitals during the cooling season that is not as evident in hotels. This suggests that hotels have lower cooling system capacities, and their cooling systems are shut down during periods of low demand, whereas hospitals have higher cooling system capacities, and their cooling systems continue to operate during periods of low demand.

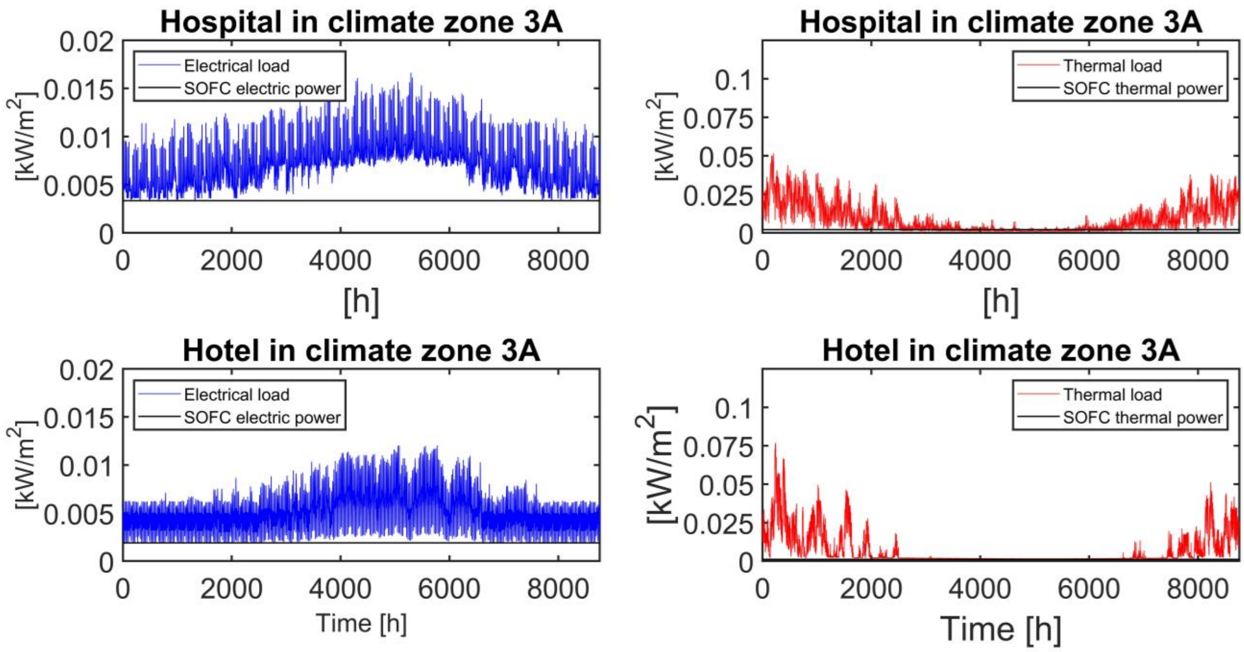


*Figure 43 - Hospitals and hotels compared: electrical and thermal profiles in climate zone 3A*

Turning to the right-hand side of the graph, which displays the specific thermal profiles, the situation is in many ways specular to the comparison between the electrical profiles. Specifically, the specific thermal power demand is more oscillatory during the heating season for hotels, in terms of the difference between minimum and peak demand, and the oscillation periods are longer, while hospitals exhibit less difference between minimum and maximum demand and shorter oscillation periods. This difference can be explained by the fact that hotels generally have a greater variability in the number of occupants throughout the year, with high and low seasons, whereas the number of occupants in hospitals is generally less variable throughout the year. Another noteworthy difference is the thermal energy demand during the summer season, which is obviously near zero for hotels (only hot water demand), while occasional heating occurs in hospitals even during the summer. The other significant difference between the thermal profiles lies in the duration of the heating season, represented by the periods of the year when the thermal demand is greater than during the summer season. This duration is greater for hospitals, with the end of the heating season occurring around June, while for hotels, it is around April. The beginning of the heating season for hotels is around November, while for hospitals, it is around the beginning of September. These last two differences between the thermal profiles can be explained by the fact that hospital patients, being fragile, require generally higher room temperatures, both in the wards and especially in the operating rooms, which is not the case for hotels.

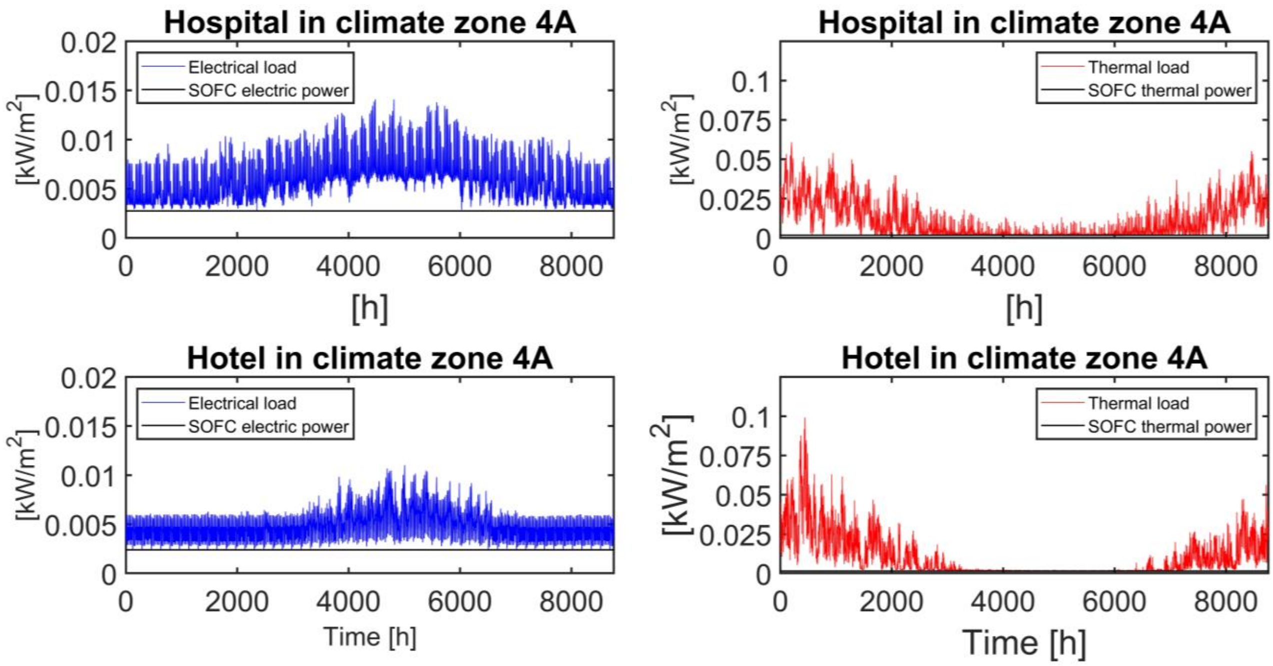


*Figure 44 - Hospitals and hotels compared: electrical and thermal profiles in climate zone 4A*

In Figure 44, the specific annual electrical and thermal profiles of hospitals and hotels located in the 4A climatic zone are compared. This zone is characterized by colder and longer winters than the 3A zone, but comparable summer temperatures. Starting with the left side of the graph showing the specific hourly electrical demand throughout the year, as in the previous comparison, hospitals exhibit higher variability between their base load and maximum electrical demand compared to hotels. However, in this case, demand peaks outside the cooling season are rarer and lower for both hospitals and hotels. The summer base load for hospitals is shorter in duration and less distant from the annual base load. Additionally, similar to the previous comparison, there are periods in which the electrical power supplied to the HVAC system for cooling is reduced even during the peak of the cooling season. On the other hand, examining the thermal profiles, an expansion of the heating season is evident for both buildings, with an increase in the specific thermal demand curves, although this phenomenon is more pronounced in hotels than in hospitals. However, the variability between minimum and maximum thermal demand during the heating season is higher in hotels than in hospitals. Furthermore, the thermal demand of hospitals during the summer is more visible than in the previous comparison, indicating a greater number of HVAC system startups and shutdowns, even though the maximum demand values are obviously still very low compared to the winter heating demand.

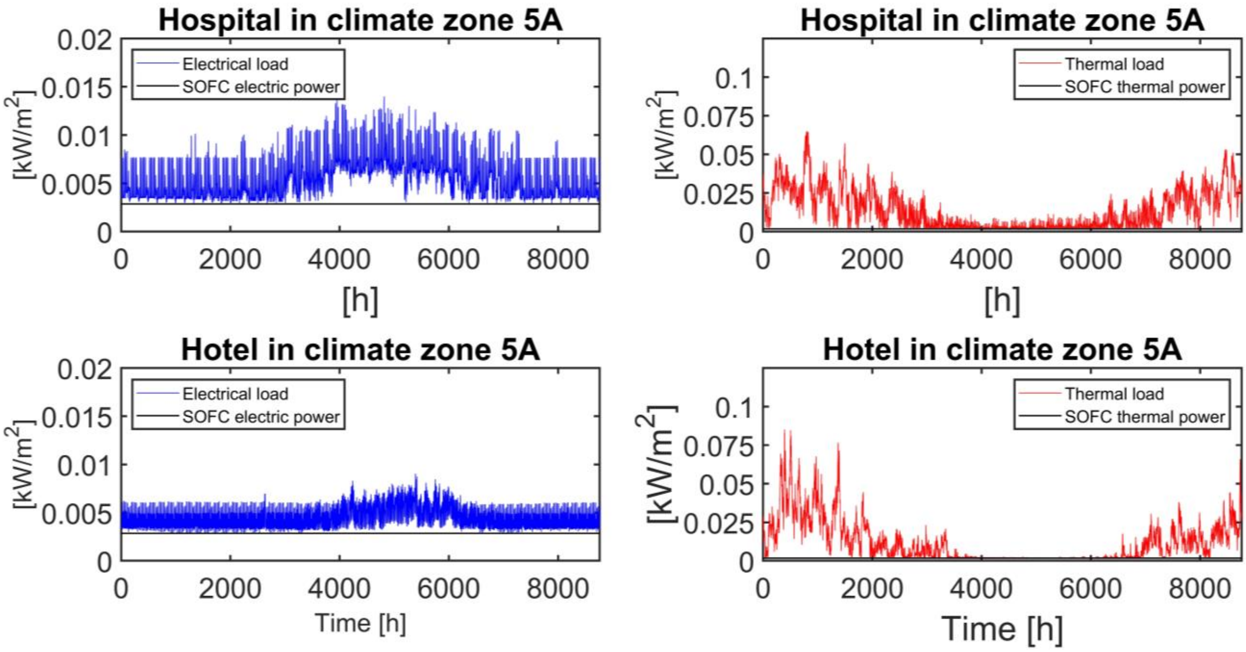


*Figure 45 - Hospitals and hotels compared: electrical and thermal profiles in climate zone 5A*

In Figure 45, the specific electrical and thermal profiles of two buildings in climatic zone 5A are compared. Looking at the electrical profiles, there is a further reduction in the duration of the cooling periods compared to the previous climatic zone, along with higher peak values for the specific electrical demand during this season, for both the hospital and the hotel. This trend is more evident when comparing the current hotel to the one in the previous climatic zone. Furthermore, off-season HVAC activations in cooling mode are less frequent, which is more evident when comparing the current hospital to the previous one.

Regarding the thermal profiles, in this case, the profiles of both the hotel and hospital are more similar compared to the previous climatic zones in terms of the duration of the heating season and the shape of the profiles. However, for the hospital, heating activations are even more frequent than the previous case, even during the summer season.

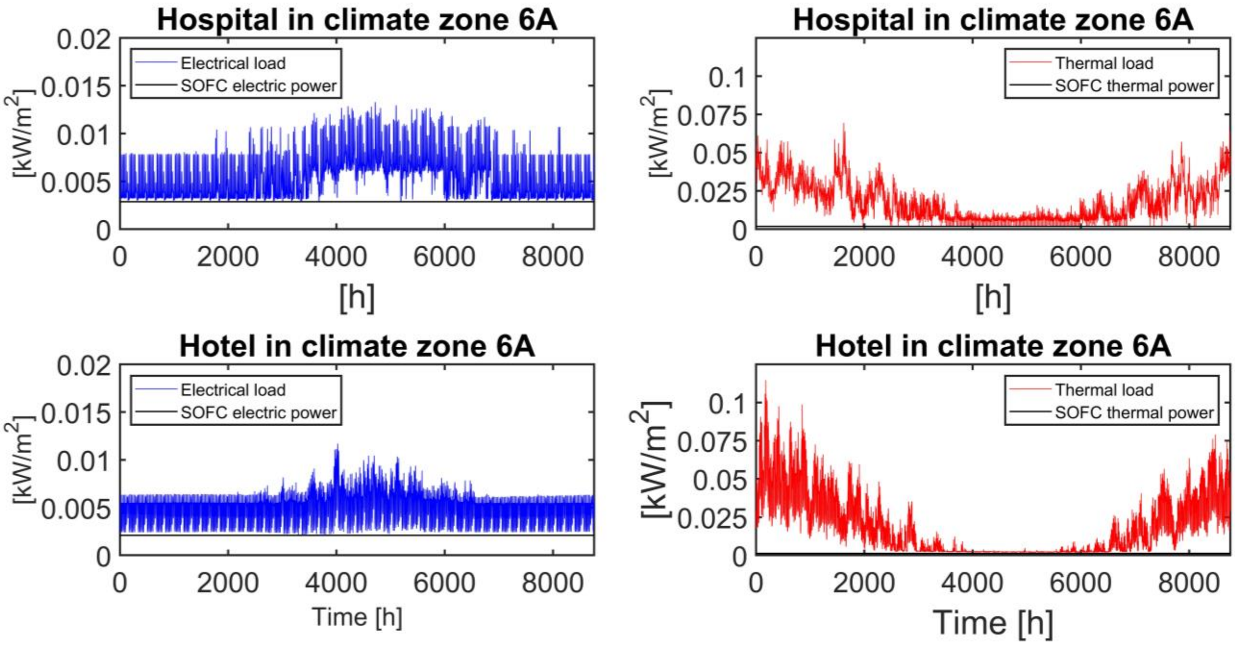


*Figure 46 - Hospitals and hotels compared: electrical and thermal profiles in climate zone 6A*

In Figure 46, the specific electrical and thermal profiles of the hospital and hotel located in the 6A climatic zone, which is the coldest in terms of heating degree days, are compared. In terms of electrical profiles, the observations made in previous climatic zones still hold true. The hospital still exhibits an electrical base load during the cooling season, while the hotel has a base load during this season that is almost imperceptibly different from the annual base load. Looking at the thermal profiles, the oscillatory thermal consumption pattern during the heating season that was observed in hotels is further accentuated in this climatic zone, with very closely spaced peaks and dips. However, it is also worth noting that during the winter season, for both types of buildings, the thermal demand never reaches the summer values observed in previous climatic zones, indicating that the HVAC heating system reduces its power during the night but does not reach very low values, except near the end or beginning of the heating season. There were no significant differences observed in the duration of the heating season, as observed in the 3A and 4A zones. The summer thermal demand of the hospital is becoming comparable to the heating demand during the transition periods between the heating and cooling seasons.

| Climate zone | Electrical intensity $\left[\frac{kWh}{m^2\,y}\right]$ | | Average electrical Intensity climate $\left[\frac{kWh}{m^2\,y}\right]$ | |
|---|---|---|---|---|
| | Hotel | Hospital | Hotel | Hospital |
| **3A** | 179.60 | 253.04 | 172.91 | 235.82 |
| **4A** | 168.49 | 208.92 | 170.33 | 209.47 |
| **5A** | 154.47 | 188.15 | 155.42 | 189.89 |
| **6A** | 166.88 | 192.36 | 168.99 | 190.74 |

*Table 20 - Intensities of electrical consumption in hospitals and hotels*

Based on the comparison between hospitals and hotels located in the same climatic zones and across different zones, certain patterns have been identified in terms of the shape of their load profiles. In the same climatic zone, hospitals generally have lower specific electricity consumption compared to hotels due to the presence of high electrical intensity medical equipment, leading to greater variability between minimum and maximum electrical demand throughout the year. The higher annual electrical demand has been confirmed in Table 20, which also shows that hotels are less energy-intensive than hospitals in the same climatic zone.

Furthermore, hospitals tend to have a longer cooling season than hotels and more frequent cooling system activations outside the cooling season. This results in a clear summer electrical base load, which is smaller in hotels where the electrical power for cooling is modulated more carefully, and the summer base load tends to disappear as the climate becomes colder.

Similarly, the duration of the heating season is generally longer in hospitals, with more frequent off-season activations than hotels, which increases as the climate becomes colder. However, the durations of the heating season become comparable between hotels and hospitals as the climate becomes colder. The different durations of both heating and cooling seasons lead to different values of E/T ratio, as shown in Table 22, with the ratio decreasing as the climate becomes colder.

| Climate zone | Thermal intensity $\left[{kWh}/{m^2\,y}\right]$ | | Average thermal Intensity climate $\left[{kWh}/{m^2\,y}\right]$ | |
|---|---|---|---|---|
| | Hotel | Hospital | Hotel | Hospital |
| **3A** | 71.90 | 93.08 | 74.33 | 90.03 |
| **4A** | 104.23 | 110.95 | 101.26 | 106.27 |
| **5A** | 121.16 | 143.59 | 125.96 | 141.13 |
| **6A** | 181.87 | 185.81 | 194.86 | 174.10 |

*Table 21 - Intensities of thermal consumption in hospitals and hotels*

At the same time, the E/T ratios for hotels are always slightly lower than for hospitals in the same climatic zone, but still comparable. This is because the greater annual electrical demand of hospitals due to highly energy-intensive medical equipment is accompanied by a greater stability of annual thermal demand, which in cold zones 5A and 6A results in hospitals using a significant amount of heating even during the summer.

In summary, at the same climatic zone, hotels, with a more constant base load throughout the year and less variation between the base load and demand peaks, can cover a greater portion of their electrical demand with a SOFC cogeneration system that operates at a constant power. On the other hand, they have greater variability in their thermal load profiles than hospitals, leading to a reduced amount of recoverable thermal energy from the waste heat from the SOFC system.

| Climate zone | E/T | | Average E/T climate | |
|---|---|---|---|---|
| | Hotel | Hospital | Hotel | Hospital |
| **3A** | 2.50 | 2.72 | 2.33 | 2.62 |
| **4A** | 1.62 | 1.88 | 1.68 | 1.97 |
| **5A** | 1.27 | 1.31 | 1.30 | 1.34 |
| **6A** | 0.92 | 1.03 | 0.87 | 1.10 |

*Table 22 - Electric to thermal ratios comparison between hospitals and hotels*

### 4.3.2 Hourly load profiles: typical days analysis

This subsection compares the specific daily electric and thermal profiles of selected hospitals and hotels for the same climatic zone, starting from the hottest zone (3A) and proceeding towards colder climates. Examining the daily electric profiles in the 3A zone, the first observation is the different magnitude of the specific energy consumption in terms of maximum and minimum values, both of which are higher in hospitals. Both buildings exhibit a peak in electric demand that starts to rise steeply around 8:30 am, reaching its peak around 10 am, before gradually decreasing towards the afternoon. Looking at the hospital profiles on the solstice days (June 21st and December 21st), the shapes of the profiles are very similar to each other except for the intensity of the demand. After the mid-morning peak, the demand starts to decrease and remains relatively stable until 4 pm, before dropping sharply. The profiles on March 20th and September 23rd also have a similar shape, with the respective highest electric demand of the day from 12 pm to 2:30 pm, followed by a rapid decrease and almost constant demand from 5:30 pm until the next day for September 23rd, while decreasing more slowly and reaching a steady state only after midnight for March 20th. On the other hand, the hotel electric profiles associated with the four typical days are less variable in the annual amplitude between minimum and maximum values than the hospitals, as previously observed in the annual profiles, but more variable in shape and time-lagged between each other.

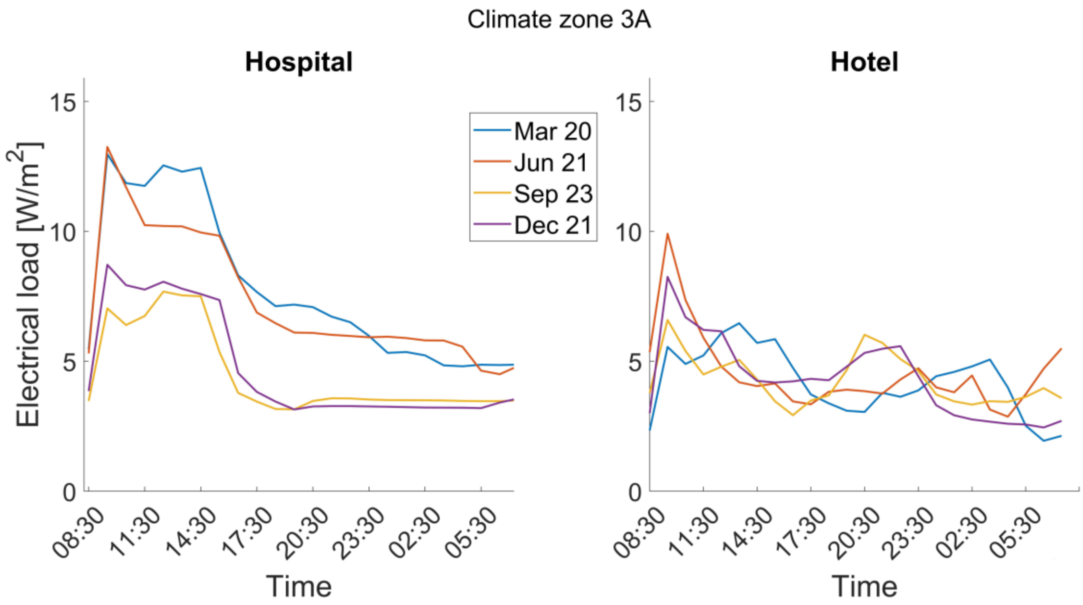


*Figure 47 - Climate zone 3A specific electrical loads*

When examining the same buildings in terms of thermal demand profiles in Figure 48, the same peak in demand that leads to the maximum thermal power demand for all the typical days and for both building types can be observed, followed by a rapid decrease in the following two hours. For the hospital, in the figure, the very similar typical days are March 20th and June 21st, and September 23rd and December 21st, with September 23rd having slightly higher thermal demand than December 21st from 8:30 pm. Looking at the four typical days of the hotel, similarities can still be observed between March 20th and June 21st, but December 21st is characterized by a much higher demand for thermal energy compared to September.

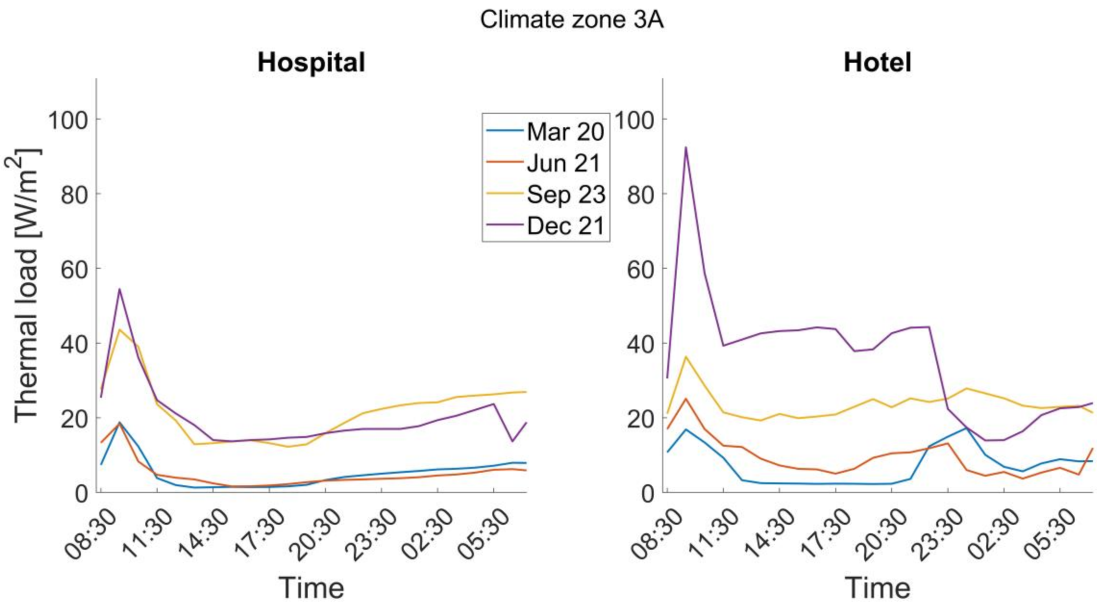


*Figure 48 - Climate zone 3A specific thermal loads*

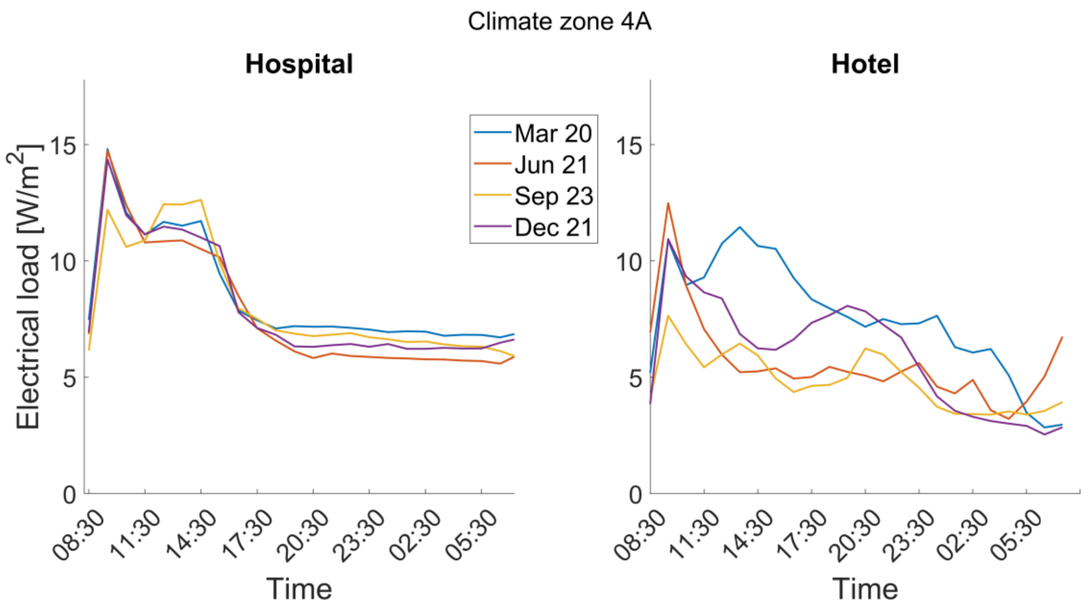


*Figure 49 - Climate zone 4A specific electrical loads*

Upon examining the comparisons in climatic zone 4A, and looking at the electric profiles in Figure 49, it is immediately noticeable how the hospital has very similar profiles across all the typical days, with the same peak in both cases occurring at 9:30 in the morning, and higher consumption in the early afternoon hours that sharply decreases in the following three hours, with the four profiles being almost overlapping. Afterward, the consumption remains almost constant until 6:00 the next day, except for June 21st, where the demand drops further until 8:30 p.m., where it stabilizes until the next day. The behavior is different in hotels, where the four typical days are characterized by significantly different electric load profiles, both in shape and intensity. In the hotel case study, it is immediately noticeable that June 21st has the highest peak due to cooling both at 9:30 a.m. and from 4:00 a.m. the next day when there is a surge in electric demand. Notably, the blue curve associated with March 20th leads to the highest daily consumption among the four days considered, followed by the purple curve associated with December 21st.

When analyzing their respective thermal demand profiles in Figure 50, the situation is the opposite of the electric demand profiles. In this case, it is the hotel that shows similar profile shapes for all 4 days, although different in height, with the December curve being above the others due to the high demand for heating.

On the other hand, looking at the hospital's thermal demand profiles, there is an immediate peak in heating demand during December 21, along with higher demand throughout the day that remains more than triple compared to the other 3 days analyzed. Another consideration is the peak demand associated with September 23, which is shifted forward by an hour compared to the other 3 days.

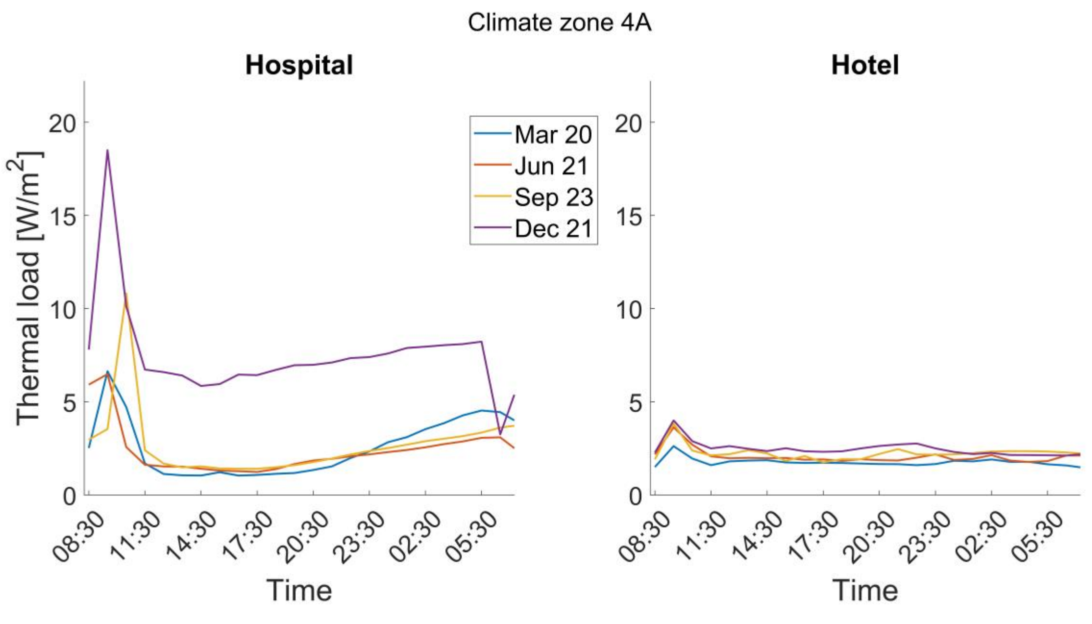


*Figure 50 - Climate zone 4A specific thermal loads*

Moving on to buildings in climate zone 5A, whose specific electric and thermal profiles are shown in Figure 51 and Figure 52, it is noticeable that, once again, the electric profiles of hospitals have a very similar shape for all four typical days, with differences only in their intensity. The lowest curve is the one for September 23, which does not differ much from that of December 21, while the highest curve is the blue one representing the daily electric profile during March 20. Looking at the hotel, the curve with the highest demand for electric energy is the blue one, with a peak demand at 4:00 PM, followed by the one for December 21.

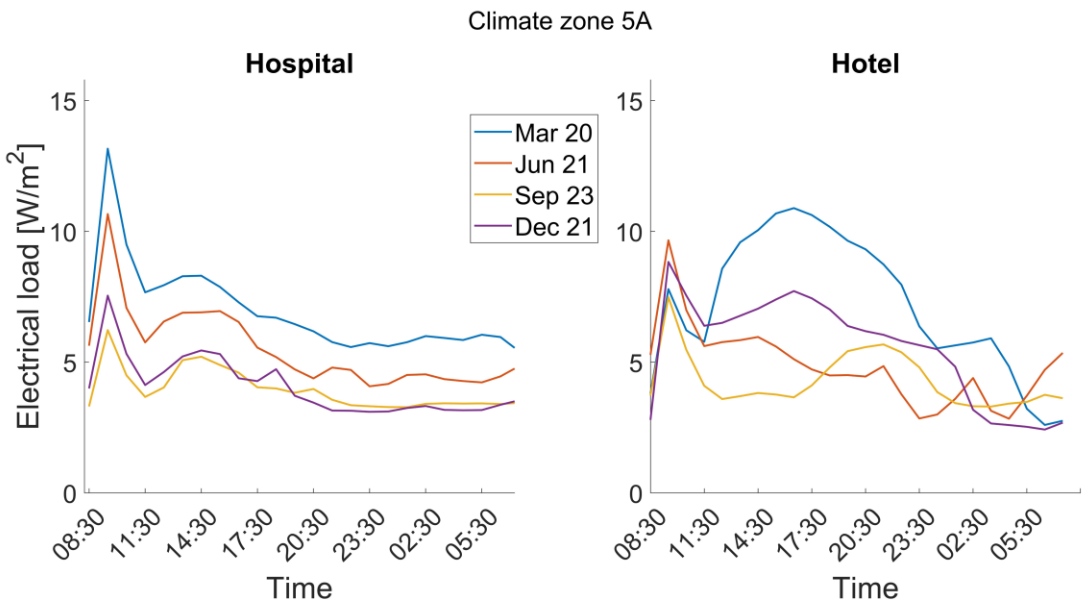


*Figure 51 - Climate zone 5A specific electrical loads*

In analyzing the specific hourly thermal profiles shown in Figure 52, as expected, the days with the highest annual thermal demand are the 21st of December, followed closely by the profiles associated with the 23rd of September, for both building types. Once again, the demand peaks for both buildings and all four days occur at 9:30 am, followed by a decrease over the next two hours to reach an absolute minimum around 2:30 pm, before starting to rise again with different slopes depending on the season being considered.

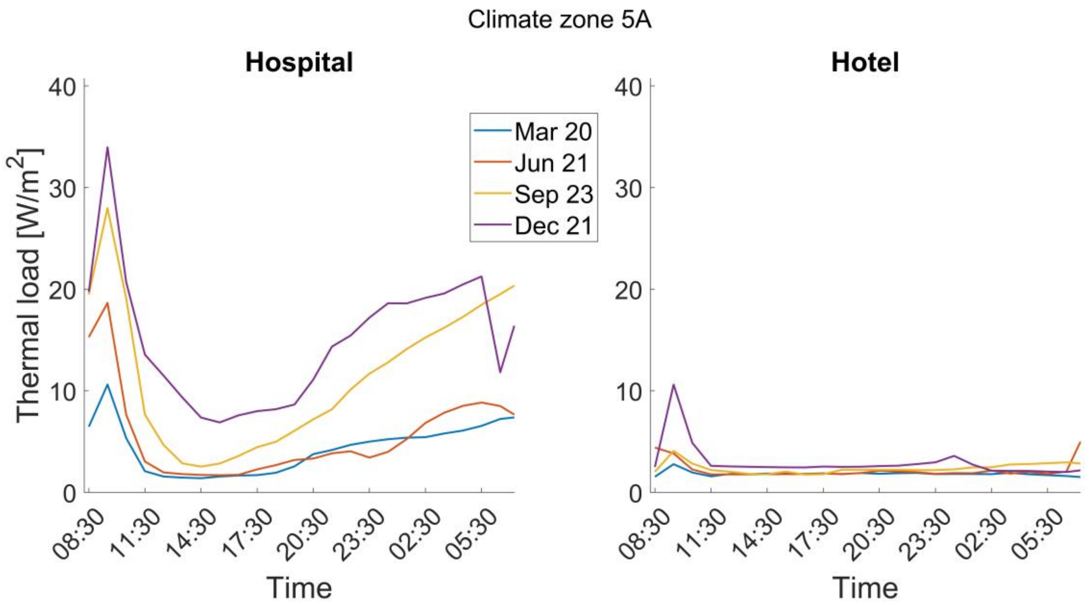


*Figure 52 - Climate zone 5A specific thermal loads*

In the final comparison, the specific daily electric and thermal profiles of hospitals and hotels in climate zone 6A, the coldest one considered, were analyzed. As in all other hospitals, the electric profiles, shown in Figure 53, have similar shapes, with the one associated with March 20th significantly differing from the others. In contrast, the hotel profiles exhibit different shapes and time shifts between minimum and maximum values depending on the day type considered, with the highest morning peak occurring on June 21st.

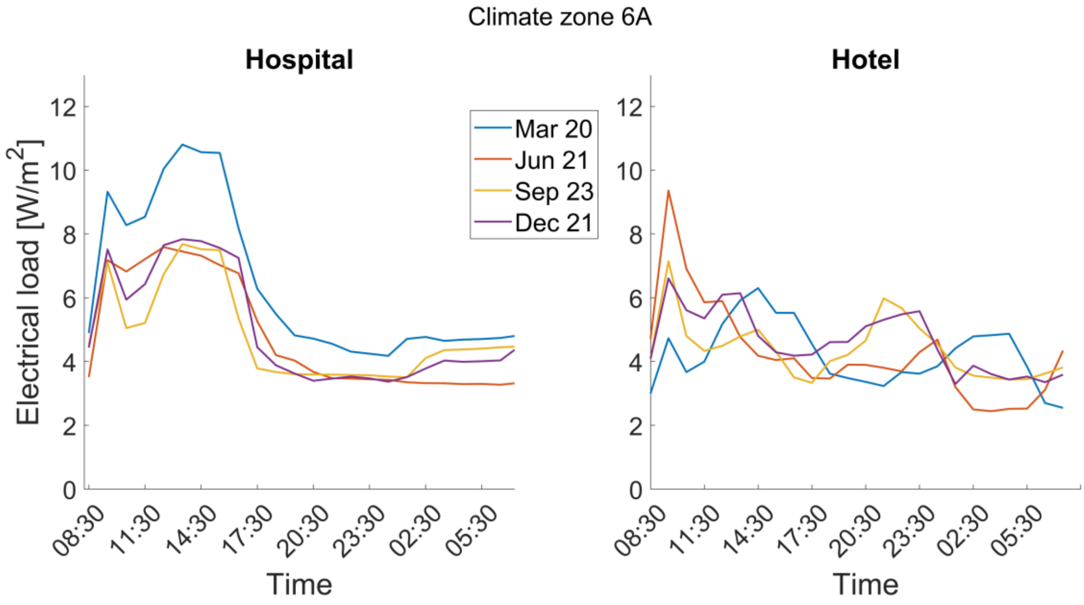


*Figure 53 - Climate zone 6A specific electrical loads*

Looking at the thermal profiles for zone 6A, shown in Figure 54, it is immediately apparent that the hospital and hotel have comparable average specific thermal consumption, unlike in zones 4A and 5A where hotel specific thermal consumption was an order of magnitude lower than the hospital's for the same climatic zone. For the hospital, due to the extremely cold winters that characterize this climatic zone, the only day with lower thermal energy demand than the others, is March 20th, while for the hotel it is September 23rd. It is worth noting that even on a relatively warm day like June 21st, the heating system still turns on in the hotel at around 4pm, which did not occur in other climatic zones except in hospitals.

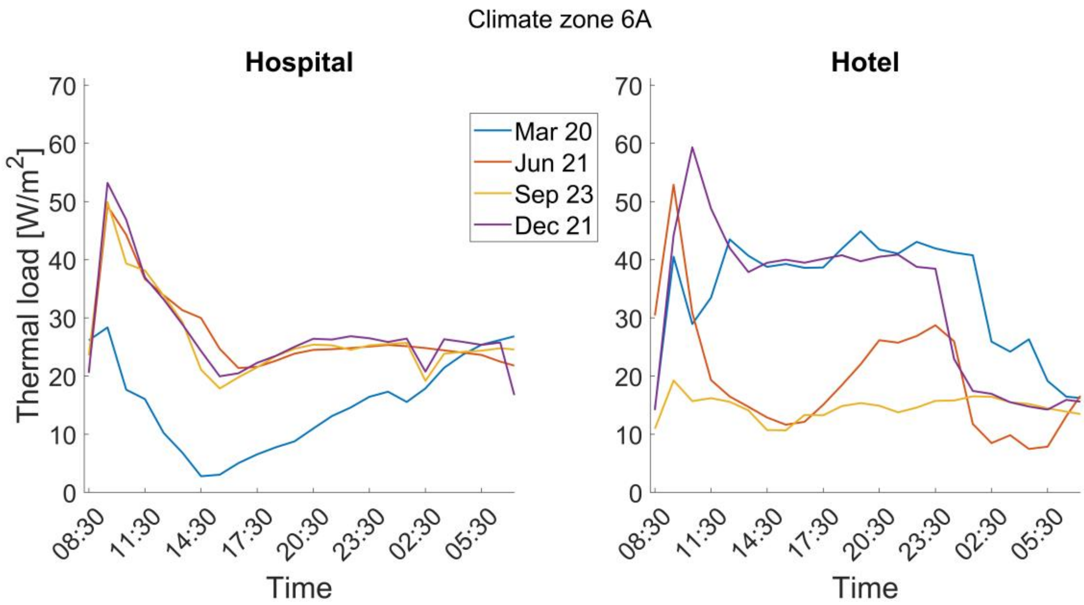


*Figure 54 - Climate zone 6A specific thermal loads*

After analyzing the specific daily load profiles of hospitals and hotels in the same climatic zone for four typical days corresponding to the solstices and equinoxes of 2018, it is possible to identify common trends among the different climatic zones.

Looking at the comparisons between specific electric load profiles, it is observed that the electric consumption of hotels is always lower than that of hospitals in the same climatic zone. The daily oscillation between minimum and maximum electric demand is always greater for hospitals than for hotels, as medical equipment and mechanical ventilation systems tend to be used more during the day due to daily medical visits, while they are used less during the night.

Regarding the trend of thermal consumption, it was noticed that hospitals have a specific daily thermal consumption profile comparable to that of hotels only in the most extreme climatic zones considered, i.e., the hottest (3A) and the coldest (6A).

These considerations suggest that, in terms of electricity, the constant electric power output from the SOFC can cover a greater percentage of the electric demand for hotels, especially in colder climates with lower cooling demand. In contrast, in terms of thermal energy, hospitals would benefit more from the coupling with SOFC, especially in climates characterized by milder winters and significant thermal energy demand even in the summer.

Overall, the results indicate that the coupling of SOFC with hospitals and hotels could offer significant advantages, but the specific characteristics of the buildings and their use patterns, as well as the local climatic conditions, should be carefully considered in order to maximize the benefits.

## 4.4 SOFC scenario

The following subsections present the results obtained in terms of LCOE and energy coupling of the SOFC with the analyzed buildings, first for hospitals and then for hotels. The last subsection shows the LCOE results obtained by assuming a future evolution of the SOFC technology characterized by lower investment costs, both for hospitals and hotels.

### 4.4.1 Results of LCOE and energy coverage for hospitals

In analyzing the results in terms of LCOE, the focus is first on the results of the study considering only each of the 4 SOFCs as the control volume for the calculation, as reported in Table 23.

| LCOE: SOFC control volume | HOSPITAL 1 | HOSPITAL 2 | HOSPITAL 3 | HOSPITAL 4 |
|---|---|---|---|---|
| **Climate zone (Building America)** | Mixed-Humid | Mixed-Humid | Cold | Cold |
| **Climate zone (ASHRAE)** | 3A | 4A | 5A | 6A |
| **Surface** $[m^2]$ | 6968 | 13935 | 6968 | 69677 |
| $P_{nom,SOFC}$ **[kW]** | 23 | 38 | 20 | 200 |
| $E/T_{avg}$ | 2.72 | 1.88 | 1.31 | 1.03 |
| **LCOE** $[€/\mathrm{kWh}]$ | 0.282 | 0.282 | 0.282 | 0.245 |

*Table 23 - Resulting LCOEs and main characteristics for hospitals: SOFC control volume*

The results show an equal value of LCOE for hospitals in climate zones 3A, 4A, and 5A, amounting to €0.282/kWh, while the hospital in climate zone 6A shows a slightly lower LCOE of €0.245/kWh. The fact that the values are the same is due to considering only the control volume of the SOFC, so the only difference among the 4 hospitals is in the natural gas price range purchased from the grid, which depends on the annual volumes of natural gas purchased. As the last hospital is the largest among the 4 considered, the calculations lead to much higher annual natural gas consumption compared to the other 3 hospitals, resulting in a reduction in the purchase price from the grid and a consequent reduction in the LCOE calculated with a control volume that includes only the SOFC.

The LCOE results for the four selected hospitals, including the building itself in the control volume along with the SOFC, are presented in Figure 55. Once again, the hospital located in the coldest climate zone among those selected proves to be the most cost-effective for installing a SOFC-based cogeneration system. This is due to a lower gas price resulting from a higher annual gas purchase volume compared to the other three cases, as well as a lower electricity price for the same reason. However, regardless of energy prices, the percentage variations in electricity and natural gas purchase volumes between the baseline scenario, where all electricity and natural gas are purchased from the grid, and the current scenario, where a lower proportion of electricity is purchased from the grid, should also be considered.

The results of these analyses are reported in Table 24, where two trends can be identified. The first trend is that as we move towards colder climatic zones, the percentage of additional natural gas to be purchased compared to the baseline scenario decreases, as the component of natural gas needed to cover the building's thermal demand decreases with colder climates. This is accompanied by an increase in the duration of the heating season and the demand for thermal energy during the summer. On the other hand, in terms of electricity not purchased from the grid, this hospital is the second among the four for the percentage of electricity saved, amounting to 52.33% less than the baseline scenario.

The second lowest LCOE value is associated with the hospital in climatic zone 3A, characterized by the lowest value of heating degree days. Despite having the highest percentage increase in natural gas consumption, exceeding 200% compared to the baseline scenario, and being in third place for electricity savings, it should be noted that this is the warmest climatic zone and therefore has the lowest annual natural gas consumption. As a result, the percentage increase in additional gas needed to power the SOFC is relatively high. However, what positively affects the LCOE is the percentage of thermal demand that can be covered by the SOFC, and this hospital has the highest percentage of thermal energy covered by SOFC due to its thermal profile in Figure 28, which is characterized by shorter duration demand peaks compared to the other three hospitals.

The hospitals in the mild 4A and the first cold 5A climatic zones have intermediate behavior in terms of the shape of the electrical and thermal profiles and the results of the associated LCOEs.

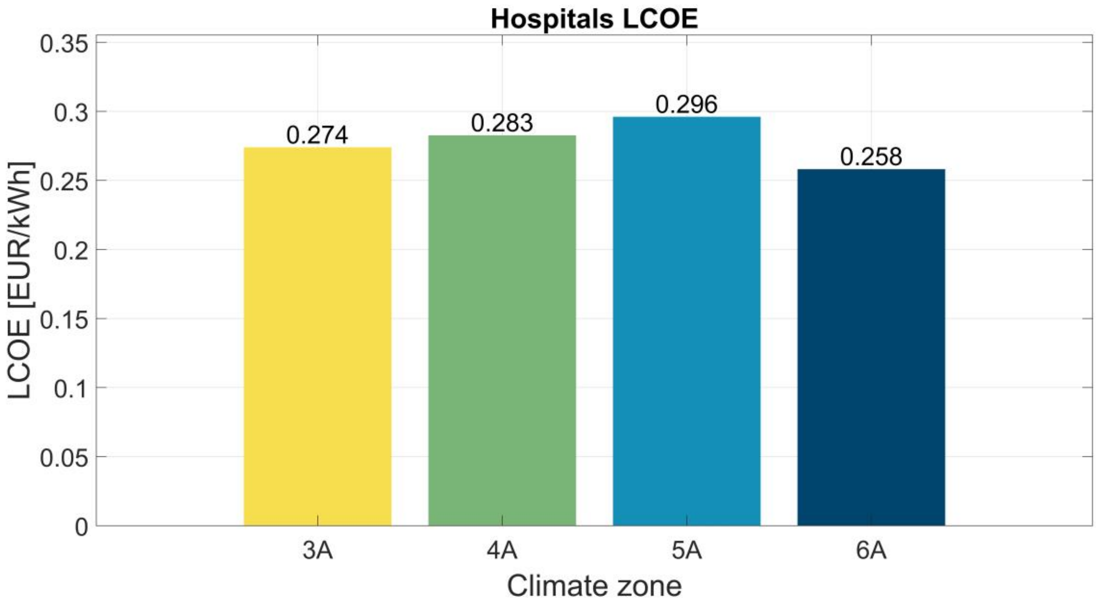


*Figure 55 – Hospitals' LCOE results*

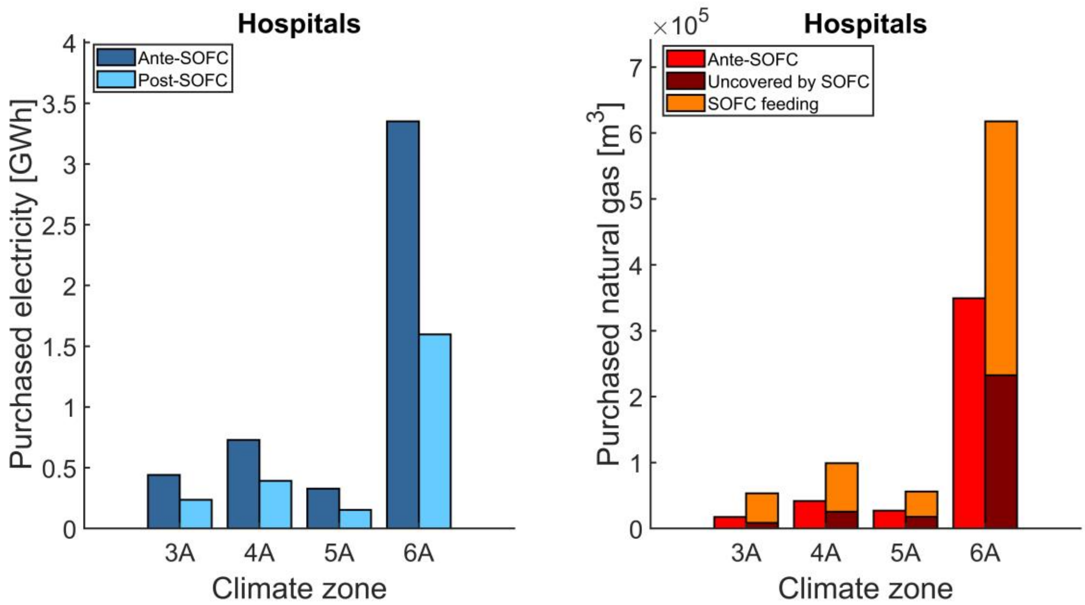


*Figure 56 - Hospitals: purchased electricity and NG before and after the implementation of SOFC-based CHP system*

| HOSPITALS | | | | |
|---|---|---|---|---|
| | **Covered thermal demand [%]** | **Additional NG [%]** | **Electricity saved [%]** | **LCOE [€/kWh]** |
| **3A** | 50.92 | +205.21 | -46.30 | 0.274 |
| **4A** | 39.04 | +137.33 | -46.03 | 0.283 |
| **5A** | 34.65 | +107.58 | -53.34 | 0.296 |
| **6A** | 33.47 | +76.76 | -52.33 | 0.258 |

*Table 24 - Hospitals LCOE and energy results*

### 4.4.2 Results of LCOE and energy coverage for hotels

In this section, the results of the LCOE calculations for the hotels under analysis are summarized. Table 25 summarizes the LCOE results calculated considering the control volume containing only the SOFC system. A value of LCOE equal to 0.282 [€/kWh] was obtained for hotels belonging to climate zones 3A and 4A, while an LCOE of 0.334 [€/kWh] was obtained for hotels in climate zones 5A and 6A. The last two hotels have such a high LCOE because they are small in size compared to the other two, and consequently, they have lower annual volumes of electricity and natural gas purchases, falling into the price bands for small consumers, which are more expensive.

| LCOE: SOFC control volume | HOTEL 1 | HOTEL 2 | HOTEL 3 | HOTEL 4 |
|---|---|---|---|---|
| **Climate zone (Building America)** | Mixed-Humid | Mixed-Humid | Cold | Cold |
| **Climate zone (ASHRAE)** | 3A | 4A | 5A | 6A |
| **Surface** $[m^2]$ | 32516 | 13935 | 1626 | 3484 |
| $P_{nom,SOFC}$ **[kW]** | 62 | 33 | 5 | 7 |
| $E/T_{avg}$ | 2.50 | 1.62 | 1.27 | 0.92 |
| **LCOE** $[€/kWh]$ | 0.282 | 0.282 | 0.334 | 0.334 |

*Table 25 - Resulting LCOEs and main characteristics for hotels: SOFC control volume*

When considering the results of LCOE calculations for the analyzed hotels with the building included in the control volume, the hotel located in climatic zone 3A has the lowest LCOE value of 0.255 [€/kWh], as shown in Figure 58, followed by the hotel in zone 4A with a value of 0.289 [€/kWh], and finally, the hotels in zones 5A and 6A with values relatively close to each other. As in the LCOE calculations with only the SOFC system as the control volume, the strong influence of the price range of natural gas and electricity purchased from the grid remains, which is dependent on the annual purchase volumes. Referring to Table 26, the performance of the SOFC cogeneration system in terms of electric and thermal demand coverage can be compared. The hotel in climatic zone 3A shows greater coverage of the total thermal demand but lower coverage of the electric demand, while the hotel in zone 5A can be considered the most energy-compatible with a SOFC-based cogeneration system, as it has the second-highest percentage of thermal energy covered by SOFC, which is very close to that of the hotel in zone 3A, and significant electric demand coverage, exceeding 60% of the annual electric demand covered.

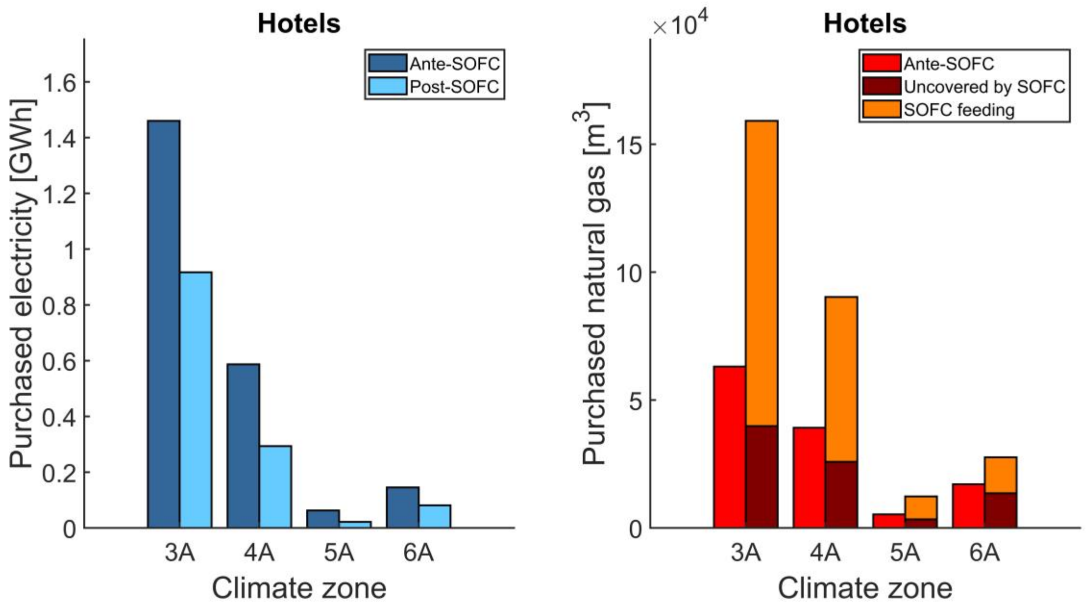


*Figure 57 - Hotels: purchased electricity and NG before and after the implementation of SOFC-based CHP system*

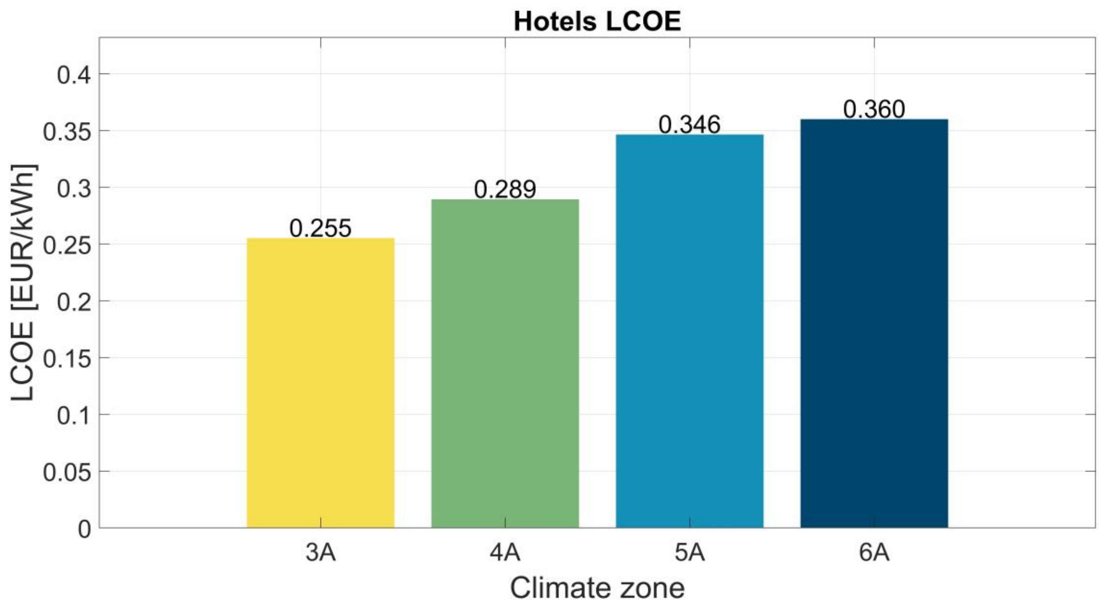


*Figure 58 – Hotels' LCOE results*

| HOTELS | | | | |
|---|---|---|---|---|
| | **Covered thermal demand [%]** | **Additional NG [%]** | **Electricity saved [%]** | **LCOE [€/kWh]** |
| **3A** | 36.91 | +152.19 | -37.20 | 0.255 |
| **4A** | 33.95 | +130.35 | -49.95 | 0.289 |
| **5A** | 36.38 | +131.82 | -64.84 | 0.346 |
| **6A** | 20.72 | +61.70 | -44.14 | 0.360 |

*Table 26 - Hotels LCOE and energy results*

### 4.4.3 Hospitals and hotels LCOE in future scenario

In this final subsection, the previously illustrated LCOE results are compared among different categories of buildings, and new LCOE values are calculated considering a possible future development of the technology and its production and sales volumes, leading to a reduction in investment costs and an increase in stack lifespan. The building with the lowest LCOE among all is the hotel located in the warmest climatic zone analyzed, where it is also the most performant in terms of annual thermal demand covered by SOFC among the buildings of its category. Similarly, the hospital in category 3A is the best performing among hospitals and overall among all buildings studied, in terms of thermal demand covered by SOFC exceeding 50%, although not in terms of LCOE due to the low volumes of electricity and gas purchased from the grid, resulting in higher energy costs compared to buildings of the same category but larger in size and therefore with higher annual consumption.

The analysis shows that, for both hotels and hospitals, the greatest coverage of the thermal demand is found in the mildest climate among those considered, due to a lower intensity of heating peak demands. However, for hospitals, at the same climate, higher coverage of thermal demand through the SOFC system is achieved, owing to a significant demand for thermal energy even during the summer season.

Regarding the reduction in electricity demand from the grid due to SOFC coverage, hotels perform better than hospitals in the mild climate of 4A and the first cold zone of 5A, while in the extreme climate zones, hospitals are better able to cover their electricity demand than hotels.

The LCOE results obtained for hotels and hospitals do not necessarily reflect the energy feasibility of adopting an SOFC cogeneration system in buildings characterized by climatic conditions that are more compatible with such a system in terms of the hourly electrical and thermal load profiles. This is because, due to the high costs of investment and stack replacement, buildings with the lowest LCOE values are not always the most energy-efficient in terms of adopting an SOFC cogeneration system. Additionally, the structure of the electricity and natural gas purchase prices, which depend on the annual energy purchase volumes, obscures which building categories and climate zones are better able to perform from an energy perspective.

To verify the aforementioned statements, the LCOE of the 8 buildings were calculated using the same prices for electricity and natural gas for all buildings, regardless of their annual purchase volumes, by taking the average value used as input in the previous LCOE calculation, as shown in Table 9. The future improvements in SOFC technology were also considered solely from an economic perspective.

Table 8 includes the current values used for the previous LCOE calculations and the potential future target values of two main economic parameters as hypothesized in the COMSOS project [26]. The technical performance improvements, such as an increase in the electrical efficiency, are also considered in the COMSOS target scenario, but in this study, they are assumed to remain unchanged to analyze the impact of the economic improvement alone on the LCOE results.

The LCOE values obtained by assuming a reduction in the investment cost of the entire SOFC system and an increase in the stack's useful life are then reported in Table 27.

| HOTELS | | | | | |
|---|---|---|---|---|---|
| | **Covered thermal demand [%]** | **Additional NG [%]** | **Electricity saved [%]** | **LCOE current [€/kWh]** | **LCOE future [€/kWh]** |
| | 36.91 | +152.19 | -37.20 | 0.255 | 0.197 |
| | 33.95 | +130.35 | -49.95 | 0.289 | 0.196 |
| | 36.38 | +131.82 | -64.84 | 0.346 | 0.191 |
| | 20.72 | +61.70 | -44.14 | 0.360 | 0.226 |
| **HOSPITALS** | | | | | |
| | **Covered thermal demand [%]** | **Additional NG [%]** | **Electricity saved [%]** | **LCOE current [€/kWh]** | **LCOE future [€/kWh]** |
| | 50.92 | +205.21 | -46.30 | 0.274 | 0.186 |
| | 39.04 | +137.33 | -46.03 | 0.283 | 0.194 |
| | 34.65 | +107.58 | -53.34 | 0.296 | 0.199 |
| | 33.47 | +76.76 | -52.33 | 0.258 | 0.208 |

*Table 27 - Hospitals and hotels current and future LCOE results*

The new LCOE results obtained assuming a reduction in the investment cost of the entire SOFC system and an increase in the stack lifespan are now more representative of buildings where both thermal and electrical demand are mostly covered by the SOFC system's constant power operation. As for hotels, the lowest LCOE is found in the system applied to the building in the 5A climatic zone, with a value of 0.191 [€/kWh], which is the building that reduces its natural gas and electricity purchased from the grid the most thanks to the SOFC system, especially from the electrical point of view, thanks to the climatic zone characterized by short summers and monthly average temperatures lower than in the warmer climatic zones, which reflects on the electrical load profiles in a lower demand for cooling annually and consequently a lower deviation from the baseload.

Regarding hospitals, the lowest LCOE value of 0.186 [€/kWh] was obtained for the hospital in climate zone 3A, which is the lowest among all the hospitals and among all the buildings analyzed. In this case, since it is a warm climate zone, the benefit of greater thermal recovery from SOFC prevails due to less deviation during the heating season in the demand for thermal energy and therefore natural gas, from the constant thermal power output from the SOFC, compared to the negative effect in terms of uncovered electrical demand due to the increased need for summer cooling that characterizes its climate zone.

Based on these new LCOE results, some conclusions can be drawn about the feasibility of installing a SOFC-based cogeneration system in hospitals and hotels in different climatic conditions.

The demand for thermal energy in a hotel is more variable throughout the year compared to a hospital in the same climatic zone. Therefore, even in warm climatic zones without excessive winter heating loads, the installation of a SOFC system without a thermal storage system allows for a lower percentage savings in natural gas compared to a hospital in the same climatic zone. This percentage savings decreases as one moves towards colder climates. Conversely, in climates that are too hot, such as zone 3A, there is a decrease in the percentage of electrical demand covered by the SOFC due to the predominance of cooling loads.

In hospitals, on the other hand, as one moves from colder to milder climates, the quantity of thermal demand that can be covered by the SOFC increases due to its less variable nature throughout the year. In addition, a non-negligible portion of natural gas savings is achieved even in summer, compared to the increase in cooling load due to rising summer temperatures and the longer annual cooling season, which does not affect annual electricity consumption as much as in the case of hotels, where it is determined to a greater extent by the use of medical equipment, mechanical ventilation, and internal lighting.

# Conclusions

The economic feasibility of a stationary SOFC-based cogeneration system is influenced by various technical and economic factors. The present work investigates the combined influence of load profiles and climate zones on the installation of SOFC-based cogeneration systems to produce local electrical and thermal power in two different categories of commercial buildings, namely hospitals and hotels, located in four different types of climates according to the ASHRAE definition of climate zones, starting from warm climates and proceeding to colder ones. This analysis uses high-reliability modeled hourly load profiles divided by end-uses of commercial buildings located in the USA, which were manipulated using self-made scripts in the MATLAB environment, and SOFC technical data retrieved from the COMSOS project.

The climate in which the buildings under analysis are located was determined based on previous literature on the feasibility of this type of cogeneration system. The evaluation of the electrical to thermal ratio (E/T ratio) of the SOFC system and the E/T ratio of commercial buildings was used to exclude climates with excessively high electrical power demand and too low thermal demand, such as very hot climates, as well as climates with excessively high thermal demand compared to electrical demand, such as very cold climates. The number of buildings per climate zone was also a factor in the selection of climate zones. Zones with a low number of buildings and limited representativeness were excluded, as they were not statistically significant due to the limited size of the dataset from which load profiles were extracted.

Before choosing the individual building models for this study, a characterization of annual energy consumption for hospitals and hotels was conducted. This was done to determine the average values per category in different climatic zones for annual electrical and thermal demand. Additionally, it was done to determine for both chosen categories which end-use distributions of thermal and electrical energy have the greatest impact on total consumption and how they vary depending on the climatic zone. The analyses in this phase of the study were conducted by comparing specific demands, i.e., per unit of area, in order to eliminate as much as possible the dependence of annual consumption on the size of individual buildings. There is a great variability in the surface areas of the buildings in the dataset. Only buildings that are powered by a natural gas HVAC system were analyzed, as a building with a fully electric HVAC system would have too low of a thermal energy demand to make integration with a cogeneration system like the one studied economically viable.

After characterizing the annual energy consumption of hospitals and hotels in different climate zones for electrical and thermal demand, the specific consumption values were determined for each category in each zone. The distributions of the energy end uses impacting total consumption and how they vary with the climate zone were also determined. Analyses were conducted on HVAC systems powered by natural gas to eliminate buildings with fully electric HVAC systems, which have insufficient thermal energy demand for cogeneration integration. Based on these analyses, a total of eight buildings were selected four hospitals and four hotels, each in one climate zone and equipped with the most common HVAC system for their category. Hourly load profiles of the eight buildings were selected using a MATLAB algorithm to find the minimum Euclidean distance between their specific annual electrical and thermal demands and the category average for each of the four climate zones. The hourly electrical and thermal profiles of the selected buildings were then compared on an annual and daily basis, using 4 typical days, within and between categories and climate zones to identify the primary similarities and differences.

Finally, a techno-economic analysis was carried out for the 8 buildings after the installation of the SOFC system. The input data used for the analysis were the techno-economic parameters of the SOFC system obtained from the COMSOS project and the purchase prices of electricity and natural gas from the commercial grid, divided by annual consumption. Results were obtained in terms of LCOE, as well as annual coverage of the electrical and thermal demand by the cogeneration system. The hotel located in climate zone 3A, the mildest among the 4 analyzed zones, had the lowest LCOE value among the 8 buildings, equal to 0.255 [€/kWh], and it was also the hotel in which the thermal demand was covered the most, reaching almost 37%, and a similar percentage of electrical energy was produced by the SOFC system. Considering both the highest electricity savings and the highest coverage of thermal demand by the cogeneration system, the most performing hotel was located in climate zone 5A, the first of the 4 cold zones analyzed based on its heating degree days and monthly average temperatures, but still below zone 6A, which is the coldest zone among those analyzed.

In this case, the coverage of the electric energy demand through the SOFC was almost 65% on an annual basis, and the coverage of thermal energy was only one percentage point lower than that of the hotel in 3A. The building that had the highest percentage of its electric demand covered by the SOFC was the hospital located in 3A, with a coverage slightly above 50%, accompanied by a coverage of the thermal demand around 46% and an LCOE of 0.274 [€/kWh], the second lowest among the 8 buildings, only higher than the hospital located in zone 6A with an LCOE of 0.258 [€/kWh]. In the latter, the SOFC system managed to cover 52% of the annual electric demand, just below one percentage point compared to the most efficient in terms of electric energy saving, located in the immediately less cold zone 6A, but from the point of view of the coverage of the thermal demand, it was the worst among the hospitals, around 33% of the total. For the two intermediate climate zones, namely mixed 3A and the first cold zone 5A, the greater coverage of the electric demand only occurred in the hotels, which in the analysis of annual and daily profiles showed a smaller deviation in the electric profiles compared to hospitals, which instead, at parity of climate zone, oscillate with greater amplitude due to the high impact on electric consumption of medical equipment and the forced ventilation system, which must cope with a highly variable number of occupants during the day and greater activity in general during the day compared to the night.

On the other hand, looking at buildings in climate zones 3A and 6A, respectively the warmest and coldest among those selected, hospitals are able to cover their electrical demand through SOFC to a greater extent than their hotel counterparts in the same climate zone. This is because the electrical demand required by the HVAC system in cooling mode increases much more the variability in annual electrical consumption in hotels than in hospitals, where it is still significant but less impactful on the total due to other consumption items such as medical equipment and mechanical ventilation systems. As climate zone 3A is characterized by the longest cooling season and higher monthly average temperatures, the deviation from the annual baseload during summer is greater, and thus, the electrical demand that cannot be covered by SOFC is higher, which has a greater impact on hotels than hospitals.

In the same climatic zone, hospitals have shown a lower LCOE compared to hotels as they are able to cover a greater portion of their electricity and thermal demand from the SOFC due to having less variable thermal load profiles throughout the year and a significant demand for thermal energy even during the summer months, compared to hotels. However, the LCOE values discussed were calculated using input data based on energy prices from the grid that are dependent on annual consumption, and the selected buildings vary in size and consequently in annual electricity and gas consumption. Buildings with higher annual consumption benefit from lower prices for electricity and gas from the grid. Another factor to consider is the current high investment costs of SOFC technology, as well as the short stack lifespan, which requires replacement three times within the 20-year project timeframe. Due to these input data, paradoxically, buildings with lower LCOE values may not necessarily be the most energy compatible with SOFC. Instead, their lower LCOE values may be due to a lower installed nominal power and consequently lower investment costs, as well as limited coverage of the energy demand covered by SOFC, compared to buildings with higher LCOE values. To highlight the positive effects of greater electricity savings from the grid and thermal coverage due to SOFC, an additional LCOE calculation was performed for the 8 buildings, considering uniform unit prices for energy purchased from the grid for all, regardless of annual purchase volumes, and a reduction in investment costs as hypothesized in future SOFC system scenarios from €11,980/kW to €3,340/kW and an increase in the fuel cell stack lifespan from 5 to 10 years.

The hotel category shows the lowest LCOE in the hotel located in the 5A climatic zone, with a value of 0.191 [€/kWh]. This building benefits the most from the SOFC system, reducing its natural gas and electricity purchased from the grid, especially in terms of electricity with a record value among the eight buildings of -65% purchased from the grid. This is due to the climatic zone having shorter summers and lower monthly average temperatures compared to the warmer zones, resulting in lower cooling demand annually and lower deviation from the baseload in electrical load profiles.

The hospital located in climate zone 3A showed the lowest LCOE value of 0.186 [€/kWh], which is the lowest among all the hospitals and buildings analyzed. This is due to the benefit of greater thermal recovery from SOFC, resulting from less deviation in the demand for thermal energy during the heating season, and therefore natural gas, because of the constant thermal power output from the SOFC. This benefit outweighs the negative effect of the increased need for summer cooling, which characterizes the warm climate zone and results in uncovered electrical demand.

In conclusion, the economic feasibility of a SOFC-based cogeneration system, which operates in a steady state, is influenced by various technical and economic factors. Once it has been identified which types of commercial buildings in which climatic zones can have their electrical and thermal demand mostly covered by SOFC, it is not necessarily the case that they are also the ones in which this system is the most economically convenient, as demonstrated in the LCOE calculations with current SOFC technology investment costs, where buildings that do not integrate well with the cogeneration system in question have lower LCOE values because it is currently more convenient to purchase electricity and natural gas directly from the grid rather than on-site production of thermal and electrical energy.

In the analysis where improvements are considered from the point of view of lowering investment costs and increasing the life of the stack, the buildings that have the highest demand for electrical and thermal energy covered by SOFC are also those with lower LCOE values. A lower investment cost, longer system life, and further improvement in electrical efficiency could make SOFC-based cogeneration systems economically convenient in the future, especially for those categories of commercial buildings characterized by a strong component of electrical baseload and limited deviation from it, as well as a ratio between electrical and thermal demand as close as possible to that characterizing the SOFC, which depends on its electrical and total efficiency. However, these considerations are valid as long as the structure of energy purchase prices from the grid does not make direct purchase more convenient, which for such a system powered by natural gas cannot ignore the purchase price of its fuel and the purchase price of electricity. In particular, as demonstrated in other studies, if the purchase price of gas from the grid rises above certain limits, together with a sufficiently low price of electricity, an SOFC system may never be cost-effective. Nevertheless, the SOFC system installed in the buildings in this study is still powered by a fossil fuel such as natural gas purchased from the grid, which in addition to environmental problems and the fact that it is not an inexhaustible source, also leads to a price that, as seen in recent years, can be strongly fluctuating depending on the geopolitical situation. However, the potential of a fuel cell also lies in fuel flexibility, allowing it to be fueled, for example, with biogas or biomethane or directly from hydrogen produced from surplus renewable energy, allowing for energy production characterized by lower CO2 emissions per kWh produced thanks to better efficiency (if H2 is not used) and a strong reduction of SOx and NOx compared to internal combustion systems powered by the same fuel.

## References


[1] IEA, “World Energy Outlook 2022,” 2022. Accessed: Mar. 01, 2023. [Online]. Available: https://www.iea.org/reports/world-energy-outlook-2022

[2] IEA, “Energy Technology Perspectives 2023,” 2023. Accessed: Mar. 01, 2023. [Online]. Available: https://www.iea.org/reports/energy-technology-perspectives-2023

[3] “Fit for 55 - The EU’s plan for a green transition - Consilium.” https://www.consilium.europa.eu/en/policies/green-deal/fit-for-55-the-eu-plan-for-a-green-transition/ (accessed Mar. 01, 2023).

[4] E. Commission, “Sustainable finance is about re-orientating investment towards environmentally friendly economic activities.”

[5] P.R. Shukla et al., IPCC, 2022: Climate Change 2022: Mitigation of Climate Change. Contribution of Working Group III to the Sixth Assessment Report of the Intergovernmental Panel on Climate Change. Cambridge, UK and New York, NY, USA, 2022. [Online]. Available: www.ipcc.ch

[6] P. J. Mago, A. Hueffed, and L. M. Chamra, “A review on energy, economical, and environmental benefits of the use of CHP systems for small commercial buildings for the North American climate,” *Int J Energy Res*, vol. 33, no. 14, pp. 1252–1265, 2009, doi: 10.1002/ER.1630.

[7] E. J. Naimaster and A. K. Sleiti, “Potential of SOFC CHP systems for energy-efficient commercial buildings,” *Energy Build*, vol. 61, pp. 153–160, 2013, doi: 10.1016/j.enbuild.2012.09.045.

[8] S. Acha *et al.*, “Fuel cells as combined heat and power systems in commercial buildings: A case study in the food-retail sector,” *Energy*, vol. 206, p. 118046, Sep. 2020, doi: 10.1016/J.ENERGY.2020.118046.

[9] R. Jing *et al.*, "Economic and environmental multi-optimal design and dispatch of solid oxide fuel cell based CCHP system," *Energy Convers Manag*, vol. 154, pp. 365–379, Dec. 2017, doi: 10.1016/j.enconman.2017.11.035.

[10] A. Alns and A. K. Sleiti, "Combined heat and power system based on Solid Oxide Fuel Cells for low energy commercial buildings in Qatar," *Sustainable Energy Technologies and Assessments*, vol. 48, Dec. 2021, doi: 10.1016/j.seta.2021.101615.

[11] F. Accurso *et al.*, "Installation of fuel cell-based cogeneration systems in the commercial and retail sector: Assessment in the framework of the COMSOS project," *Energy Convers Manag*, vol. 239, Jul. 2021, doi: 10.1016/j.enconman.2021.114202.

[12] S. Acha *et al.*, "Fuel cells as combined heat and power systems in commercial buildings: A case study in the food-retail sector," *Energy*, vol. 206, Sep. 2020, doi: 10.1016/j.energy.2020.118046.

[13] N. R. E. L. (NREL) Eric J.H. Wilson et al., End-Use Load Profiles for the U.S. Building Stock: Methodology and Results of Model Calibration, Validation, and Uncertainty Quantification. Carolrhoda Books, 2022.

[14] A. B. Stambouli and E. Traversa, "Solid oxide fuel cells (SOFCs): A review of an environmentally clean and efficient source of energy," *Renewable and Sustainable Energy Reviews*, vol. 6, no. 5, pp. 433–455, 2002, doi: 10.1016/S1364-0321(02)00014-X.

[15] S. Zarabi Golkhatmi, M. I. Asghar, and P. D. Lund, "A review on solid oxide fuel cell durability: Latest progress, mechanisms, and study tools," *Renewable and Sustainable Energy Reviews*, vol. 161, p. 112339, Jun. 2022, doi: 10.1016/J.RSER.2022.112339.

[16] M. L. Faro, S. Trocino, S. C. Zignani, and A. S. Aricò, "Solid oxide fuel cells," *Compendium of Hydrogen Energy*, pp. 89–114, Jan. 2016, doi: 10.1016/B978-1-78242-363-8.00004-9.

[17] D. Chiappini, A. L. Facci, L. Tribioli, and S. Ubertini, "SOFC management in distributed energy systems," *J Fuel Cell Sci Technol*, vol. 8, no. 3, 2011, doi: 10.1115/1.4002907.

[18] Y. Shiratori, T. Ijichi, T. Oshima, and K. Sasaki, "Internal reforming SOFC running on biogas," *Int J Hydrogen Energy*, vol. 35, no. 15, pp. 7905–7912, Aug. 2010, doi: 10.1016/J.IJHYDENE.2010.05.064.

[19] M. Deru *et al.*, "U.S. Department of Energy Commercial Reference Building Models of the National Building Stock," 2011. [Online]. Available: http://www.osti.gov/bridge

[20] U. S. D. of E. Pacific Northwest National Laboratory, "Building America and IECC Climate Zones by U.S. County Boundaries (Detailed) - Panoramica." https://www.arcgis.com/home/item.html?id=8e5c3c6e1fa94e379553e199dcc4e777 (accessed Jan. 24, 2023).

[21] ASHRAE, "Climatic Data for Building Design Standards." Accessed: Feb. 17, 2023. [Online]. Available: https://xp20.ashrae.org/standard169/169_2013_a_20201012.pdf

[22] "NSRDB | TMY." https://nsrdb.nrel.gov/data-sets/tmy (accessed Feb. 04, 2023).

[23] "DOE climate zones and representative cities | Download Table." https://www.researchgate.net/figure/DOE-climate-zones-and-representative-cities_tbl1_225647810 (accessed Feb. 18, 2023).

[24] Y. Ruan, Q. Liu, W. Zhou, R. Firestone, W. Gao, and T. Watanabe, "Optimal option of distributed generation technologies for various commercial buildings," *Appl Energy*, vol. 86, no. 9, pp. 1641–1653, Sep. 2009, doi: 10.1016/J.APENERGY.2009.01.016.

[25] F. Accurso *et al.*, "Installation of fuel cell-based cogeneration systems in the commercial and retail sector: Assessment in the framework of the

COMSOS project," *Energy Convers Manag*, vol. 239, p. 114202, Jul. 2021, doi: 10.1016/J.ENCONMAN.2021.114202.

[26] P. Marocco, M. Gandiglio, and M. Santarelli, "When SOFC-based cogeneration systems become convenient? A cost-optimal analysis," *Energy Reports*, vol. 8, pp. 8709–8721, Nov. 2022, doi: 10.1016/J.EGYR.2022.06.015.

[27] "Eurostat - Data Explorer, 2022b. Gas prices for non-household consumers - biannual data (from 2007 onwards). http://appsso.eurostat.ec.europa.eu/nui/ show.do?dataset=nrg_pc_203&lang=en."

[28] "Eurostat - Data Explorer, 2022a. Electricity prices for non-household consumers - bi-annual data (from 2007 onwards). http://appsso.eurostat.ec.europa.eu/ nui/show.do?dataset=nrg_pc_205&lang=en."

[29] K. F. Beckers, M. Z. Lukawski, T. J. Reber, B. J. Anderson, M. C. Moore, and J. W. Tester, "INTRODUCING GEOPHIRES V1.0: SOFTWARE PACKAGE FOR ESTIMATING LEVELIZED COST OF ELECTRICITY AND/OR HEAT FROM ENHANCED GEOTHERMAL SYSTEMS," *PROCEEDINGS, Thirty-Eighth Workshop on Geothermal Reservoir Engineering*.

[30] "High-rise buildings much more energy-intensive than low-rise | UCL News - UCL – University College London." https://www.ucl.ac.uk/news/2017/jun/high-rise-buildings-much-more-energy-intensive-low-rise (accessed Mar. 07, 2023).

[31] E. Resch, R. A. Bohne, T. Kvamsdal, and J. Lohne, "Impact of Urban Density and Building Height on Energy Use in Cities," *Energy Procedia*, vol. 96, pp. 800–814, 2016, doi: 10.1016/J.EGYPRO.2016.09.142.

[32] "Climate Zones - DOE Building America Program | U.S. Energy Atlas." https://atlas.eia.gov/datasets/0c432b67293048b6a4704232a26ca99f_0/explore?location=34.518973%2C-95.221420%2C4.10&showTable=true (accessed Jan. 24, 2023).

[33] "Climate Zones | Department of Energy." https://www.energy.gov/eere/buildings/climate-zones (accessed Feb. 04, 2023).

# APPENDIX A1

In this section the main parameters which can be obtained from the dataset or were used by authors to model it are reported

HVAC systems share in COMSTOCK dataset

| HVAC system | [%] | HVAC system | [%] |
|---|---|---|---|
| 'PSZ-AC with gas coil' | 39.65% | 'PVAV with gas boiler reheat' | 0.17% |
| 'PSZ-HP' | 11.48% | 'VAV district chilled water with district hot water reheat' | 0.17% |
| 'PSZ-AC with no heat' | 10.67% | 'Fan coil chiller with no heat' | 0.15% |
| 'PSZ-AC with electric coil' | 10.48% | 'Residential AC with baseboard electric' | 0.15% |
| 'PTAC with gas coil' | 3.20% | 'Residential forced air furnace' | 0.14% |
| 'PTAC with no heat' | 3.02% | 'Direct evap coolers with forced air furnace' | 0.14% |
| 'PSZ-AC with gas boiler' | 2.18% | 'PSZ-AC district chilled water with electric coil' | 0.13% |
| 'Gas unit heaters' | 1.95% | 'PTAC with gas unit heaters' | 0.13% |
| 'Baseboard electric' | 1.76% | 'Direct evap coolers with baseboard electric' | 0.13% |
| 'PTAC with baseboard electric' | 1.57% | 'Fan coil district chilled water with district hot water' | 0.06% |
| 'Residential AC with residential forced air furnace' | 1.34% | 'PSZ-AC district chilled water with district hot water' | 0.06% |
| 'Forced air furnace' | 1.29% | 'DOAS with fan coil chiller with boiler' | 0.05% |
| 'PTAC with baseboard gas boiler' | 1.13% | 'Water source heat pumps cooling tower with boiler' | 0.04% |

| | | | |
|---|---|---|---|
| 'Water source heat pumps with ground source heat pump' | 0.96% | 'Water source heat pumps fluid cooler with boiler' | 0.04% |
| 'PSZ-AC with baseboard gas boiler' | 0.87% | 'DOAS with fan coil air-cooled chiller with boiler' | 0.02% |
| 'PTHP' | 0.82% | 'DOAS with water source heat pumps cooling tower with boiler' | 0.02% |
| 'Residential AC with no heat' | 0.72% | 'Baseboard district hot water' | 0.02% |
| 'PSZ-AC with baseboard electric' | 0.57% | 'DOAS with fan coil district chilled water with district hot water' | 0.02% |
| 'Baseboard gas boiler' | 0.52% | 'Fan coil district chilled water with boiler' | 0.01% |
| 'Direct evap coolers with gas unit heaters' | 0.50% | 'VAV chiller with district hot water reheat' | 0.01% |
| 'PSZ-AC with gas unit heaters' | 0.45% | 'PSZ-AC with district hot water' | 0.01% |
| 'Fan coil chiller with boiler' | 0.38% | 'PVAV with gas heat with electric reheat' | 0.01% |
| 'PVAV with PFP boxes' | 0.35% | 'Direct evap coolers with no heat' | 0.01% |
| 'DOAS with VRF' | 0.32% | 'Fan coil air-cooled chiller with baseboard electric' | 0.01% |
| 'Fan coil air-cooled chiller with boiler' | 0.30% | 'VAV chiller with gas coil reheat' | 0.01% |
| 'VAV air-cooled chiller with gas boiler reheat' | 0.30% | 'Fan coil chiller with baseboard electric' | 0.01% |
| 'PTAC with baseboard district hot water' | 0.27% | 'PSZ-AC with baseboard district hot water' | 0.00% |
| 'PTAC with electric coil' | 0.27% | 'DOAS with fan coil chiller with district hot water' | 0.00% |

| | | | |
|---|---|---|---|
| 'PTAC with gas boiler' | 0.27% | 'PVAV with district hot water reheat' | 0.00% |
| 'VAV chiller with gas boiler reheat' | 0.26% | 'DOAS with water source heat pumps district chilled water with district hot water' | 0.00% |
| 'Fan coil chiller with district hot water' | 0.20% | 'Fan coil air-cooled chiller with no heat' | 0.00% |
| 'DOAS with water source heat pumps with ground source heat pump' | 0.19% | 'VAV chiller with PFP boxes' | 0.00% |

*Table 28 - HVAC system share: all buildings*

## COMSTOCK modeling data sources

| Data Sources | ComStock Inputs |
|---|---|
| 2015 U.S. Lighting Market Characterization | Interior/exterior lighting power density. |
| ASHRAE 62.1 | Ventilation rates. |
| ASHRAE 90.1 | Nominal efficiency levels for lighting, HVAC, and envelope properties. |
| ASHRAE Service Life and Maintenance Cost Database | Distribution shapes for equipment lifespans. |
| Building Codes Assistance Project | Timeline of energy code adoption by state. |
| DOE Prototype Buildings | Lighting power density, efficiency, occupancy. |
| CoStar Real Estate Data (2017) | Fine geospatial resolution for buildings that are part of an active real estate market: Building type, vintage, floor area, number of stories, location |

| | |
|---|---|
| Database for Energy Efficiency Resources (DEER) | Building system lifespans. For Buildings in California, schedules and power densities for interior lighting and interior equipment, building program, HVAC system controls and efficiencies, ventilation rates, infiltration rate. |
| Commercial Building Stock Assessment 4 (2019) Final Report | Lighting power density, lifespan of windows. |
| DOE Commercial Prototype Buildings | Loads, efficiency, occupancy, space type ratio and zone definition. |
| EIA Commercial Building 2012 Energy<br>Consumption Survey (CBECS) 2012 | Coarse geospatial resolution: Building type, vintage, floor area, number of stories, energy sources, conditioned floor space, HVAC and water heating equipment, hours of operation, aspect ratio, window-to-wall ratio, thermostat setback saturation, data center saturation, heating (space and water) saturation, other equipment saturation. |
| Guidehouse Commercial Fenestration Market Study | Window characteristics and window-to-wall ratio (WWR). |
| Homeland Security Infrastructure Plan<br>(HSIP) Gold 2012 Database | Fine geospatial resolution for buildings that are not part of an active real estate market (hospital, schools): Building type, number of beds (hospitals), enrollment (schools), location |
| Proprietary End-Use Submeter Data | Schedules and power densities for interior lighting and interior equipment, HVAC operation patterns, thermostat setpoints. |

| | |
|---|---|
| Strip Mall Restaurant Surveying | Percentage of restaurants in strip malls. |
| U.S. Census Bureau Public Use Microdata Sample (PUMS), 5-yr 2017. | Heating fuel distributions are inferred from distributions of heating fuel for residential dwelling |

*Table 29 - Data sources for ComStock building stock definition.*

## Climate zones by surface in USA

| IECC Climate Zone | IECC Moisture Regime | Building America Climate Zone | Coun ties | Area in Square Kilometers |
|---|---|---|---|---|
| 1 | A | Hot-Humid | 1 | 3.114,438 |
| 2 | A | Hot-Humid | 222 | 446.974,572 |
| 2 | B | Hot-Dry | 6 | 99.450,251 |
| 2 | B | Hot-Humid | 14 | 57.250,911 |
| 3 | A | Hot-Humid | 192 | 322.850,72 |
| 3 | A | Mixed-Humid | 385 | 635.487,049 |
| 3 | B | Hot-Dry | 109 | 629.575,395 |
| 3 | C | Marine | 14 | 57.054,198 |
| 4 | A | Mixed-Humid | 738 | 856.408,343 |
| 4 | B | Cold | 1 | 11.724,646 |
| 4 | B | Mixed-Dry | 56 | 296.556,435 |
| 4 | C | Marine | 38 | 148.879,498 |
| 5 | A | Cold | 616 | 966.304,848 |
| 5 | B | Cold | 150 | 1.223.562,697 |
| 6 | A | Cold | 337 | 764.947,398 |
| 6 | B | Cold | 125 | 851.577,168 |
| 7 | N/A | Very Cold | 122 | 829.414,269 |
| 8 | N/A | Subarctic | 8 | 1.012.324,775 |

*Table 30 - ASHRAE/IECC USA Climate zone [32]*

### ASHRAE climate zones definitions

| Building America climate zone | ASHRAE Climate zones | Quantitative description | Precipitation regime (annual) |
|---|---|---|---|
| Hot-Humid | 1A<br>2A<br>3A | • A 67°F (19.5°C) or higher wet bulb temperature for 3,000 or more hours during the warmest six consecutive months of the year; or<br>• A 73°F (23°C) or higher wet bulb temperature for 1,500 or more hours during the warmest six consecutive months of the year. | > 20 inches (50 cm) |
| Mixed-Humid | 3A<br>4A | has approximately 5,400 heating degree days (65°F basis) or fewer, and where the average monthly outdoor temperature drops below 45°F (7°C) during the winter months. | >20 inches (50 cm) |
| Hot-Dry | 2B<br>3B | the monthly average outdoor temperature remains above 45°F (7°C) throughout the year. | < 20 inches (50 cm) |
| Mixed-Dry | 4B | , has approximately 5,400 heating degree days (65°F basis) or less, and where the average monthly outdoor temperature drops below 45°F (7°C) during the winter months. | < 20 inches (50 cm) |
| Cold | 5<br>6 | between 5,400 and 9,000 heating degree days (65°F basis). | none |
| Very Cold | 7 | between 9,000 and 12,600 heating degree days (65°F basis). | none |

| | | | |
|---|---|---|---|
| Subarctic | 8 | 12,600 heating degree days (65° basis) or more. The only subarctic regions in the United States are in found Alaska | |
| Marine | 3C<br>4C | A coldest month mean temperature between 27°F (-3°C) and 65°F (18°C)<br>• A warmest month mean of less than 72°F (22°C)<br>• At least 4 months with mean temperatures higher than 50°F (10°C)<br>• A dry season in summer. The cold season is October through March in the Northern Hemisphere and April through September in the Southern Hemisphere. | The month with the heaviest precipitation in the cold season has at least three times as much precipitation as the month |

*Table 31 - Climate zones: from Building America to Ashrae definitions [33]*

### COMSTOCK buildings' models characteristics

| Input parameter | Unit of measure | Description |
|---|---|---|
| in.sqft | $ft^2$ | Building total floor area, per i confronti posso tenere conto dei consumi specifici riferiti al m2 |
| in.aspect_ratio | – | Aspect ratio of building geometry which is the ratio of North/South Facade Length Relative to East/West Facade Length |
| in.rotation | ° | Building Rotation off of North axis |

| | | |
|---|---|---|
| in.weekday_operating_hours | hr | Building duration of weekday hours of operation which influences duration of schedules |
| in.weekday_opening_time | hr | Building weekday start hour which impacts the start time of schedules |
| in.weekend_operating_hours | hr | Building duration of weekend hours of operation which influences duration of schedules |
| in.weekend_opening_time | hr | Building weekend start hour which impacts the start time of schedules |
| in.tstat_clg_delta_f | F | Cooling thermostat unoccupied setpoint temperature delta from primary occupied cooling setpoint. A value of '999' indicates default values were used for model |
| in.tstat_clg_sp_f | F | Cooling thermostat occupied setpoint. A value of '999' indicates default values were used for model |
| in.tstat_htg_delta_f | F | Heating thermostat unoccupied setpoint temperature delta from primary occupied heating setpoint. A value of '999' |

| | | |
|---|---|---|
| | | indicates default values were used for model |
| in.tstat_htg_sp_f | F | Heating thermostat occupied setpoint. A value of '999' indicates default values were used for model |
| in.number_of_stories | | Specifies the number of stories of the building |
| in.hvac_system_type | | Building primary HVAC system type |
| stat.occupant_density_ppl_per_m_2 | $\frac{people}{m^2}$ | Occupant density, people per unit area |

*Table 32 - Building metadata extracted using MATLAB[13]*

### COMSTOCK buildings' models characteristics

| | |
|---|---|
| 'applicability' | 'in_number_of_stories' |
| 'in_upgrade_name' | 'in_sqft' |
| 'in_tstat_clg_delta_f' | 'in_hvac_system_type' |
| 'in_tstat_clg_sp_f' | 'in_weekday_operating_hours' |
| 'in_tstat_htg_delta_f' | 'in_weekday_opening_time' |
| 'in_tstat_htg_sp_f' | 'in_weekend_operating_hours' |
| 'in_aspect_ratio' | 'in_weekend_opening_time' |
| 'in_building_subtype' | 'stat_occupant_density_ppl_per_m_2' |
| 'in_county' | 'in_rotation' |
| 'in_building_type' | |

*Table 33 - Building metadata: geometry, thermostats setpoint, hours of schedule, HVAC data[13]*

## COMSTOCK dataset calibration parameters

| |
|---|
| 'qoi_report_maximum_daily_timing_shoulder_hour' |
| 'qoi_report_maximum_daily_timing_summer_hour' |
| 'qoi_report_maximum_daily_timing_winter_hour' |
| 'qoi_report_maximum_daily_use_shoulder_kw' |
| 'qoi_report_maximum_daily_use_summer_kw' |
| 'qoi_report_maximum_daily_use_winter_kw' |
| 'qoi_report_minimum_daily_use_shoulder_kw' |
| 'qoi_report_minimum_daily_use_summer_kw' |
| 'qoi_report_minimum_daily_use_winter_kw' |

*Table 34 - Building metadata: energy peak timing and magnitude[13]*

## COMSTOCK buildings' models technical characteristics

| |
|---|
| 'in_heating_fuel' |
| 'in_service_water_heating_fuel' |
| 'stat_air_system_fan_total_efficiency' |
| 'stat_average_boiler_efficiency' |
| 'stat_average_dx_cooling_cop' |
| 'stat_average_dx_heating_cop' |
| 'stat_average_gas_coil_efficiency' |
| 'stat_design_dx_cooling_cop' |
| 'stat_design_dx_heating_cop' |

*Table 35 - Building metadata: fuel, HVAC, and efficiencies[13]*

## COMSTOCK buildings’ models input data

| |
|---|
| 'in_energy_code_followed_during_last_exterior_lighting_replaceme' |
| 'in_energy_code_followed_during_last_hvac_replacement' |
| 'in_energy_code_followed_during_last_interior_equipment_replacem' |
| 'in_energy_code_followed_during_last_interior_lighting_replaceme' |
| 'in_energy_code_followed_during_last_roof_replacement' |
| 'in_energy_code_followed_during_last_service_water_heating_repla' |
| 'in_energy_code_followed_during_last_walls_replacement' |
| 'in_energy_code_followed_during_last_windows_replacement' |
| 'in_energy_code_followed_during_original_building_construction' |

*Table 36 - Building metadata: energy codes used in simulations [13]*

## COMSTOCK buildings’ models energy consumption by end-use

| | |
|---|---|
| 'out_district_cooling_cooling_energy_consumption' | 'out_electricity_refrigeration_energy_consumption_intensity' |
| 'out_district_cooling_cooling_energy_consumption_intensity' | 'out_electricity_water_systems_energy_consumption' |
| 'out_district_heating_heating_energy_consumption' | 'out_electricity_water_systems_energy_consumption_intensity' |
| 'out_district_heating_heating_energy_consumption_intensity' | 'out_natural_gas_heating_energy_consumption' |
| 'out_district_heating_water_systems_energy_consumption' | 'out_natural_gas_heating_energy_consumption_intensity' |
| 'out_district_heating_water_systems_energy_consumption_intensity' | 'out_natural_gas_interior_equipment_energy_consumption' |
| 'out_electricity_cooling_energy_consumption' | 'out_natural_gas_interior_equipment_energy_consumption_intensity' |
| 'out_electricity_cooling_energy_consumption_intensity' | 'out_natural_gas_water_systems_energy_consumption' |
| 'out_electricity_exterior_lighting_energy_consumption' | 'out_natural_gas_water_systems_energy_consumption_intensity' |
| 'out_electricity_exterior_lighting_energy_consumption_intensity' | 'out_other_fuel_heating_energy_consumption' |

| | |
|---|---|
| 'out_electricity_fans_energy_consumption' | 'out_other_fuel_heating_energy_consumption_intensity' |
| 'out_electricity_fans_energy_consumption_intensity' | 'out_other_fuel_water_systems_energy_consumption' |
| 'out_electricity_heat_recovery_energy_consumption' | 'out_other_fuel_water_systems_energy_consumption_intensity' |
| 'out_electricity_heat_recovery_energy_consumption_intensity' | 'out_district_cooling_total_energy_consumption' |
| 'out_electricity_heat_rejection_energy_consumption' | 'out_district_cooling_total_energy_consumption_intensity' |
| 'out_electricity_heat_rejection_energy_consumption_intensity' | 'out_district_heating_total_energy_consumption' |
| 'out_electricity_heating_energy_consumption' | 'out_district_heating_total_energy_consumption_intensity' |
| 'out_electricity_heating_energy_consumption_intensity' | 'out_electricity_total_energy_consumption' |
| 'out_electricity_interior_equipment_energy_consumption' | 'out_electricity_total_energy_consumption_intensity' |
| 'out_electricity_interior_equipment_energy_consumption_intensity' | 'out_site_energy_total_energy_consumption' |
| 'out_electricity_interior_lighting_energy_consumption' | 'out_site_energy_total_energy_consumption_intensity' |
| 'out_electricity_interior_lighting_energy_consumption_intensity' | 'out_natural_gas_total_energy_consumption' |
| 'out_electricity_pumps_energy_consumption' | 'out_natural_gas_total_energy_consumption_intensity' |
| 'out_electricity_pumps_energy_consumption_intensity' | 'out_other_fuel_total_energy_consumption' |
| 'out_electricity_refrigeration_energy_consumption' | 'out_other_fuel_total_energy_consumption_intensity' |

*Table 37 - Building metadata: yearly energy consumption by end use [13]*

### COMSTOCK buildings' models geographic informations

| |
|---|
| 'in_nhgis_tract_gisjoin' |
| 'in_nhgis_county_gisjoin' |
| 'in_state_name' |
| 'in_state_abbreviation' |
| 'in_census_division_name' |
| 'in_census_region_name' |
| 'in_weather_file_2018' |
| 'in_weather_file_TMY3' |
| 'in_climate_zone_building_america' |
| 'in_climate_zone_ashrae_2004' |
| 'in_iso_region' |
| 'in_reeds_balancing_area' |
| 'in_resstock_county_id' |
| 'in_nhgis_puma_gisjoin' |

*Table 38 - Building metadata: geographical, climate and weather information [13]*

# APPENDIX A2

## SOFC sizing

In this section, the sizing of the SOFC to meet the electrical demand of each of the eight buildings is presented. The annual electric and thermal profiles for each building are reported, along with the baseline electric load on which the SOFC is sized, and the available thermal power output from the SOFC.

### Hospitals

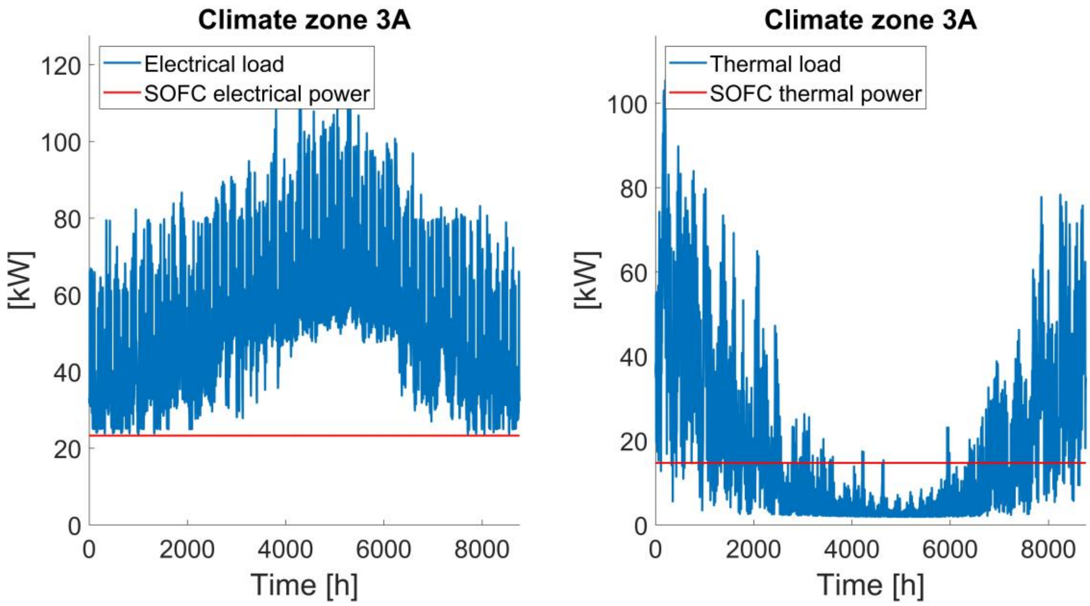


*Figure 59 - Sizing of SOFC for hospital in climate 3A*

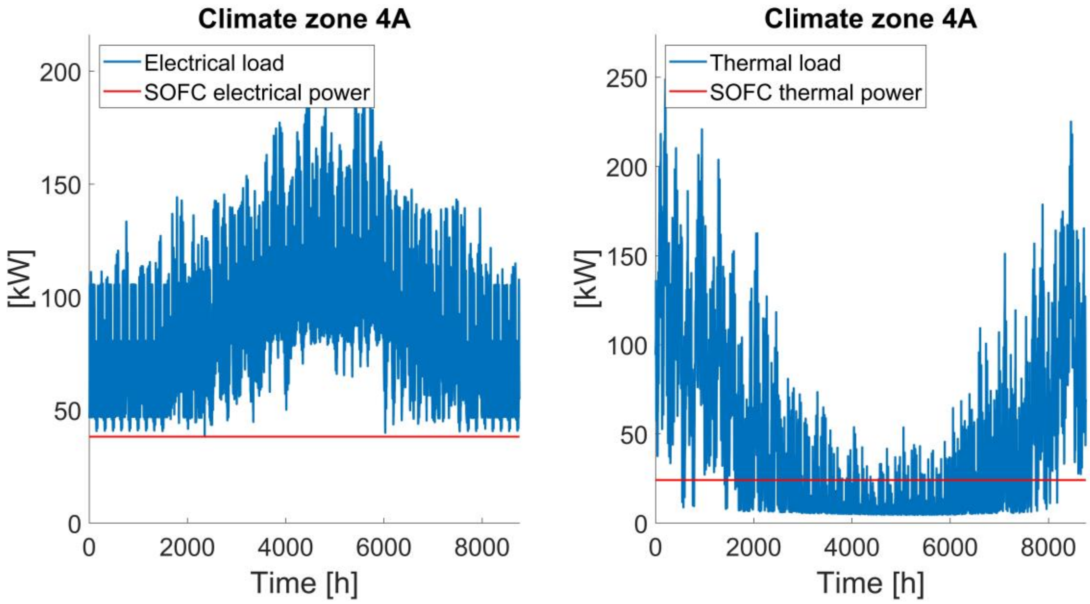


*Figure 60 - Sizing of SOFC for hospital in climate 4A*

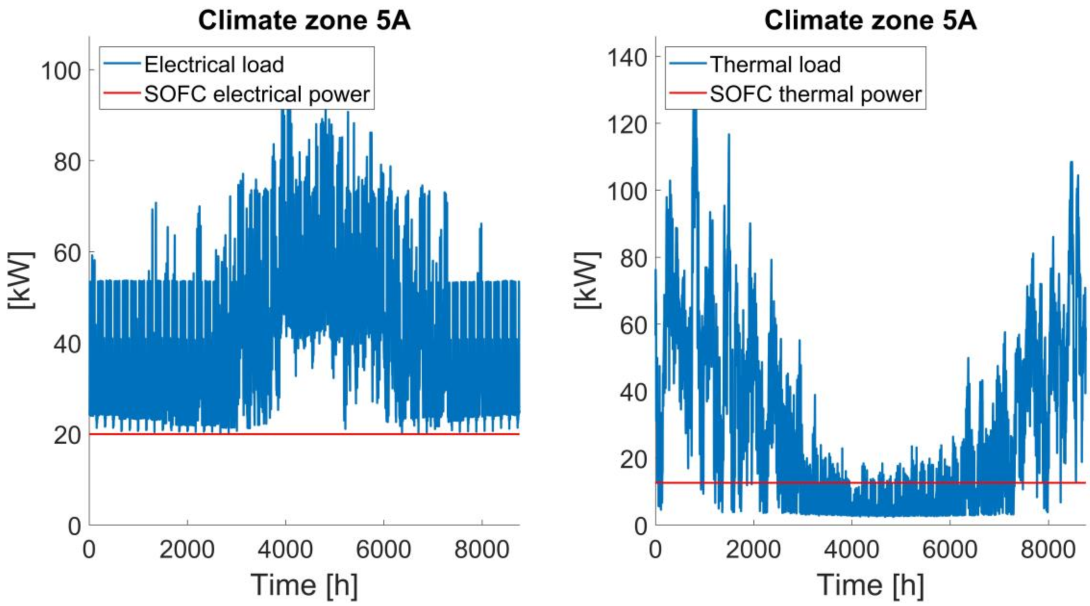


*Figure 61 - Sizing of SOFC for hospital in climate 5A*

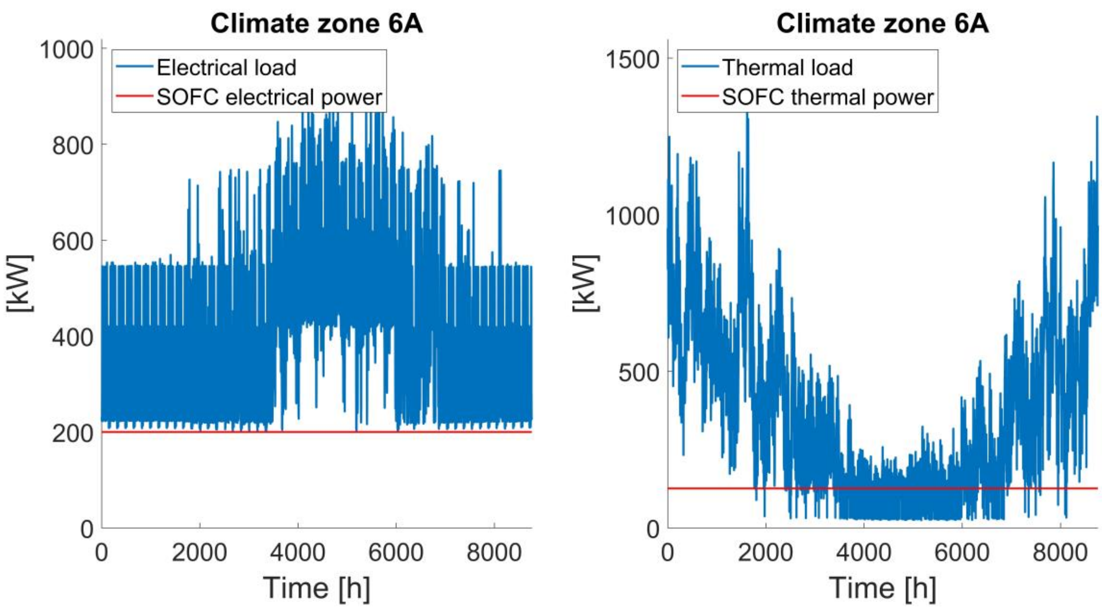


*Figure 62 - Sizing of SOFC for hospital in climate 6A*

## Hotels

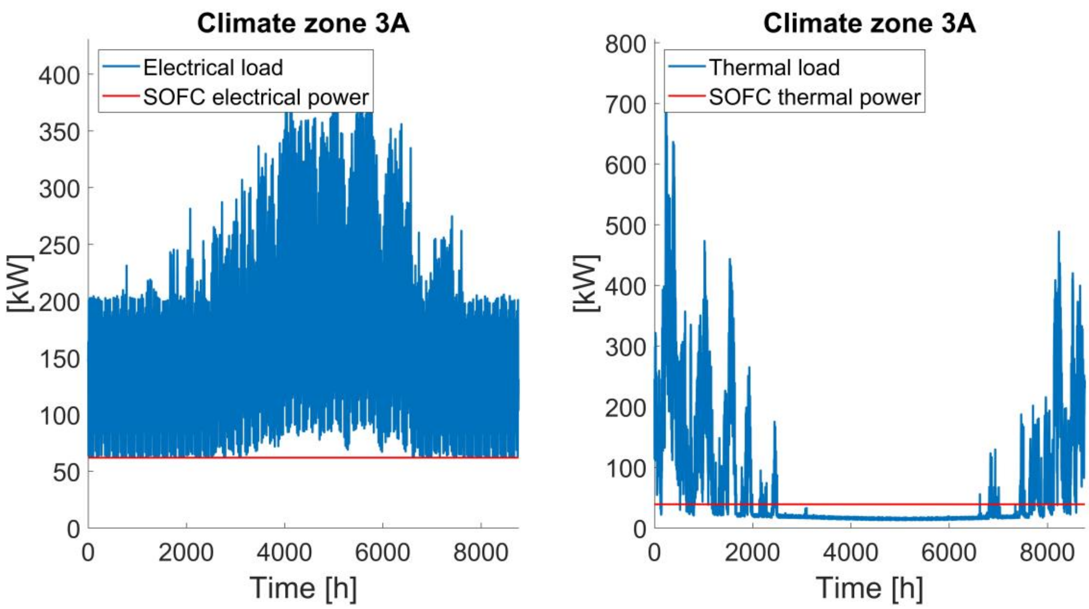


*Figure 63 - Sizing of SOFC for hotel in climate 3A*

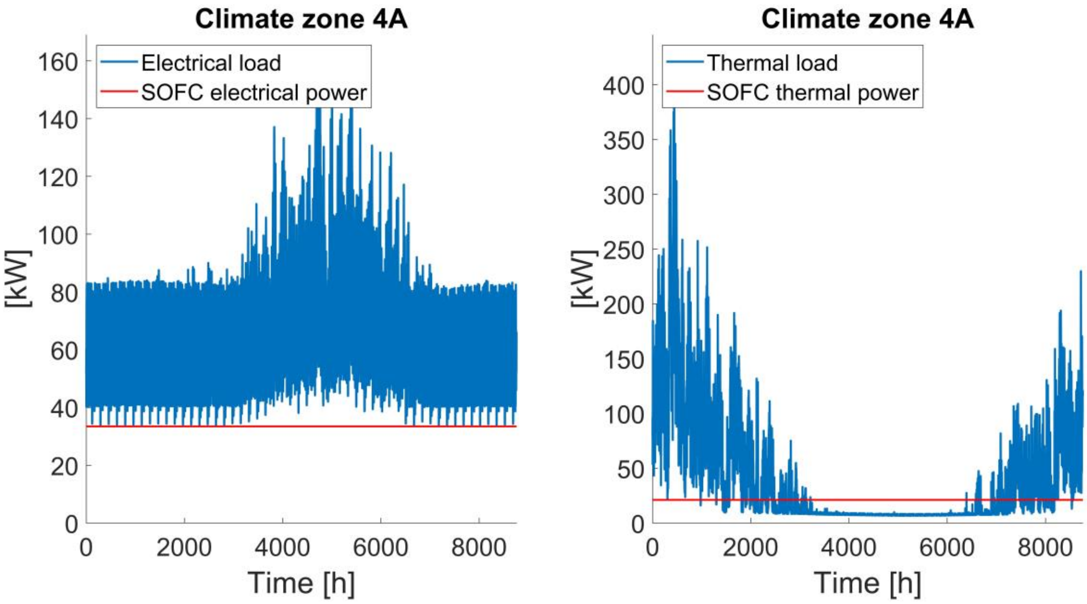


*Figure 64 - Sizing of SOFC for hotel in climate 4A*

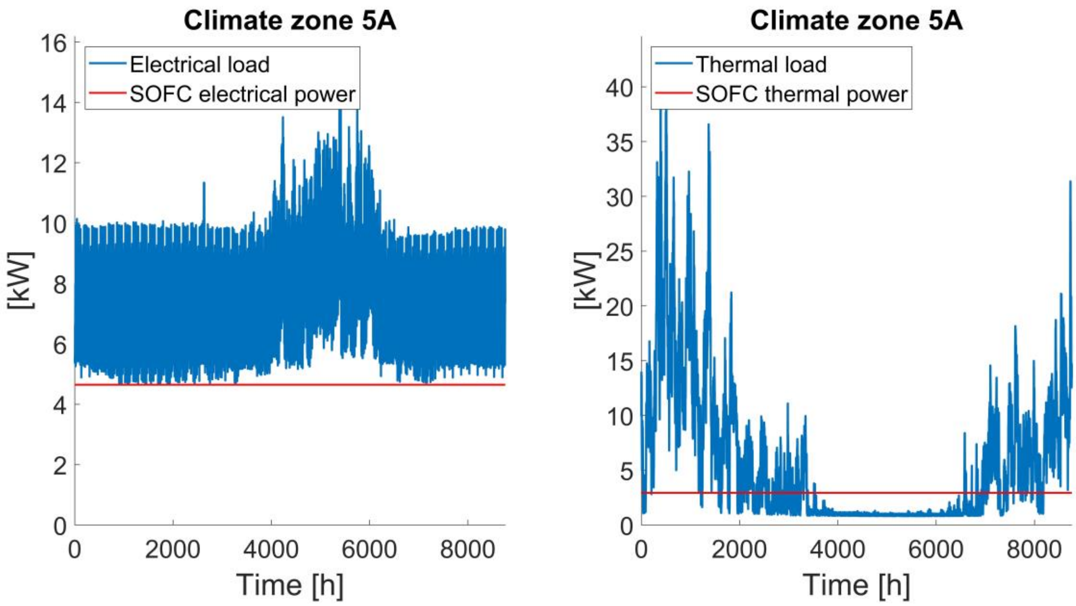


*Figure 65 - Sizing of SOFC for hotel in climate 5A*

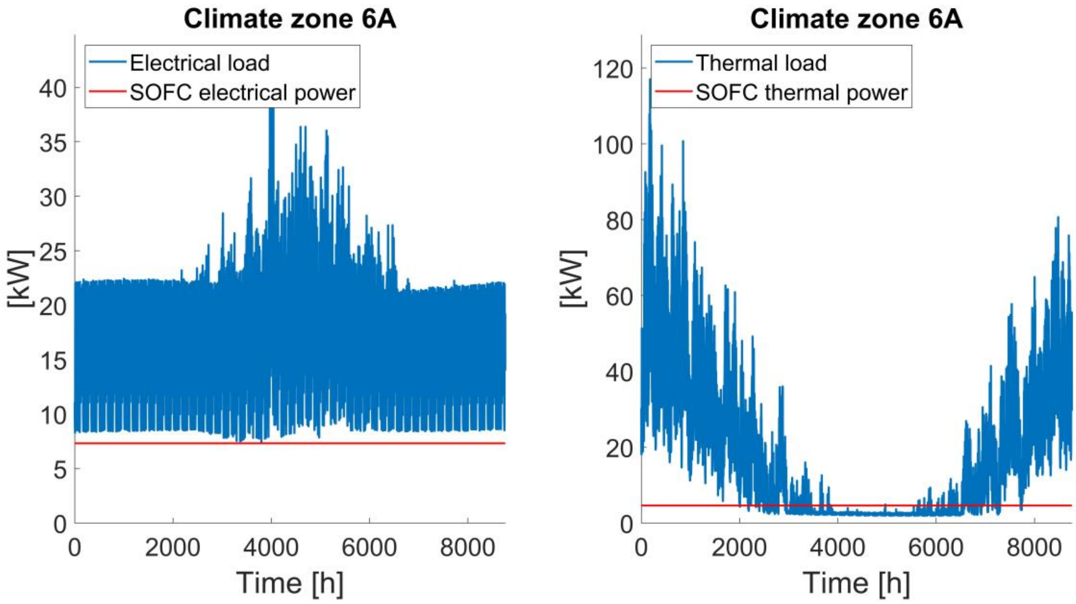


*Figure 66 - Sizing of SOFC for hotel in climate 6A*